Energy-Efficient Electronic Health Monitoring System with Wireless Body Area Networks

by

Osama Amjad

Graduate Program

in

Department of Electrical and Computer Engineering

A thesis submitted in partial fulfillment of the requirements

for the degree of Doctor of Philosophy (Ph.D.)

Faculty of Graduate Studies

Lakehead University

Thunder Bay, Ontario, Canada

August 2022

Examining Committee Membership

The following served on the Examining Committee for this thesis. The decision of the Examining Committee is by majority vote.

External Examiner: Aissa Ikhlef
Associate Professor, Department of Engineering,
Durham University, United Kingdom

Internal Member(s): Apparao Dekka
Assistant Professor, Dept. of Electrical Engineering,
Lakehead University, Canada

Shafiqul Hai
Assistant Professor, Dept. of Electrical Engineering,
Lakehead University, Canada

Supervisors: Salama Ikki
Associate Professor, Dept. of Electrical Engineering,
Lakehead University, Canada

Ebrahim Bedeer
Assistant Professor, Dept. of Electrical Engineering,
University of Saskatchewan, Canada

Author's Declaration

I hereby declare that I am the sole author of this thesis. This is a true copy of the thesis, including any required final revisions, as accepted by my examiners.

I understand that my thesis may be made electronically available to the public.

Abstract

Recent evolution and technological advancement in wireless communications and microelectronics have enabled enhanced research trends toward wireless body area networks (WBANs). This emerging new field of research plays an important role in medical and healthcare services. An electronic health (eHealth) monitoring system is one of the major applications of WBANs that in addition to saving lives can provide cost-effective healthcare services by replacing the need for costly in-hospital monitoring with wearable or implanted monitoring systems that help early detection and prevention of any abnormal physiological activities that could risk the patients' lives. Such a system continuously monitors the patient's vital signs and helps patients to involve in their routine activities of daily life without requiring intensive or specialized medical services all the time, thus creating significant enhancement in the standard of living. One of the key challenges that limit the widespread usage of eHealth solutions in practical healthcare facilities is the limited battery life of sensor nodes (SNs) that are needed to be replaced/recharged manually once the energy is depleted. In most scenarios, battery replacement is not preferable, and it becomes highly unsuitable and impractical, especially when the SNs are implanted inside the human body. This limited battery capacity of SNs not only causes a performance bottleneck but is also likely to disrupt the future operations of SNs, which may cause a life hazard. Therefore, in order to have seamless and efficient implementation of an eHealth monitoring WBAN, improving the SNs' lifetime or energy efficiency (EE) is of paramount importance.

EE is one of the fundamental design objectives that greatly affects the performance of the eHealth system, and optimizing the EE enables efficient use of energy-constrained SNs. In this regard, this thesis has threefold objectives. Firstly, a linear fractional EE optimization problem is formulated and solved for an eHealth monitoring WBAN consisting

of SNs equipped with energy harvesting capabilities communicating with an aggregator. The EE objective function is defined as the ratio of the overall source rate of all the SNs to the total power consumption of WBAN by considering energy harvesting and power budget constraints. Secondly, a robust communication scheme for eHealth monitoring WBAN is proposed that can characterize the propagation characteristics of various patient activities by only utilizing the generalized gamma distribution that can efficiently model various body movements. In this regard, a novel EE optimization problem is formulated and solved that does not require channel state information (CSI) from transmitting SNs to the aggregator while optimizing the transmit power and encoding rate of each SN by considering outage probability and packet retransmission. Last but not the least, an energy-efficient resource allocation framework is proposed to maximize the EE of an eHealth monitoring WBAN assisted with backscatter communication (BackCom) and energy harvesting technologies, subject to quality of service (QoS) and power budget constraints. More specifically, the optimization problem optimizes the transmit power of the aggregator, transmission time, and backscatter time of WBAN consisting of energy-constrained SNs which have the ability to harvest energy from the signals transmitted by the aggregator.

Acknowledgements

First and foremost, I am grateful to Almighty Allah (Subhanahu Wa Taala) for his countless blessings and for giving me the strength to accomplish my research work.

I would like to express my deepest gratitude to my supervisors, Dr. Salama Ikki and Dr. Ebrahim Bedeer. Thank you for your continuous guidance, support, encouragement, and insightful feedback throughout my research studies that helped improve the technical and presentation quality of my work. Without your guidance, advice, and valuable input on my research ideas and writings, this work would not have been possible. I have always been inspired by your in-depth knowledge in diverse fields of wireless communications.

I am also grateful to Dr. Aissa Ikhlef, Dr. Apparao Dekka, and Dr. Shafiqul Hai for serving on my thesis committee as examiners and providing constructive feedback. I also appreciate Dr. Krishnamoorthy Natarajan for serving as a member of my comprehensive exam and seminar committee and providing valuable feedback on my work.

I sincerely thank my colleagues at Lakehead University, Electrical and Computer Engineering department for making my Ph.D. study such an exceptional learning experience. I appreciate your friendship, support, and useful discussions.

Last but not the least, I would like to express my deepest gratitude to my parents, sister, brother, and my in-laws. I am extremely fortuitous and honored to have them in my life. Without their prayers, support, encouragement, and eternal love I would never be able to accomplish this goal. I can not thank enough my mother for her encouragement, prayers, and sacrifices throughout her life for my better future. I like to pay regard to my late father (may his soul rest in peace) who always wanted to see me in a position of high esteem. Special thanks to my wife for her love, support, and sacrifices for the family, and to my beautiful son Ibrahim for bringing happiness and hope to my life.

Dedication

I would like to dedicate this thesis to my deceased father, Amjad Pervez. He was my mentor and a source of inspiration who always encouraged me to aim higher in life. May his soul be pleased to see me accomplish this milestone.

May Allah ((Subhanahu Wa Taala) grant him the highest place in the heavens.

Table of Contents

List of Figures

Abbreviations

ADC analog-to-digital converter 13, 83, 86

AP access point 22

BackCom backscatter communication v, 4, 5, 7, 9, 10, 28, 29, 72–78, 80–84, 87, 88, 93, 100, 102, 105, 106, 108–110, 112, 113, 115

BP blood pressure 14, 15

BSN body sensor network 18

CNR channel gain to noise ratio 58, 61

CSI channel state information v, 7, 9, 57, 58, 62, 64, 65, 112

CSMA/CA carrier-sense multiple access with collision avoidance 32

CW continuous wave 28, 80

ECG electrocardiogram 14

EE energy efficiency iv, v, 3–7, 9, 10, 31–34, 41–48, 50–53, 55–57, 61, 62, 64, 65, 68–70, 72, 74, 75, 77, 78, 81, 82, 91–94, 96, 97, 99–117

EEG electroencephalography 14

eHealth electronic health iv, v, 2–6, 9, 10, 13–15, 18, 23, 27–31, 34, 38, 47, 53–56, 65, 71–73, 76, 77, 79, 87, 92, 100, 102, 104, 109, 111–114

ENO energy neutral operation 31

H-AP hybrid access point 73

HD hybrid device 74, 75

HTT harvest-then-transmit 74–77, 82, 84, 106, 108, 109

IoT Internet-of-Things 5, 28, 75

KKT Karush-Kuhn-Tucker 7, 78, 95, 98

LFP linear fractional programming 42, 43

MAC medium access control 5, 32, 33

MIMO multi-input-multi-output 113

PB power beacon 74, 75

PD personal device 16

PDA personal digital assistant 16

PTT pulse transmit time 15

QoS quality of service v, 3, 7, 31–34, 56

RC resistor/capacitor 29, 83

RF radio frequency 4, 5, 26–29, 72, 73

SN sensor node iv, v, 3–7, 9, 13, 16–18, 22, 23, 25, 30–42, 46, 47, 49–51, 53, 55–57, 71–77, 79–82, 84–87, 92, 93, 100, 102, 104–106, 108–112, 114, 115, 117

SNR signal-to-noise ratio 73, 75

TDMA time division multiple access 32, 35, 56, 58, 82, 85

UAV unmanned aerial vehicle 75

WBAN wireless body area network iv, v, 3–7, 9, 10, 12–15, 17–24, 27, 28, 30–35, 37, 40, 41, 45, 47, 49, 53, 55–58, 60, 62–65, 70–82, 84, 87, 88, 90–93, 100, 102, 104–107, 109–115, 117

WPCN wireless powered backscatter communication network 74, 75

WPCN wireless powered communication network 73, 74, 83

WSN wireless sensor network 12, 18

Chapter 1

Introduction

1.1 Background and Motivation

The population of the world is increasing rapidly, and every country around the globe is experiencing growth in the number of older people in their population. According to a report on world population aging statistics [1], there were 703 million people aged 65 years or over in the world in 2019, and from 2025 to 2050, the elderly population is projected to nearly double at least to 1.6 billion globally, as shown in Fig. 1.1. Furthermore, the number of people living alone is increasing day by day, and the majority of older people are facing chronic diseases. However, conventional medical treatment which needs patients to go to a medical facility or doctor when they feel sick, cannot confront these situations in a timely manner. It is expected that this increase in the number of adults will overburden the efficient performance of the health care systems, thus considerably affecting the quality of life. Based on these statistics it is necessary to have a dramatic shift in currently available health care systems towards more affordable and adaptable health solutions [2–4].

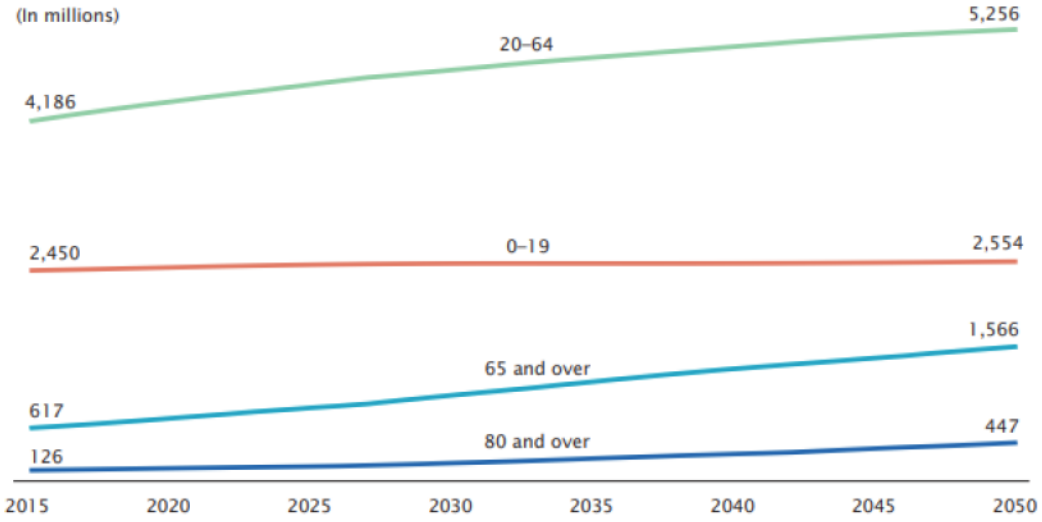

Fig. 1.1: World population (in millions) by age group: 2015 to 2050 [1].

On the other hand, hundreds of thousands of patients die every year from various fatal and chronic diseases such as cancer, cardiovascular disease, Parkinson's, diabetes, asthma, obesity, etc [5]. In most cases, the patients suffering from such fatal diseases experience the symptoms of illness and have been diagnosed with the disease when it is too late. Most of the research studies have shown that many of these diseases can be cured if they are detected during their early stages. Therefore, future health care solutions need to offer dynamic wellness management and focus on early detection and prevention of any signs of illness. In this regard, with the evolution of wearable sensors and the advancement in wireless communication technologies, eHealth monitoring system arises as an emerging research field in the academics and R&D industries worldwide [6–9].

eHealth system serves as a promising solution that provides cost-effective healthcare services through wearable or implanted monitoring systems that help early detection and prevention of any abnormal physiological activities that could risk the patients' lives. Such a system continuously monitors the patient's vital signs and helps patients to involve

in their routine activities of daily life without requiring intensive or specialized medical services all the time thus creating significant enhancement in the standard of living. Such seamless medical and healthcare services can only be acquired through a smart network consisting of low-power microelectronics and nanotechnology based actuators and SNs that can be deployed on the body surface as wearable devices or implanted inside the patient's body. Such networks are commonly called as WBANs [10–12]. In comparison with the conventional healthcare services, eHealth systems with WBAN take advantage of portable health monitoring devices to offer location-independent healthcare facilities. In addition to saving lives, the prevalent use of WBANs will reduce health care costs by removing the need for costly in-hospital monitoring of patients [2].

1.2 Research Challenges and Possible Solutions

To facilitate the efficient and seamless implementation of eHealth monitoring WBANs, such as to be adopted widely, certain challenges need to be addressed. In this regard, increasing the battery life with sustainable energy supply, QoS guarantee of the data, and high EE with minimal power consumption are of significant importance [8, 13, 14]. Body SNs require a sustainable energy supply to perform their activities and perpetual operation. Conventionally, these SNs are powered by batteries, which have a limited lifetime and are needed to be replaced/recharged manually once the energy is consumed. Moreover, battery maintenance and replacement are not preferable sometimes, and it becomes unsuitable when sensors are implanted within the human body. Furthermore, the evolution of battery technologies is not yet capable of meeting the energy demand to develop WBAN with sufficient lifetime and satisfactory cost; thus there exists a vast gap between the energy demand of the wireless devices and the energy density resulting from the development

in battery technology. That said, improving the SNs' lifetime or EE is of paramount importance for the widespread adoption of eHealth monitoring systems in the practical healthcare environment.

Numerous research efforts are carried out in the literature at different layers with a focus on minimizing the energy constraints by designing energy-efficient protocols, energy conservation strategies, and effective network topology designs. As a result of recent technological breakthroughs, various battery recharging techniques have been developed to overcome the limited battery life of the SNs that remained a major hurdle making the WBAN use less appealing. One such alternative is wireless energy harvesting, which serves as a promising approach and helps enable the self-sustained body SNs operations. In this technique, SNs are equipped with energy harvesting capabilities that allow them to scavenge energy from ample biochemical and biomechanical energy sources present in the human body or ambient green sources (e.g., solar, thermal, vibrational, radio frequency (RF)) [15–18]. However, the energy recharging rate is usually slow and varies from time to time; therefore a body sensor may deplete its energy before its battery is recharged which creates a disturbance in the eHealth monitoring system. This interruption may cause a hazard if the vital information of a serious patient is not received on time. Nevertheless, the harvested energy requires effective energy management schemes such as EE maximization that focuses on saving the energy of WBAN given the available resources while maintaining the satisfactory performance level of the network in terms of data transmission.

Recently BackCom has emerged as an evolving paradigm that serves as a communication technology for the next-generation wireless networks such as eHealth monitoring WBANs [19]. BackCom can provide nearly limitless chances to connect wireless devices due to this revolutionary way of communication by reflecting and modulating the incident signal. BackCom is considered a key enabler to tackle the issue of limited battery capacities

in wireless devices, therefore can be utilized to enable pervasive connectivity in a variety of applications, including wearable devices, smart connected homes, industrial Internet-of-Things (IoT), and small embedded devices. In contrast to a conventional radio architecture that requires a chain of power-hungry modules, a backscatter node does not comprise any active RF components, therefore, can be deployed to have miniature hardware with exceptionally low power consumption [20]. Furthermore, BackCom is envisioned to revolutionize the healthcare supplied through embedded microelectronics and wearable devices by efficiently transmitting the data under a low-power budget. Consequently, this technology helps enable customized self-managing and self-monitoring eHealth systems [21].

1.3 Objectives and Thesis Contributions

As discussed earlier, the main objective of an eHealth monitoring system is to serve with continuous and high-quality service to the subscribers. A sustainable service necessitates that the system can operate without interference for an adequately prolonged stretch of time with the end goal that adequate information can be gathered for a patient. Due to limited battery life, improving the SNs lifetime or EE is of significant importance to realize smart healthcare solutions in real life. However, such a design objective has been overlooked in the literature, and most of the existing research on eHealth monitoring WBANs is based on aspects of designing the medium access control (MAC) protocols [13, 22, 23] and maximizing the throughput of WBANs that focuses on transmitting the maximum data by utilizing all the available power [24–26].

In comparison with the existing literature on WBANs, the objective of this thesis is to design an energy-efficient eHealth system by considering EE as the design objective. EE is one of the fundamental design objectives that greatly affects the performance of an eHealth

system. In this regard, this research proposes new solutions for achieving enhancements in the eHealth monitoring system by considering different system models and various design parameters with the principle aim of saving the power of energy-constrained WBAN. In addition, the discussion and insight into future research directions with potential scope of improvements and opportunities for further research are provided. The main contributions (also summarized in Fig. 1.2) of this thesis are briefly described as follows:

1. An optimization problem is proposed and solved to maximize the EE of an eHealth monitoring WBAN. The proposed system model consists of SNs equipped with energy harvesting capabilities communicating with an aggregator, and the corresponding energy harvesting process of the SNs is modeled using the discrete-time Markov chain. The EE objective function is defined as the ratio of the sum of the source rate of all the SNs to the power consumption of all SNs in the network. The formulated linear fractional EE optimization problem is converted to an equivalent linear form by using the Charnes-Cooper transformation. The optimization problem aims to maximize the overall EE of the self-sustained eHealth monitoring system with WBAN by optimally allocating each SN source rate such that the overall EE of the WBAN system is maximized. Moreover, the structure of the optimization problem is analyzed to provide a suboptimal solution at lower computational complexity, and mathematical expressions of upper and lower bounds of the source rates of the SN are derived. Extensive simulations are performed to evaluate the performance of the proposed scheme, which reveal that the optimal allocation of the source rate to energy-constrained SNs improves the performance of WBAN in terms of EE.

2. A robust eHealth monitoring communication system is proposed that can characterize the propagation characteristics of various patient conditions by only utilizing

the generalized gamma distribution that supports various patient conditions and can efficiently model both everyday and dynamic activities. More specifically, an optimization problem is formulated to optimize the EE of WBAN without requiring the CSI from the transmitting SNs to the aggregator. The optimization problem optimizes the transmit power and encoding rate of each SN such as to optimize the EE (measured in J/bits) by considering outage probability and packet retransmission. It is shown that the formulated optimization problem is semi-strictly quasi-convex in each decision variable, and an alternative optimization approach is proposed to determine its solution.

3. A resource allocation framework is proposed to maximize the EE of WBAN assisted with BackCom, subject to QoS and power budget constraints. More specifically, the optimization problem optimizes the transmit power of the aggregator, transmission time, and backscatter time of WBAN consisting of energy-constrained SNs which have the ability to harvest energy from the signals transmitted by the aggregator. A generalized gamma distribution is adopted to characterize the channel propagation characteristics of patients under different arbitrary body movements/activities. The formulated EE optimization problem is shown to be a quasi-concave nonlinear fractional problem, which is transformed to an equivalent parametric problem by using the Dinkelbach approach, and the corresponding Karush-Kuhn-Tucker (KKT) conditions are solved to obtain the solution. Furthermore, a low-complexity iterative-based suboptimal heuristic is proposed with performance fairly close to the optimized solution. Simulation results demonstrate the effectiveness of the proposed scheme in maximizing EE of the WBAN by considering relaxing, walking, and running states. Additionally, comparisons with the related work from the literature are performed that reaffirm the superiority of the proposed algorithm.

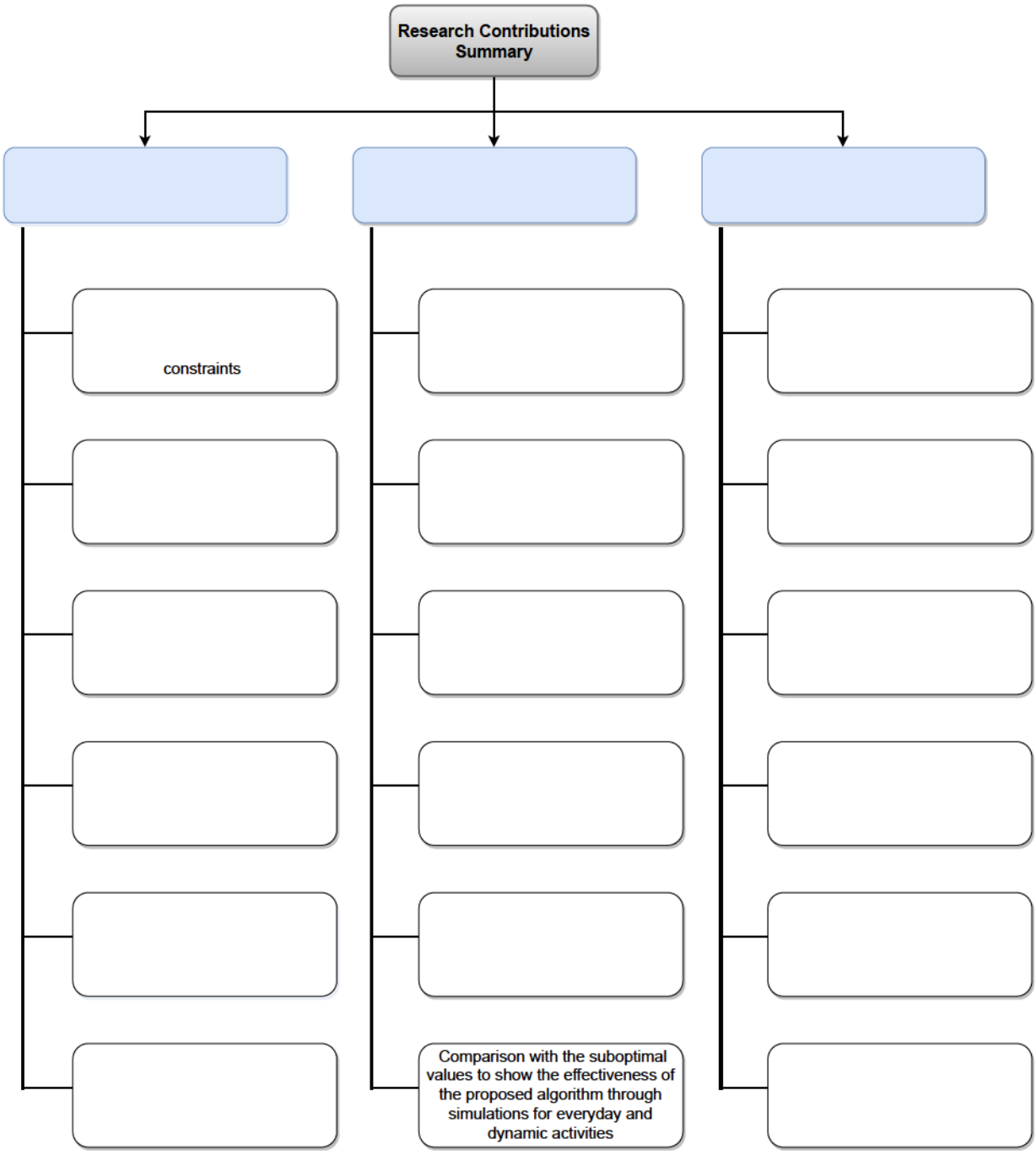

Fig. 1.2: Summary of the research contributions in the dissertation.

1.4 Thesis Outline

The thesis is organized as follows:

In Chapter 2, the general architecture of WBAN and its various medical and non-medical applications including eHealth monitoring system is discussed. The taxonomy of WBANs including different modules and a brief overview of the classification of WBAN devices according to their functionalities are also highlighted. The different communication architectures are also discussed to provide an idea about different communication tiers in WBANs. Moreover, energy harvesting in WBANs is discussed and a classification of the available energy resources that can be utilized for harvesting energy are also provided. Last but not the least, a brief over of BackCom in eHealth monitoring WBAN is discussed to highlight the advantages in overcoming the issue of limited battery capacities in eHealth systems by enabling pervasive connectivity.

In Chapter 3, a self-sustained WBAN system model is presented in which the energy harvesting mechanism of the SN is modeled using the discrete-time Markov chain. In this regard, an EE maximization problem formulation and its solution are discussed that intends to maximize the EE of energy-constrained SNs equipped with energy harvesting capabilities communicating with an aggregator. Finally, the suboptimal solution at a lower computational complexity is also discussed in this chapter.

In Chapter 4, a WBAN system model with a robust communication scheme that focuses on saving the power of energy-constrained SNs is presented. In this regard, an EE optimization problem without having the CSI from the transmitting SNs to the aggregator is formulated and solved. Moreover, a generalized gamma distribution is adopted that can support different patient conditions during daily life activities and can efficiently model both everyday and dynamic activities.

In chapter 5, a BackCom based eHealth monitoring system model is proposed that aims to provide sustainable and high-quality medical services. Based on that, an energy-efficient optimization framework is studied on a transmission frame consisting of two phases, i.e., passive BackCom phase, and active data transmission phase to maximize the EE of energy-constrained WBAN equipped with energy harvesting capabilities. Moreover, a generalized gamma distribution is adopted to model various patients' conditions by considering relaxing, walking, and running states. Last but not the least, extensive simulations are performed to evaluate the performance of the optimized and suboptimal solutions in comparison with the related literature to show the effectiveness of the proposed scheme in maximizing the EE of WBAN.

In Chapter 6, a summary of our investigation and important conclusions regarding the research are drawn by summarising the important findings from each research contribution. It also includes discussion on future research directions in the field of eHealth monitoring WBAN that are expected to be a source of inspiration for future innovations and developments in WBANs.

1.5 List of Publications

I, Osama Amjad, hold a primary author status for all the published manuscript discussed in the chapters (Chapter 3 - 5) of this dissertation. Whereas, my supervisors and co-researchers, are co-authors on each research article, whose time and guidance, careful assessment, and constructive feedback throughout this research have helped improve the technical and presentation quality of the work and development of these publications indicated below.

1. O. Amjad, E. Bedeer, and S. Ikki, "Energy-Efficiency Maximization of Self-Sustained Wireless Body Area Sensor Networks," *IEEE Sensors Letters*, vol. 3, no. 12, pp. 14, Oct. 2019.

2. O. Amjad, E. Bedeer, N. A. Ali, and S. Ikki, "Robust Energy Efficiency Optimization Algorithm for Health Monitoring System with Wireless Body Area Networks," *IEEE Communications Letters*, vol. 24, no. 5, pp. 11421145, Feb. 2020.

3. O. Amjad, E. Bedeer, N. A. Ali, and S. Ikki, "Energy Efficient Resource Allocation for eHealth Monitoring Wireless Body Area Networks with Backscatter Communication," Accepted, *IEEE Sensors Journal*, 2022.

Chapter 2

Wireless Body Area Networks: Background and Preliminaries

2.1 Introduction

The recent evolution and technological advancements in wireless communication and microelectronics have enabled the enhanced research trends towards the development of low-power, inexpensive, miniaturized smart wireless devices that can be implanted underneath the skin or attached to the human body surface as wearables sensors, or integrated with accessories and clothing. This set of bio-medical sensors can be connected to form a network referred to as WBAN that enables advanced continual monitoring applications without disturbing the daily-life activities of the patients. The sole standard available for WBAN is IEEE 802.15.6, which was issued in 2012. IEEE 802.15.6 defines WBAN as a specific form of wireless sensor network (WSN) [27]. IEEE 802.15.6 offers reliable communication over a short distance and a wide range of data rates to serve a variety of applications.

WBANs help enable the SNs to continuously monitor various physiological attributes of the body during stationary or mobility states. The SNs sense the patients' vital information such as heart rate, blood pressure, respiratory measurement, body temperature, pulse rate data, and blood glucose level from the body and translate this information into data packets which are wirelessly transmitted to the central coordinator node known as aggregator/gateway. Most importantly, the information collected by an eHealth monitoring WBAN provides the medical facility and healthcare providers with a clear picture of the patient's status as this data is gathered during a patient's daily-life routine activities in a natural environment [28].

2.1.1 Taxonomy of WBAN Devices

As discussed earlier, a WBAN system consists of miniature devices with communication capabilities to sense the information through various SNs and transmit that information as data packets over wireless channels. Based on their functionalities and roles, these devices can be categorized into three classes. This section details a brief overview of the classification of WBAN devices according to their functionality.

i. **Wireless Sensor Node:** A SN senses the physiological attributes, performs the data processing of the sensed information by using the analog-to-digital converter (ADC), and transmits that in the form of data packets to the aggregator using wireless communication technology. The general architecture of a wireless SN comprises four components as shown in Fig. 2.1: a radio transceiver, storage battery, microprocessor, and the sensor component [29]. When connected to the power supply the SNs are activated to provide wireless monitoring for anybody, anywhere, and anytime. SNs in WBAN are categorized according to their location on the body, as follows

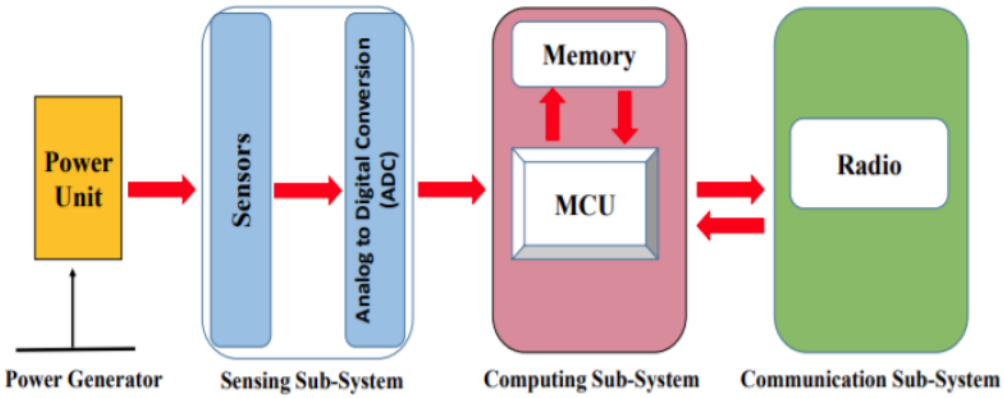

Fig. 2.1: Illustration of different modules of a wireless sensor node [29].

- **Wearable Sensor:** These devices are placed on the body surface or attached to the clothes for gathering vital signs. Some existing varieties of these sensors can be embedded in a smart wristwatch, smartphone, or earphone of the patient, allowing continuous monitoring independent of the patient's location. For example, peripheral oxygen measures the saturation level of oxygen in the human blood. The electrocardiogram (ECG) sensor investigates the functionality of the heart by sampling the heart muscle propagation waveform with respect to time. The electroencephalography (EEG) sensor utilizes the electro-physiological monitoring method to record the electrical activity of the brain. The various types of available sensors for eHealth monitoring WBAN are temperature sensor, motion sensor, blood pressure (BP), blood glucose, pulse rate, motion sensor [2, 4].

  With the advancements in wearable devices, the trend of measuring the BP using the sensors has increased [30,31]. It is due to the fact that measuring a BP using a cuff-based technology is sometimes distressing as it utilizes an inflatable cuff that is wrapped on an arm and pressure is applied to the artery by increasing the pressure on the arm and then gradually releasing the pressure from the

cuff, thus enabling the measurement of the systolic and diastolic BP. Due to the inflation and the deflation, a cuff-based BP measurement takes a few minutes for the arteries to recover fully. As a result, cuff-based BP measurement technology is considered obstructive and unsuitable for wearable-based eHealth monitoring WBANs [32]. There are various studies in the literature regarding the cuffless and wearable technologies to measure the BP using several indirect techniques such as tonometry and pulse transmit time (PTT) methods as discussed in [33, 34]. Due to its ability to track BP change, as well as its benefits as a noninvasive, continuous, and most importantly cuffless instrument for BP measurement, the PTT method has attracted much interest in recent decades. Most industry and academia efforts for cuffless BP monitoring are now focused on PTT to reduce the distress caused due to the cuff inflations. In [31], a cuff-less based BP estimation system is designed that uses only one sensor for photoplethysmography that is expected to provide a wearable device for continuous and stress-free BP monitoring. The studied research evaluates and validates the clinical application of cuffless BP estimation in compliance with the IEEE standard for wearable cuffless BP measuring devices (issued by IEEE to publicize the development of cuffless BP measurement) [35].

- **Implantable Sensor:** These devices are placed beneath the skin surface or even injected into the body tissue or in the bloodstream to access the health parameters. These sensors can constantly assess metabolite levels irrespective of the patient's physiological condition (rest, sleep, etc.) [36]. For example, in Parkinson's disease, these sensors are used to send electrical impulses to the brain through neural simulators [37]. One of the distinguished applications of an implantable sensor in healthcare is the ability of retina prosthesis chips implanted

within a human eye to assist visually impaired or patients with no vision to see at a decent level [36].

ii. **Actuators:** Actuators are used to administer medicine to a patient. The required drug is administered directly in a predefined manner when a sensor detects an abnormality or when it is triggered by an external source, according to the doctors decision. Similar to a SN, an actuator consists of a transceiver, battery, memory, and the actuator hardware that holds and manages the drug. The actuator is activated upon receiving data from the sensors. Its function is to offer network feedback by acting on sensor data such as injecting the right amount of dose to control the blood pressure, body temperature and to treat many other illnesses [38].

iii. **Wireless Personal Device:** A personal device (PD) is responsible for collecting the incoming data information transmitted from the sensors. It is also called a body control unit, gateway/aggregator, or sink [2, 8]. It is the central unit that is responsible for establishing communication between sensors, actuators, and a cellular phone in a wireless fashion. PD can be a specialized dedicated unit, a personal digital assistant (PDA) or a smartphone. A smart cellular phone, for example, can be configured to transmit information to and from the human body to external healthcare providers. This device is usually more resource-rich than the SNs. Its main components are a transceiver, a rich power source, a large processor, and a large memory. It can also provide coordination by sending the device configuration updates or medical alerts from the service provider to the SNs. Unlike the energy-constrained SNs, a PD is usually energy sufficient, and normally it has stable charging access within reach such as a power outlet, or high capacity portable power bank to recharge its battery.

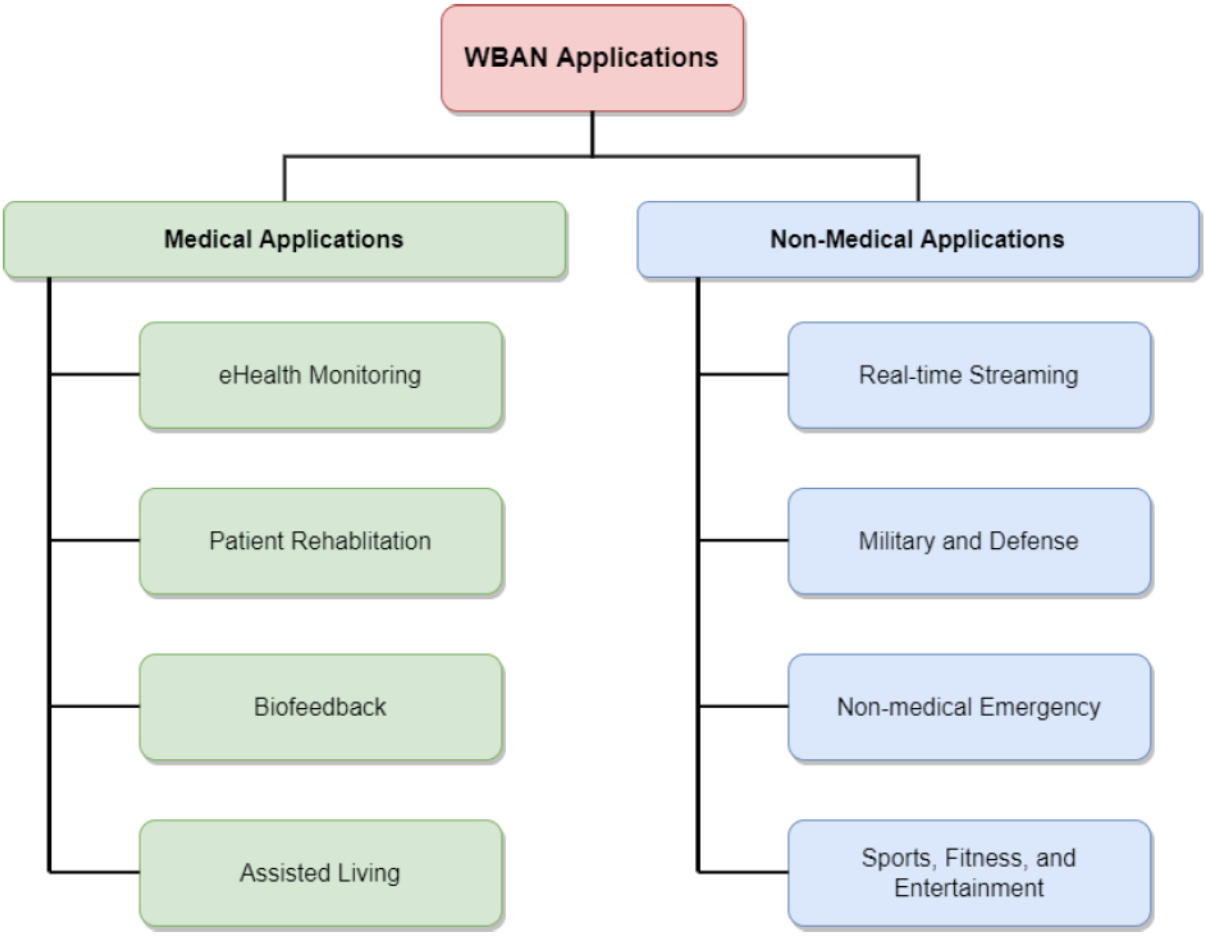

Fig. 2.2: Medical and non-medical applications of WBANs [39].

2.2 Applications of WBANs

In this section, the applications of WBANs are discussed that can help reduce medical expenses and provide enhancement in quality of life. WBANs applications can be mainly classified into medical and non-medical applications. Fig. 2.2 shows some interesting and innovative medical and non-medical applications that WBANs can support. The low power and the low cost of individual SNs are the key factors due to which WBAN applications

span diverse fields including, but not limited to, eHealth monitoring, stress control, patient rehabilitation, tracking records of patient bio-metrics, managing chronic diseases, together with the non-medical applications such as intelligent environmental surveillance, disaster, and emergency management for workers safety in hazardous workplaces (e.g., building workers, firefighters, soldiers, etc.), human activity recognition such as sports, and fitness tracking [39, 40]. The common aspect of all WBAN applications is to improve the user's standard of living.

2.2.1 Electronic Health Monitoring

WBANs have a great potential to revolutionize the future of the healthcare field by identifying several life-threatening disorders and by enabling real-time continuous patient monitoring via eHealth system. Fig. 2.3 illustrates the general architecture of eHealth monitoring system with WBAN [41]. It has two main modules that include a body sensor network (BSN) and an eHealth service provider. BSNs are the type of WSNs that consists of several body SNs and the central coordinator node known as an aggregator. As discussed earlier, the aggregator could be a handheld device such as a smart cell phone. The SNs are deployed on the body surface, or they can be implanted inside the human body [2, 8, 40]. These sensors continuously monitor and collect the patient's required information and send it wirelessly to the aggregator. The aggregator wirelessly transmits the collected data to the base station. Further, the information from the base station is sent to the eHealth service provider over the wired channels for further processing and analysis. eHealth monitoring provides medical facilities at multiple places that may include the patient's home, shopping mall, and the hospital and they will be continuously monitored as far as they are in one of the eHealth locations.

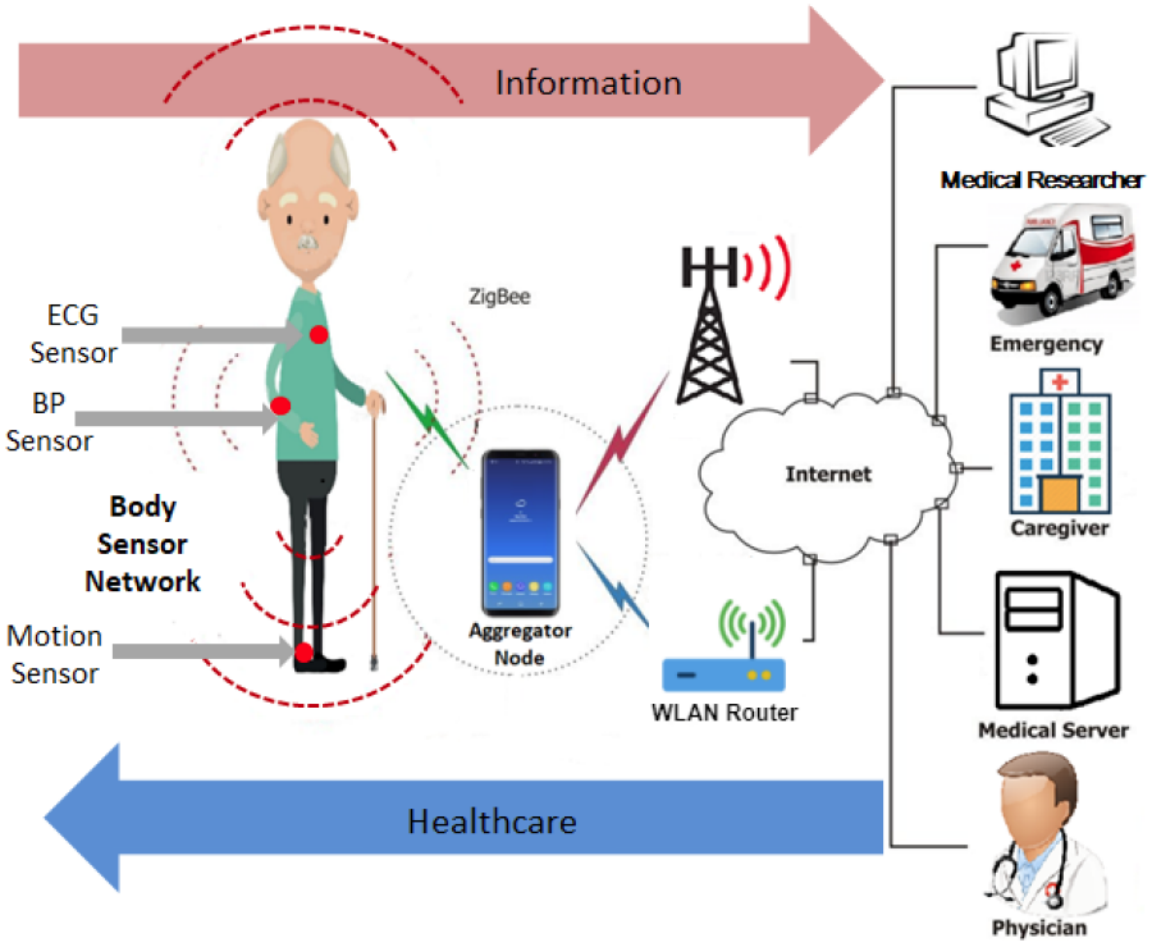

Fig. 2.3: General architecture of an eHealth monitoring system with WBAN [41].

2.2.2 Patient Rehabilitation

WBANs have significant developments in continuous patient monitoring and administering appropriate medication when needed. In this regard, WBANs are also equally useful with high potential in the rehabilitation process of individuals suffering from mobility issues, such as those recuperating from a stroke or traumatic brain injury. They play a significant role in keeping track of a patient's physical activities and exercises in order to:

- Avoid improper exercises
- Update difficulty level of exercises
- Observe recovery
- Compare alternative treatment protocols
- Enable telerehabilitation

The purpose of a WBANs in rehabilitation is typically to capture patients' movements and posture during motor activities. The velocity and acceleration of limbs and joints are traditionally measured using accelerometers, gyroscopes, and magnetometers. Those tools have primarily been employed for gait analysis [40, 42].

2.2.3 Assisted Living

Assisted living facilities have evolved as a viable housing option for elderly with disabilities who are not regarded as independent but do not require round-the-clock medical assistance, such as provided by nursing or retirement centers. As a result, assisted living encourages independence and self-respect in the aging population while also lowering medical expenses. As a result, smart homes have developed as an effective tool for monitoring patients' activities and lifestyles by utilizing a sensor network containing wearable and living space sensors that can sense and regulate the characteristics of the environment before sending body data to a central station. The patient's health can be evaluated based on their heart rate, blood pressure, and environmental data. In an event of significant changes in the measured parameters or deviations from the usual range, the system may be connected to a healthcare facility for surveillance and emergency help [39, 40].

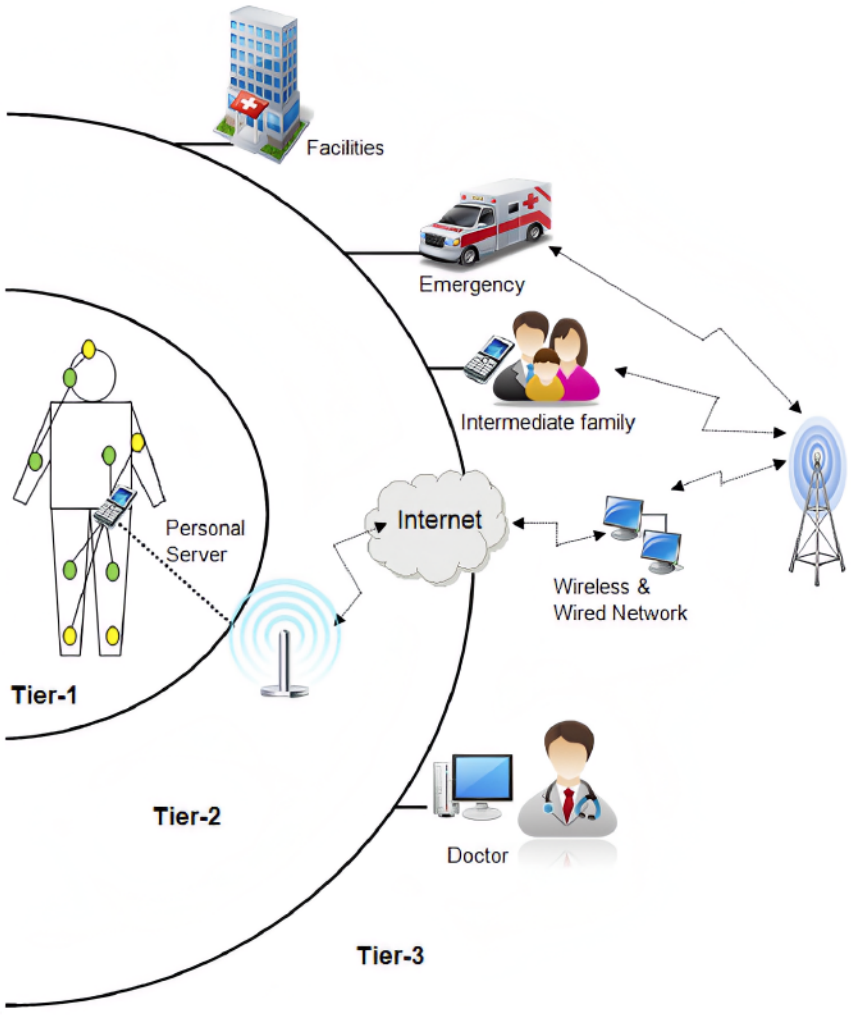

Fig. 2.4: Communication architecture of WBAN with different tiers [2].

2.3 Communication Architecture of WBAN

The communication architecture of WBANs as presented in Fig. 2.4, can be separated into three different tiers as follows

- Tier-1: Intra-WBAN communication

- Tier-2: Inter-WBAN communication
- Tier-3: Beyond-WBAN communication

Fig. 2.4 illustrates the network communication within a WBAN and between the WBAN and among multiple tiers in an efficient, component-based system. The devices are dispersed all over the body in a centralized network architecture where the exact location of a device is application specific. However, due to the random body movements during daily-life activities (e.g. running, walking), the ideal body location of SNs is not always the same; hence, WBANs are not always regarded as being static.

Tier-1: Intra-WBAN communication - Tier-1 depicts the network interaction of SNs and their corresponding transmission ranges ($\sim$ 2 meters) in and around the human body. In Tier-1 communication, different wearable and implantable sensors are used to transmit the vital information from the patient's body to the personal server, also known as the aggregator node, located in Tier-1. The collected physiological data is then processed and wirelessly transmitted to an access point in Tier-2.

Tier-2: Inter-WBAN communication - Tier-2 communication is usually between the aggregator and one or more access points (APs). The APs can be considered as part of the infrastructure or even deliberately placed in a dynamic environment to manage emergency circumstances. Tier-2 communication focuses on connecting WBANs with other networks, including cellular networks and the Internet, that may be conveniently accessed in daily life. The more technologies supported by a WBAN, the easier for them to be integrated within applications.

Tier-3: Beyond-WBAN Communication - This communication tier is intended for use in metropolitan areas. In other words, from the Internet to the healthcare facility in a particular application, a gateway, such as an aggregator can be utilized to bridge

the link between Tier-2 and Tier-3. However, the design of Tier-3 for communication is application-specific. In principle, a database is one of the most crucial elements of Tier-3 in a medical setting because it contains the patient's medical history and profile. As a result, either the Internet or short message service can be used to inform doctors or patients of an emergency situation. Additionally, Tier-3 allows restoring all necessary information of a patient which can be used for their treatment.

2.4 Energy Harvesting in WBANs

Energy harvesting is a promising alternative that has gained significant attention in the communication solutions in WBANs by allowing the energy-constrained SNs to harvest energy and perform the required operations [16]. In eHealth monitoring solutions, the energy harvesting technology is considered a feasible solution for increasing the operational time of the network or may even replace the battery of SNs with a continuous energy supply. In eHealth monitoring, energy harvesting can enable the real-time monitoring of various vital parameters of the patients, resulting in a self-sustainable system [17].

Energy can be harvested from a variety of different types of energy sources available in the surrounding environment and converting it to usable electrical form. However, the availability of a specific energy source may vary depending on the patient's body state and surrounding environment, or the battery capacity, location, or function of a particular SN. Even though it is not a novel concept, knowing that it has been deployed on a vast scale around the world, its application in small devices such as SNs is an emerging topic in academics and industry. Along with minimizing the network expenses, it reduces the electrical waste in the form of drained or dead batteries, thus promoting the concept of green energy supply as well. Moreover, recent technological advancements have also made

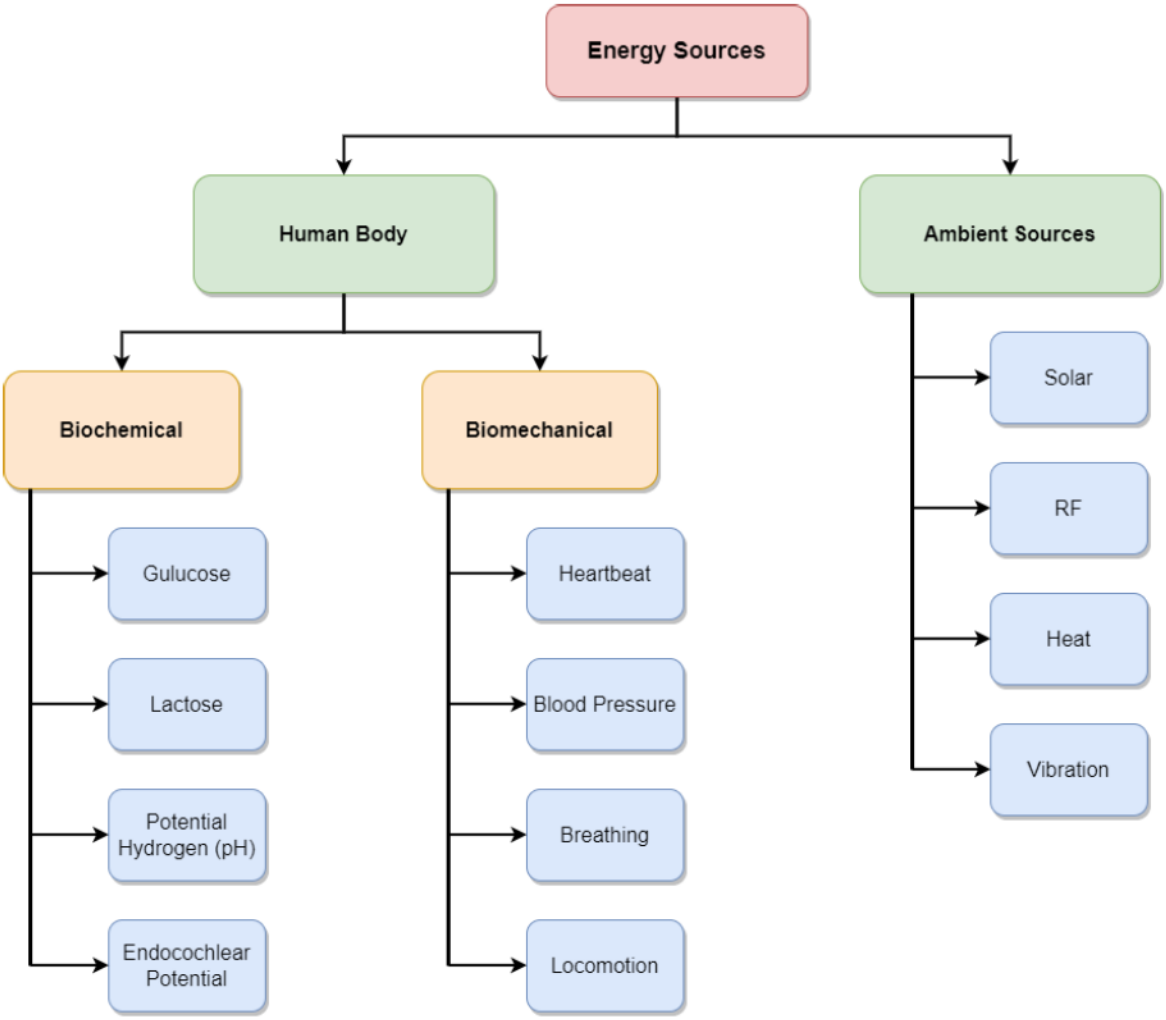

Fig. 2.5: Classification of energy sources available for energy harvesting in WBANs [15].

it possible to harvest energy from a variety of sources present within the human body, which was previously unimaginable [15]. WBANs can harvest energy from a range of ambient sources available in the surrounding environment and human body, as summarized in Fig. 2.5. In this section, a brief overview of two main categories of energy sources, i.e., ambient and human body sources available for harvesting energy in WBANs are discussed.

2.4.1 Energy Harvesting from the Human Body

In the human body, there are plenty of energy sources that can be exploited to power both in/on-body SNs. Based on the type of energy, the energy sources available in the human body can be categorized into biomechanical and biochemical energy sources. The former source is mobility dependent and based on the voluntary and involuntary movement of the human body, which can be converted into electrical energy. The latter deals with harvesting energy from the electrochemical reactions inside the human body that generate energy and can be utilized for the purpose of harvesting energy.

i. **Biochemical Energy Sources:** Inside the human body, biofluids include a wide range of chemicals and active enzymes that supply energy to the body. Biofuel is the key enabler technology for harvesting energy that relies on converting chemical energy into electrical energy from the chemical compounds by using electrochemical processes under appropriate conditions [43]. The scavenged energy can be used to power low-power SNs embedded inside the body. The amount of harvestable chemicals in the body fluctuates with age and is mostly determined by an individual's health and daily food and nutrition intake. In general, these sources can be harvested whenever necessary, as long as the body has an adequate quantity of potential chemicals.

   As an example, among the different chemical substances that the body extracts from dietary substances, glucose is among the most common sources of energy. By utilizing an implantable enzymatic biofuel cell that helps to digest glucose into acid and releases electrons, which can be subsequently used to generate electrical energy. Lactate is another chemical found in high concentrations in human saliva or sweat. A noninvasive tattoo-based biofuel cell design that can be externally positioned on a human body can also be used to harvest energy [44].

ii. **Biomechanical Energy Sources:** Another type of source associated with the human body is biomechanical energy which exists in the form of kinetic energy obtained through various internal and external movements of the human body. These body movements can be involuntary and voluntary activities. The involuntary movements refer to the body's continual actions, such as breathing, heartbeat, blood pressure, and other muscular movements, irrespective of a human's desire. Whereas walking, exercising, and other similar activities connected corresponding to physical movements are examples of voluntary movements [45].

The human body movements account for a large portion of biomechanical sources, which include footsteps, knee movement, and arm motion. Various piezoelectric and mechanical generators can be used to harvest energy from these sources. Foot taps during walking can generate a significant quantity of energy, which can be scavenged by employing piezoelectric polymers in the shoe sole. The energy produced can be utilized to power biometric sensors. In addition, considerable amounts of vibrations occur at the knee during movements that generate kinetic energy, which can also be used to scavenge energy [15, 46].

2.4.2 Energy Harvesting from Ambient Sources

Energy can also be harvested from various ambient sources, such as RF radiation, thermal, and solar. These sources can generate a considerable amount of energy, which, if utilized effectively, can power a variety of embedded and wearable devices.

Light is the most dominant of these ambient sources, and it may be scavenged in both outdoor environments from the natural sunlight and indoor settings from artificial light sources. In outdoor locations, the amount of energy harvested from sunshine varies greatly

depending on the time of day, region, and environmental circumstances, but successful solar harvesting can result in a full day or several days of operational time. However, indoor artificial light does not have the same intensity as natural sunshine; thus, it can only generate a small amount of energy [42]. Similarly, the human body continuously dissipates a reasonable amount of heat throughout the day. This heat is a reliable source of thermal energy that can be harvested by using the thermoelectric transducer to charge wearable devices [47].

With the explosive increase in the growing wireless devices, RF radiations available in the surrounding environment have also increased significantly. Consequently, Wi-Fi routers, cellular and radio towers, and TV broadcasting towers utilize the electromagnetic spectrum, in particular, RF radiations for data communication [15]. These signals can be captured by utilizing a rectifying antenna which is a specific type of efficient antenna connected to special hardware known as an energy harvester. This rectifying antenna converts the received radiations into usable DC electrical energy [48]. However, one of the drawbacks is that the amount of harvested energy is dependent on the distance between the transmitter and the receiver device. Even though there may be a lot of electromagnetic radiation available for harvesting nearby a transmitting source, as it radiates and spreads farther out, the amount of energy available for harvesting also decreases. Therefore, by taking the distance into consideration, this method of harvesting energy can provide a promising solution for lower-power devices in eHealth monitoring WBANs. In addition, dedicated RF sources include specially designed and configured transmitters that emit radio waves and act as a reliable source of transmitting energy signals, e.g., TX91501b powercaster transmitter [49].

2.5 Backscatter Communication in eHealth Systems

BackCom has emerged as an evolving paradigm that serves as a communication technology for the next-generation wireless networks such as eHealth monitoring WBANs [19]. BackCom can provide nearly limitless chances to connect wireless devices due to this revolutionary way of communication by reflecting and modulating the incident signal. BackCom is considered a key enabler to tackle the issue of limited battery capacities in wireless devices, therefore can be utilized to enable pervasive connectivity in a variety of applications, including wearable devices, smart connected homes, industrial IoT, and small embedded devices.

As illustrated in Fig. 2.6, a basic BackCom system consists of two components: a Tag, which is a mobile backscatter node, and a Reader [50]. The Tag is a passive device that harvests energy from a sinusoidal continuous wave (CW) emitted by the Reader and modulates and reflects the incident signal back to the Reader. The signal reflection is caused by an intended impedance mismatch between the antenna and the load impedance. The reflection coefficient varies as the load impedance varies, followed by a random sequence that modulates the reflected signal with Tag's data information bits. This modulation scheme is known as backscatter modulation. In BackCom, the Reader transmits a binary intensity modulated signal to the Tag. The Tag connects its information decoder and utilizes the received RF signal for RF energy harvesting and energy-detection based demodulation. The decoding mechanism is used for ultra-low power designs that allow the receiver to decode the data information with high efficiency by only utilizing an average envelope detector and a threshold computation circuit. Firstly, the envelope detector smoothes/averages out the variations of the received signals, and then based on the two signal levels produced at the output, a threshold value is calculated. Finally, the comparison circuit consisting of

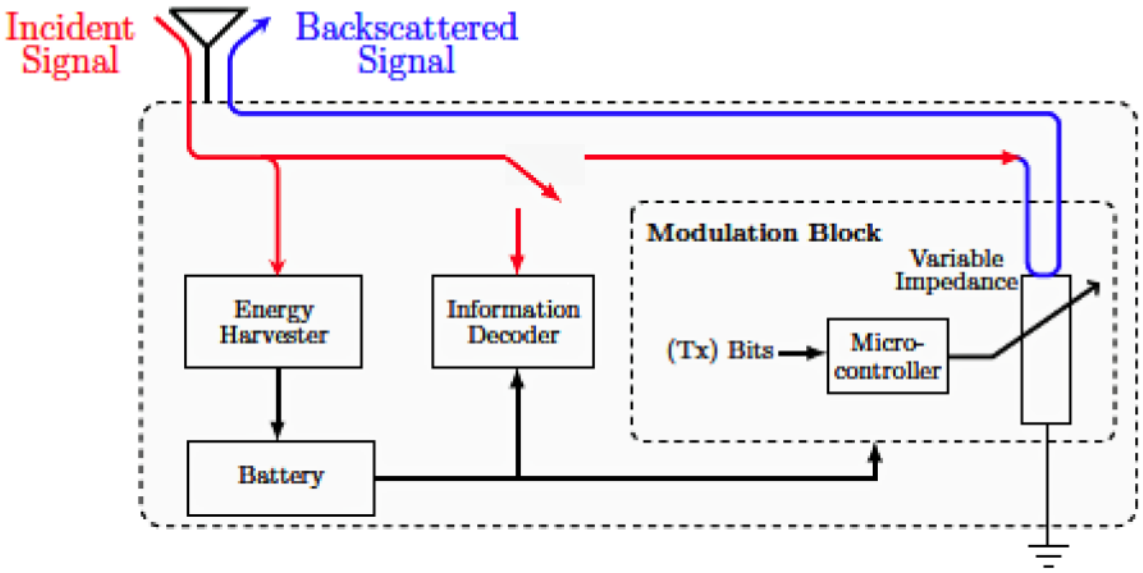

Fig. 2.6: A general architecture of a backscatter tag [50].

an resistor/capacitor (RC) circuit and a comparator compares the average envelope signal and the threshold to distinguish between the output bits.

In contrast to a conventional radio architecture that requires a chain of power-hungry modules, a backscatter node does not comprise any active RF components, therefore, can be deployed to have miniature hardware with exceptionally low power consumption [20]. Furthermore, BackCom is envisioned to revolutionize the healthcare facilities supplied through embedded microelectronics and wearable devices by efficiently transmitting the data under a low-power budget. Therefore the potential benefits of BackCom are considered to have a considerable impact on how doctors and patients engage with wireless devices. Consequently, this technology can help enable customized self-managing and self-monitoring eHealth systems [21].

Chapter 3

Energy Efficiency Maximization of Self-Sustained Wireless Body Area Sensor Networks

3.1 Introduction

eHealth monitoring system with WBANs helps integrate the patient's data processing and communications technologies into traditional medical facilities and serves as a promising approach to boost healthcare efficiency. In a WBAN, the SNs monitor the patient's vital signs and send the data wirelessly to the aggregator. These SNs are conventionally powered by batteries, which are needed to be replaced once the energy is consumed. Moreover, battery replacement is not preferable sometimes, and it becomes highly impractical and infeasible in the case of implanted SNs. Therefore, wireless energy harvesting serves as an alternative approach that enables self-sustained SNs operations by scavenging energy from

various biomechanical, biochemical, and ambient sources (e.g., thermal, electromagnetic radiations) [15]. Nevertheless, the harvested energy necessitates appropriate energy management techniques such as EE maximization, which focuses on conserving WBAN energy given available resources while maintaining a satisfactory network performance level in terms of data transmission.

3.1.1 Related Work

As discussed earlier, in order to realize an efficient eHealth system in real-life healthcare environments, improving the lifetime of energy-constrained SNs or EE is of paramount importance. EE is one of the important design objectives that have a significant effect on the performance of an eHealth system. However, such a crucial design objective has not been thoroughly investigated for different eHealth systems. More specifically, in [51], an efficient power QoS control scheme for WBAN is proposed in which the SNs are powered by human body energy harvesting. The proposed algorithm utilizes the concept of an energy neutral operation (ENO) based power management to prolong the network lifetime and achieve continuous operation as long as there are no faults in the system hardware. In other words, a SN that utilizes energy harvesting is said to be in the ENO state if its power consumption is less or equal to the energy scavenged from the surrounding environment. In this regard, the proposed ENO inspired algorithm focuses on achieving the best possible QoS by efficiently transmitting the data packets under different human activities and ensuring that the SNs can detect any medical condition by considering various human body movements.

In [52], stochastic modeling of wirelessly powered wearables is proposed that provides an analytical framework for the SNs' ability to notify the medical staff about the patient's

condition promptly by deriving the probability of correct notification in a cluster-based hospital environment. More practically, in order to be approved by the medical community such as to be widely adopted in real-life healthcare facilities, wearables must have a perpetual lifetime and reliable data communication. In these situations, it is critical to understand the likelihood of accurate notification, which is primarily affected by the deployment of wireless wearables and their power source. Since the hospital rooms frequently house numerous patients, therefore in order to obtain more reliable results, a cluster-based communication model is adopted in which there are multiple clusters with each containing multiple patients distributed around the cluster head/gateway according to the Poisson cluster process.

In [13], a MAC layer protocol for health monitoring WBAN is proposed that utilizes the carrier-sense multiple access with collision avoidance (CSMA/CA) and time division multiple access (TDMA) hybrid schemes to extend the lifetime and EE of SNs suffering from the energy shortage challenge. In the proposed protocol, the concept of awaiting orders (AO) is proposed that refers to a specific type of idle state in which a SN's synchronous clock keeps working, whereas all other operations are stopped to help save energy. Anytime a SN needs to transmit or receive data information, it can promptly switch to the active state from an AO state. In addition, the transmission overhead in the proposed protocol is put on the aggregator's side to save the energy of SNs. Simulation results in comparison with the related literature show that the proposed MAC protocol consumes less energy.

In [53], a MAC protocol for WBAN is proposed that deals with the two important challenges associated with the WBANs, i.e., to maintain a satisfactory QoS and ensure the EE of energy-constrained system. In this regard, a TDMA based MAC protocol is proposed that ensures to tackle these challenges in the power-constrained network by dynamically adjusting the transmission order and by optimizing the transmission slot such as the en-

ergy consumption of the SNs is minimized. Simulation results show that in comparison with the related literature, the proposed scheme is energy-efficient in terms of less power consumption.

The cooperative energy harvesting-adaptive MAC protocol proposed in [23] improves the WBAN performance in terms of delay, EE, and throughput by changing its operation based on the energy harvesting conditions. In [54], a point-to-point communication system is studied for a WBAN consisting of SNs that can harvest energy from radio signals. In the proposed system, power splitting and power switching protocols are considered for normal and abnormal situations, respectively, and the corresponding power spilling and time switching ratios are derived for each protocol. The goal of this study is to maximize the information throughput in uplink from the SNs to the access point by optimizing the time in the command transfer/ energy harvesting phase and information transfer phase while considering the energy constraint.

In [8], the authors investigated two important challenges associated with WBANs, i.e., the need for sustainable energy supply for the SNs and the QoS guarantee of the data. Resource allocation optimization is used to provide high quality and sustainable health monitoring system by formulating and solving two resource allocation optimization problems. In the first problem, named as a steady-rate optimization problem, the source rate of each SN is optimized to minimize the source rate fluctuations with reference to the average sustainable source rate, while considering the power budget constraints. The energy harvesting process of a SN is modeled using the discrete-time Markov chain and the theoretical relationship between the source rate and the uninterrupted lifetime of a SN is analyzed. Based on the optimal source rates obtained from the steady-rate problem, the second optimization problem called as QoS optimization problem is formulated. In this problem, the transmission power and the transmission rate are optimized jointly for

each SN to ensure a QoS guarantee of the data transmission. Simulation results show that optimal resource allocation of transmit power and transmission rate can improve the performance of the eHealth monitoring system in terms of sustainability and guarantee satisfactory QoS.

3.1.2 Contributions

Compared to the existing work discussed above, in this chapter, an energy-efficient optimization problem is formulated and solved that focuses on maximizing the EE of energy-constrained WBAN by using optimization techniques. The linear fractional EE objective function is defined as a ratio of the sum of the source rate of all the SNs in the network to the total power consumption of WBAN. In a WBAN system model, the SNs are considered to be equipped with energy harvesting capabilities that allows them to harvest energy, whereas the corresponding energy harvesting process is modeled using a discrete-time Markov chain. To facilitate obtaining the solution, the Charnes-Cooper transformation is used to convert the defined linear fractional EE optimization problem to an equivalent linear form. More precisely, the goal of the optimization problem is to maximize the overall EE of the self-sustaining eHealth monitoring WBAN by optimally assigning the source rate to each SN, such that the overall EE of the WBAN system is maximized. Furthermore, the structure of the optimization problem is investigated in order to propose a suboptimal solution with lower computational complexity, and to obtain the mathematical expressions of the SN's upper and lower bounds of the source rates. Extensive simulations are performed to assess the performance, revealing that allocating the source rate optimally to energy-constrained SNs enhances WBAN's system performance in terms of EE under various body movements/activities of the patients during daily life.

3.2 System Model

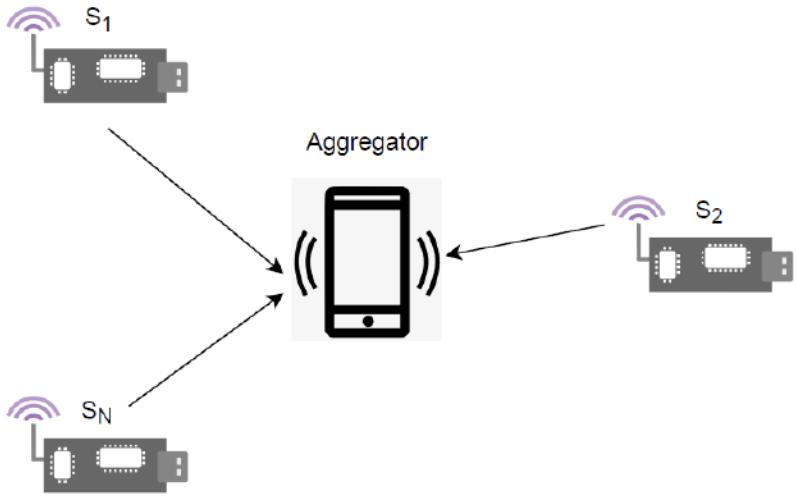

Fig. 3.1: WBAN system model.

We consider a WBAN with one aggregator carried by the patient which acts as the gateway as shown in Fig. 3.1. There are N SNs in the network deployed on the patient's body in a star topology such that each node directly communicates with the aggregator. The aggregator is assumed to be connected with a reliable energy source, whereas the SNs are energy-constrained and are supposed to have a rechargeable battery that can harvest energy from biochemical and biomechanical energy sources available in the human body. In WBAN, each SN inquires a dedicated guaranteed time slot from the aggregator, during which it periodically transmits its data using the standard TDMA scheme [13].

3.2.1 Energy Harvesting Model

In WBAN, energy can be harvested from the human body that includes biochemical energy, thermal energy, and biomechanical energy generated by the motion, and the movement of limbs of the human body [16]. The amount of available energy depends on the size and

efficiency of the energy harvesting device, as well as the availability of energy sources. In recent years energy harvesting from the human body has been a topic of great interest for energizing the wearable and implantable SNs due to their almost ubiquitous availability.

The available power density from human body energy harvesting can provide a considerable amount of energy that can potentially operate the low power SNs [47, 55]. Due to the universal availability of energy, many studies in the literature model the energy harvesting process by utilizing the energy sources available in the human body as described in [8, 56]. Therefore in this work, we model the energy harvesting process in which the SNs are assumed to be compatible with harvesting energy available in the human body.

The energy harvesting of a SN is a random process and it depends on the type of energy harvesting technology used and the state of the subscriber. In the case of energy harvesting from the human body, the state/posture of the subscriber, the motion during daily activities, and the environmental conditions are time-varying, due to which the energy recharging rate is time-varying. Therefore, the energy harvesting rate of each SN is also varying during different positions (e.g., relaxing, walking, running). However, in each time slot, based on the state of the patient, the SN i can harvest different amounts of energy that follows a uniform distribution in a range of $[E_i^{\min}, E_i^{\max}]$, denoting the minimum energy level required to be maintained and the maximum battery capacity of SN i, respectively [56].

The energy harvesting process in this work is modeled by adopting the discrete-time Markov chain model in [8]. Since the source rate and the energy recharging rate during each time slot remains constant, the energy harvesting process at SN i can be modeled as a discrete-time Markov chain [8, 51] represented as $\{\mathbf{A}_i, \mathbf{P}_i\}$, where $\mathbf{A}_i$ is the set of states in the Markov chain model, and $\mathbf{P}_i$ is the transition probability matrix. The energy recharging rate at state m ($m \in \mathbf{A}_i$) is expressed as $g_i^{(m)}$. Fig. 3.2 shows the two-state Markov chain with transition probabilities P_{10}, and P_{01} from state S_1 to S_2, and from state S_2 to S_1,

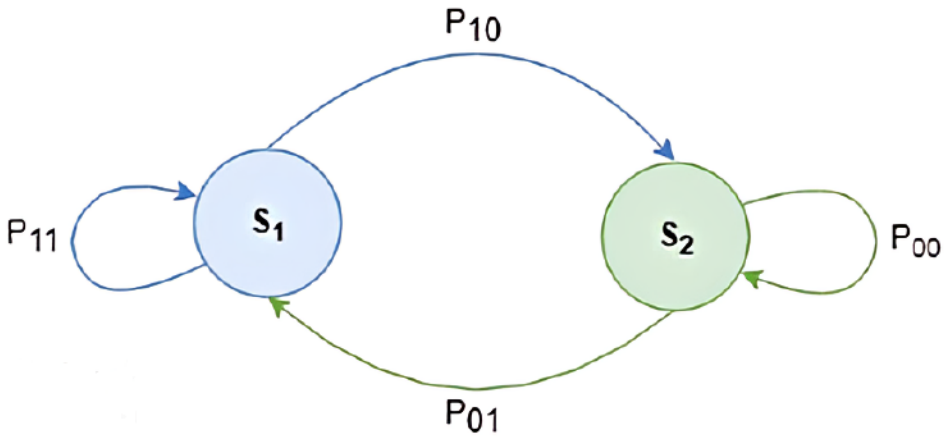

Fig. 3.2: Two state discrete Markov chain of energy harvesting process.

respectively. The states in $\mathbf{A}_i$ are arranged in an increasing order as $g_i^{(1)} \leq g_i^{(2)} \cdots \leq g_i^{|\mathbf{A}_i|}$, where $|\mathbf{A}_i|$ is the cardinality of $\mathbf{A}_i$ and represents the number of the states in $\mathbf{A}_i$. Let $\mathbf{\Pi}_i$ be the steady-probability vector at SN i, that can be calculated as follows: $\mathbf{\Pi}_i^T \mathbf{P}_i = \mathbf{\Pi}_i^T$, and $\mathbf{\Pi}_i^T \mathbf{I} = 1$, where $\mathbf{I}$ is the identity vector with all entries equal to 1. The long-term average recharging rate of SN i is then written as $g_i^{avg} = \mathbf{\Pi}_i^T \mathbf{g}_i$, where $\mathbf{g}_i$ is the vector of the recharging rates at SN i.

3.2.2 Power Consumption Model

In WBAN, the power consumption of a SN depends on: sensing power consumption and transmission power consumption. The SNs monitor and capture the patient's vital information/readings and translate these readings to data packets and send them wirelessly to the aggregator. The sensing power consumption is the energy consumed by the SN during its sensing operation. If a SN senses more readings/sec, the sensing power consumption will be higher, and it will have a higher amount of data to be sent to the aggregator and vice-versa. Therefore the sensing power consumption at a SN i is proportional to the source

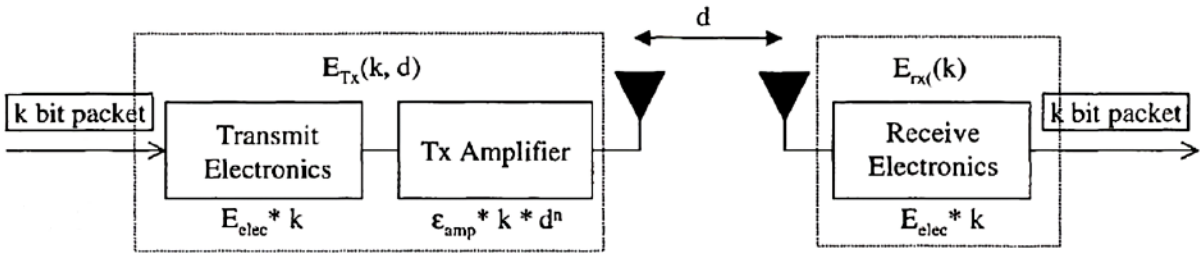

Fig. 3.3: Radio energy dissipation model [57].

rate r_i modeled as: $P_{s,i} = \psi_i r_i$, where ψ_i is the energy cost of sensing at SN i [8].

In an eHealth system, most of the wearable devices and SNs are fastened to the human body; therefore communication between the SNs and the aggregator occurs along the surface of the human body, which contributes towards the attenuation of the transmitted radio signal. Furthermore, the random body movements of the subscriber cause changes in the distance and the direction of the SN to the aggregator that results in the change of path loss and ultimately attenuates the transmission power consumption $P_{t,i}$.

According to the radio energy dissipation model [57] as shown in Fig. 3.3, the transmitter depletes the energy to operate the radio electronics and the transmit amplifier of the SN, and on the receiving end, the receiver consumes the energy to operate the radio electronics. The signal power attenuates as the signal propagates a certain distance d from the SN to the aggregator. Therefore, the power control can be utilized to invert this propagation loss by adjusting the power amplifier such as to guarantee a certain power at the receiver/aggregator. Thus, the energy consumption model to transmit and receive k-bits data over a distance d can be given as follows [57]

$$\begin{aligned} E_{TX}(k, d, m_p) &= kE_{Tx-elec} + kE_{Tx-amp}d^{m_p}, \\ E_{RX}(k) &= kE_{Rx-elec} \end{aligned} \tag{3.1}$$

where $E_{Tx-elec}$ and $E_{Rx-elec}$ are the energy consumption costs dissipated by the radio to run the circuitry for the transmit and receive electronics, respectively. E_{Tx-amp} is the energy cost of transmit amplifier (in J/b/m^{m_p}), and m_p is the path loss exponent. As discussed, the power amplifier can be adjusted to control the propagation loss between the transmitter and the receiver, therefore we are only interested in the transmit amplifier term to determine the required transmit power as a function of receiver threshold and the distance between the SN and the aggregator. Thus, in terms of transmit power consumption, (3.1) can be written as follows

$$P_t = E_{Tx-amp} R_b d^{m_p}, \tag{3.2}$$

where P_t is the transmitted power consumption equal to the transmit energy per bit, and R_b is the bit-rate of the radio. According to the Friis free space equation, the received power P_r is given as follows

$$P_r = \frac{E_{Tx-amp} R_b G_t G_r \lambda^2}{(4\pi)^2}. \tag{3.3}$$

Since we have to adjust the P_t such that the received power at the aggregator is above a specific threshold $P_{r-thresh}$. Therefore the parameter E_{Tx-amp} can be found by setting (3.3) equal to $P_{r-thresh}$ written as follows

$$E_{Tx-amp} = \frac{P_{r-thresh}(4\pi)^2}{R_b G_t G_r \lambda^2}, \tag{3.4}$$

where G_t and G_r are the transmitting and receiving antenna gains, respectively. λ represents the wavelength. By using the value of E_{Tx-amp} from (3.4) the transmit power P_t can be found from (3.2) as follows

$$P_t = \frac{P_{r-thresh}(4\pi)^2 d^{m_p}}{G_t G_r \lambda^2}, \tag{3.5}$$

Finally, the required transmitted power consumption P_t, as a function of receiver threshold and the distance between the SN and the aggregator can be written as

$$P_t = \Upsilon P_{r-thresh} d^{m_p}. \tag{3.6}$$

where $\Upsilon = \frac{(4\pi)^2}{G_t G_r \lambda^2}$. Therefore, according to the radio energy model in [57], to guarantee a certain minimum received power at the aggregator, $P_{t,i}$ takes $d_i^{m_p}$ as a path loss and the energy cost due to a channel variation in respect with distance d_i between SN i and the aggregator, and thus makes the received power independent of $d_i^{m_p}$. The transmission power consumption depends on the path loss model of the wireless channels in WBAN as illustrated in [8]

$$PL(d_i) = PL(d_o) + 10\, m_p \log_{10}\left(\frac{d_i}{d_o}\right) + X_\sigma, \quad \forall i \in N, \tag{3.7}$$

where $PL(d_o)$ is the path loss at reference distance d_o, m_p is the path loss exponent. The transmission power consumption at SN i can be modeled as $P_{t,i} = 10^{\frac{X_\sigma}{10}} \beta_i r_i + \theta_i$, where θ_i is the constant energy cost of transmit electronics of SN i, β_i is the transmission energy consumption cost of SN i given by $\beta_i = \zeta_i d_i^{m_p}$, and ζ_i is a coefficient term associated with the energy cost of transmit amplifier. X_σ is the Gaussian random variable that represents shadowing, and denoted as $\mathcal{N}(0, \sigma_s^2)$. The standard deviation σ_s depicts the different postures of the body such as relaxing, walking or running [58]. The total power consumption at SN i is the sum of $P_{s,i}$ and $P_{t,i}$ given as

$$\begin{aligned} P_i &= P_{s,i} + P_{t,i} = \psi_i r_i + 10^{\frac{X_\sigma}{10}} \beta_i r_i + \theta_i, \\ &= (\psi_i + 10^{\frac{X_\sigma}{10}} \zeta_i d_i^{m_p}) r_i + \theta_i, \quad \forall i \in \{1, \ldots, N\}. \end{aligned} \tag{3.8}$$

3.3 Energy Efficiency Optimization Problem

In this section, we propose and solve an optimization problem to maximize the EE of the WBAN subject to energy harvesting constraints. Furthermore, the structure of the optimization problem is analyzed to propose a suboptimal solution at a significantly lower computational complexity.

3.3.1 Problem Formulation and Optimal Solution

The proposed optimization problem aims to maximize the EE of the WBAN, consisting of SNs equipped with energy harvesting capabilities. The EE objective function is defined as the ratio of the sum of source rate of all the SNs to the power consumption of all the SNs in the network. Mathematically the problem can be formulated as follows

$$
\begin{aligned}
\underset{r_i}{\text{maximize}} \quad & \frac{\sum_{i=1}^{N} r_i^{(t)}}{\sum_{i=1}^{N} P_i^{(t)}} \\
\text{subject to} \quad & C_1: \quad P_i^{(t)} = (\psi_i + 10^{\frac{X_\sigma}{10}} \zeta_i d_i^{m_p}) r_i^{(t)} + \theta_i, \qquad \forall i, \\
& C_2: \quad E_i^{(t+1)} = E_i^{(t)} + \tau \phi_i^{(t)} - \tau P_i^{(t)} - F_i^{(t)}, \\
& C_3: \quad E_i^{\min} \leq E_i^{(t+1)} \leq E_i^{\max}, \qquad \forall i, \\
& C_4: \quad r_i^{(t)} \geq 0, \qquad \forall i.
\end{aligned} \tag{3.9}
$$

In problem (3.9), the constraint $\mathcal{C}_1$ represents the total power consumption at SN i during time slot t. $\mathcal{C}_2$ represents the energy at the beginning of time slot $(t+1)$, $E_i^{(t)}$ is the energy of SN i at the beginning of time slot t, the length of the time slot is τ, and $\phi_i^{(t)}$ is the energy recharging rate of SN i at time slot t. $F_i^{(t)}$ is the amount of energy wasted

by SN i during time slot t due to battery overflow. $\mathcal{C}_3$ shows that the energy at time slot $(t+1)$ must not be less than the minimum energy level $E_i^{\min}$ required to be maintained at SN i and should not be larger than the maximum battery capacity $E_i^{\max}$ of SN i.

3.3.2 Linear Fractional Programming

The optimization problem in (3.9) is in linear fractional form and a problem of optimizing such a ratio of affine functions is known as linear fractional programming (LFP). A LFP problem can be transformed into an equivalent linear program (LP) with the help of a Charnes-Cooper transformation [59]. A LP can be viewed as a special case of the LFP problem, in which the objective function is transformed from the ratio of two linear functions to an equivalent linear function in which the denominator is a constant function equal to one. The standard LFP problem can be written as follows

$$f_o(\vec{r}) = \frac{\vec{x}^T\vec{r} + d}{\vec{e}^T\vec{r} + f}, \tag{3.10}$$

From the standard LFP problem defined in (3.10), the EE objective function in (3.9) can be written in standard linear fractional form as follows

$$f_o(\vec{r}) = \frac{\vec{x}^T\vec{r}}{\vec{e}^T\vec{r} + f}, \tag{3.11}$$

where $\vec{r}$ is a $n \times 1$ vector that contains the source rate of each sensor given as $\vec{r} = \left[r_1^{(t)}\ r_2^{(t)} \cdots\ r_n^{(t)}\right]^T$, and the coefficients of objective function $\vec{x}$ is a $n \times 1$ vector of ones such as $\vec{x} = \left[1\ 1\ \cdots\ 1\right]^T$. Similarly $\vec{e}$ is a $n \times 1$ vector written as follows $\vec{e} = \left[\lambda_1\ \lambda_2\ \cdots\ \lambda_n\right]^T$, where, $\lambda_j = \psi_j + 10^{\frac{X_\sigma}{10}}\zeta_j d^{m_p}$. The sum of the energy cost of transmit electronics of the N sensors in the network can be expressed as $f = \theta_1 + \theta_2 + \ldots + \theta_N$ and $d = 0$ in our case.

3.3.3 Transforming to a Linear Program

From equation (3.11), it can be seen that the EE optimization problem can be written as a standard LFP problem. Now, in order to apply the Charnes-Cooper transformation to the EE objective function in (3.11), multiply both the numerator and the denominator of the objective function by a positive constant value α such that the objective function value does not change.

That said, the EE objective function in (3.11) can be re-written as a standard linear-fractional optimization problem as

$$f_o(\vec{z}) = \frac{\vec{x}^T \vec{z}}{\vec{e}^T \vec{z} + f\alpha}, \tag{3.12}$$

where $\vec{z} = \vec{r}\alpha$, and the value of α can be selected such that the denominator of the objective function in (3.12) is equal to one, i.e., $\vec{e}^T \vec{z} + f\alpha = 1$. In order to show the equivalence, it can be noted that if $\vec{r}$ is feasible in (3.11), then $\vec{z}$ is feasible in (3.12), with the denominator function equal to one and with the same objective function value equal to $f_o(\vec{z}) = \vec{x}^T \vec{z}$. The equivalent LP of the (3.9) can be written as follows

$$\begin{aligned}
\underset{\alpha,\vec{z}}{\text{maximize}} \quad & \vec{x}^T \vec{z} \\
\text{subject to} \quad & \mathcal{C}_1: \ \alpha P_i^{(t)} = (\psi_i + 10^{\frac{X_\sigma}{10}} \zeta_i d_i^{m_p}) z_i + \alpha \theta_i, \qquad \forall i, \\
& \mathcal{C}_2: \ E_i^{(t+1)} = E_i^{(t)} + \tau \phi_i^{(t)} - \tau P_i^{(t)} - F_i^{(t)}, \\
& \mathcal{C}_3: \ E_i^{\min} \leq E_i^{(t+1)} \leq E_i^{\max}, \qquad \forall i, \\
& \mathcal{C}_4: \ \vec{e}^T \vec{z} + f\alpha = 1, \\
& \mathcal{C}_5: \ z_i \geq 0, \qquad \forall i, \\
& \mathcal{C}_6: \ \alpha > 0.
\end{aligned} \tag{3.13}$$

It can be noted, that the EE optimization problem defined in (3.13) has a linear objective function with a set of linear equations and inequalities, and an additional equality constraint $\mathcal{C}_4$ has been added as a constraint after applying the LP transformation.

The constraints can be further simplified by substituting the constraint $\mathcal{C}_1$ and $\mathcal{C}_2$ in $\mathcal{C}_3$ of the problem (3.13), the resultant EE optimization problem can be written as follows

$$\begin{aligned}
&\underset{\alpha,\vec{z}}{\text{maximize}}\ \vec{x}^T\vec{z} \\
&\text{subject to}\ \ \mathcal{C}_1:\ \alpha E_i^{\min} \leq \alpha E_i^{(t)} - \tau[(\psi_i + 10^{\frac{X_\sigma}{10}}\zeta_i d_i^{m_p})z_i + \alpha\theta_i] \\
&\qquad\qquad + \alpha\tau\phi_i^{(t)} - \alpha F_i^{(t)} \leq \alpha E_i^{\max}, \qquad \forall i, \\
&\qquad\quad \mathcal{C}_2:\ \vec{e}^T\vec{z} + f\alpha = 1, \\
&\qquad\quad \mathcal{C}_3:\ z_i \geq 0, \qquad \forall i, \\
&\qquad\quad \mathcal{C}_4:\ \alpha > 0.
\end{aligned} \tag{3.14}$$

Further, simplifying the compound inequality constraint $\mathcal{C}_1$ in (3.14), the EE optimization problem with the linear objective function, and the simplified set of constraints with decision variables $\vec{z}$ and α can be written as follows

$$\begin{aligned}
&\underset{\alpha,\vec{z}}{\text{maximize}}\ \ \vec{x}^T\vec{z}, \\
&\text{subject to}\ \ \mathcal{C}_1:\ \tau(\psi_i + 10^{\frac{X_\sigma}{10}}\zeta_i d_i^{m_p})z_i + (E_i^{\min} + F_i^{(t)} + \tau\theta_i - E_i^{(t)} - \tau\phi_i^{(t)})\alpha \leq 0, \\
&\qquad\quad \mathcal{C}_2:\ -\tau(\psi_i + 10^{\frac{X_\sigma}{10}}\zeta_i d_i^{m_p})z_i + (E_i^{(t)} + \tau\phi_i^{(t)} - \tau\theta_i - F_i^{(t)} - E_i^{\max})\alpha \leq 0, \\
&\qquad\quad \mathcal{C}_3:\ \vec{e}^T\vec{z} + f\alpha = 1, \\
&\qquad\quad \mathcal{C}_4:\ z_i \geq 0, \qquad \forall i, \\
&\qquad\quad \mathcal{C}_5:\ \alpha > 0.
\end{aligned} \tag{3.15}$$

The EE optimization problem defined in (3.15) can be written in a generalized form as

$$\begin{aligned}
\underset{\alpha,\vec{z}}{\text{maximize}} \quad & \vec{x}^T\vec{z} \\
\text{subject to} \quad & \mathcal{C}_1: \quad a_i z_i + b_i\alpha \leq 0, \qquad \forall i, \\
& \mathcal{C}_2: -a_i z_i + c_i\alpha \leq 0, \qquad \forall i, \\
& \mathcal{C}_3: \quad \vec{e}^T\vec{z} + f\alpha = 1, \\
& \mathcal{C}_4: \quad z_i \geq 0, \qquad \forall i, \\
& \mathcal{C}_5: \quad \alpha > 0.
\end{aligned} \tag{3.16}$$

where a_i can be written as, $a_i = \tau(\psi_i + 10^{\frac{X_\sigma}{10}}\zeta_i d_i^{m_p})$, $b_i = E_i^{\min} + F_i^{(t)} + \tau\theta_i - E_i^{(t)} - \tau\phi_i^{(t)}$, and c_i can be given as follows $c_i = E_i^{(t)} + \tau\phi_i^{(t)} - \tau\theta_i - F_i^{(t)} - E_i^{\max}$. The optimization problem to maximize the EE of WBAN is now in a standard form and can be solved to obtain the optimal solution using the simplex method [60].

3.3.4 Suboptimal Solution

In this subsection, we exploit the structure of the EE optimization problem in (3.16) and provide a suboptimal solution with lower computational complexity. The optimization problem finds the source rate of each sensor in the network and based on that information, the power consumption, and ultimately the EE of the overall WBAN is calculated. From the constraints $\mathcal{C}_1$ and $\mathcal{C}_2$ of the optimization problem defined in (3.16), the source rate of the sensor i can be written as

$$r_i^{(t)} \leq \frac{E_i^{(t)} + \tau\phi_i^{(t)} - \tau\theta_i - F_i^{(t)} - E_i^{\min}}{\tau(\psi_i + 10^{\frac{X_\sigma}{10}}\zeta_i d_i^{m_p})} = r_i^{\max}, \tag{3.17}$$

$$r_i^{(t)} \geq \frac{E_i^{(t)} + \tau\phi_i^{(t)} - \tau\theta_i - F_i^{(t)} - E_i^{\max}}{\tau(\psi_i + 10^{\frac{X_\sigma}{10}}\zeta_i d_i^{m_p})} = r_i^{\min}. \tag{3.18}$$

Alternatively by using (3.17) and (3.18), the source rate of SN i can be written as a compound inequality as follows

$$r_i^{min} \leq r_i^{(t)} \leq r_i^{max} \tag{3.19}$$

According to (3.19), the source rate of the SN i can take any value between the minimum $r_i^{\min}$ and the maximum source rate $r_i^{\max}$. By analyzing the optimization problem in (3.16), it can be noticed that by relaxing the $\mathcal{C}_3$ that is coupling the decision variables in the constraints together, the source rate of each sensor can take either the maximum or minimum source rate values only. In order not to deviate much from the original optimization problem and the optimal solution, constraint $\mathcal{C}_3$ and its effect on the source rates has to be determined. It can be observed that $\mathcal{C}_3$ is contributing towards the denominator of the objective function in (3.12), where the source rate of each sensor is coupled with other sensors in the network.

The main idea of the suboptimal solution is to choose the source rates such as to maximize the EE objective function, i.e., to keep the denominator of the objective function as minimum as possible as the numerator is the equal-weighted sum of the SNs' source rates. That said, we propose to allocate either the maximum or the minimum source rates to each SN (based on the coefficients λ_i) to minimize the denominator in (3.12). In particular, the SN with a higher coefficient λ_i should take the minimum source rate, and the SN with a lower coefficient λ_i will be allocated by the maximum source rate equation. From the system model, the higher λ_i means that the SN is far from the aggregator and on the other hand, the lower coefficient λ_i means that the SN is near to the aggregator. Consequently, it

can be concluded from our analysis, that the SN close to the aggregator should transmit its data with maximum source rate $r_i^{\max}$, and the SN far from the aggregator should transmit the data by minimum source rate $r_i^{\min}$.

The question now is to determine the number of SNs transmitting with maximum and minimum rates for a given set of parameters. To address this question, we propose a suboptimal Algorithm 1 that has twofold objectives: 1) It separates the source rate of each sensor into two groups that either satisfy the maximum or minimum source rate equation. 2) Based on the selection of source rates of each sensor, it finds the maximized EE of the overall eHealth monitoring WBAN. The proposed algorithm calculates the EE of the WBAN by selecting the optimal source rates combination from either maximum or minimum source rate for each SN, such as to achieve the maximum EE. The basic idea of the algorithm is to assume all the sensors will have a minimum source rate. Then we incrementally assign the maximum source rate for each sensor based on its distance from the aggregator and calculate the EE. The source rate combinations that result in the maximum EE is the required suboptimal solution. The proposed suboptimal Algorithm 1 is formally summarized at the top of the next page.

3.3.5 Complexity Analysis

The worst case computational complexity of the suboptimal solution can be analyzed as follows: starting from line 1 of the Algorithm 1, taking input for N number of sensors is independent of any parameters in the optimization problem; therefore its complexity does not scale with the value of N. For remaining inputs $\mathbf{R_{min}}$, $\mathbf{R_{max}}$, $\mathbf{P_{min}}$, and $\mathbf{P_{max}}$ have the complexity of $\mathcal{O}(N)$ each. Since the complexity scales linearly with the number of SNs, the overall complexity of the input is $\mathcal{O}(N)$. The complexity of the **for** loop at line 2 is

Algorithm 1 Proposed suboptimal algorithm for energy efficiency optimization problem

1: **INPUT:** N, $\mathbf{R_{min}}, \mathbf{P_{min}}, \mathbf{R_{max}}, \mathbf{P_{max}}$
2: **for** $i = 0, \ldots, n+1$ **do**
3: **if** $i \neq 0$ **then**
4: Replace $R_{\max}[i-1]$ with $R_{\min}[i]$
5: Replace $P_{\max}[i-1]$ with $P_{\min}[i]$
6: **end if**
7: Get sum of all $R_{\min}$ source rates
8: Get sum of all $P_{\min}$ power consumption
9: Find the energy efficiency
10: **if** $i = 0$ **then**
11: push energy efficiency value in new array $K[\,]$
12: **else**
13: push energy efficiency value in new array $K[i]$
14: **end if**
15: Increment i
16: **end for**
17: **OUTPUT:** Find the maximum energy efficiency from the array $K[i]$ and get the index of the maximum element.

$\mathcal{O}(N+2)$ as the loop repeats $N+2$ times. From line 3 to line 6, the overall computational complexity is $\mathcal{O}(N+1)$. For line 7 and line 8, the complexity is $\mathcal{O}(N+1)$ each. From line 9 to line 12, each has a complexity of $\mathcal{O}(1)$ as this computation is independent of N. The line 13 executes $N+1$ times, which makes its complexity equals to $\mathcal{O}(N+1)$. Hence, the overall worst-case computational complexity of the suboptimal EE optimization Algorithm 1 is $\mathcal{O}(N+2)\mathcal{O}(N+1) + \mathcal{O}(N) = \mathcal{O}(N^2)$, which is the polynomial time complexity of N. In comparison, the computational complexity of the optimal solution that utilizes the simplex method has a worst-case computational complexity of $\mathcal{O}(2^N)$ [60].

3.4 Results and Discussion

We considered a WBAN with 10 SNs to evaluate the performance of the proposed scheme. By following the simulation parameters of [8], the distance between SNs and aggregator is uniformly distributed between 0.3 and 0.7 m. The initial energy E^{ini} of each SN is set to 0.1 J. The maximum battery capacity $E^{\max}$ of each SN is 0.11 J. The minimum energy $E^{\min}$ required for each SN is 0.01 J. In the power consumption model, the energy cost of sensing ψ_i and transmit electronics θ_i of SN i is set as 2×10^{-8} J/b and 6×10^{-8} J/b respectively. Similarly, the energy cost of transmit amplifier ζ is chosen as 8×10^{-8} J/b/m^{m_p}. The path loss exponent m_p of the SNs is set between 1.4 to 4.4. In the energy harvesting Markov chain model, from state 1 to state 2, the transition probability is uniformly distributed between 0.6 and 0.8. From state 2 to state 1, the transition probability is uniformly distributed between 0.2 and 0.4. The length of the time slot τ is set as 5 s.

A statistical model of the dynamic on-body time-varying channel based on an experimental measurement campaign for different human body movements is proposed in [58]. The model considers different body movements of various human subjects to study the effect of human activities on propagation channel behavior. The measurement results reveal that the movement conditions of the subject are strictly shadowing dependent. Moreover, the shadowing conditions also depend on the human subject's way of movement, and shadowing conditions remain identical if the subject does not show any movement. Due to the random movements of the patient during daily life activities, the direction, and the distance from the SN to the aggregator changes, which results in the variation of path loss. Since, the transmission power consumption is a function of distance, the change in distance affects the transmission power consumption. Therefore, in our work, the variations of the transmission power consumption $P_{t,i}$ during different postures are modeled as

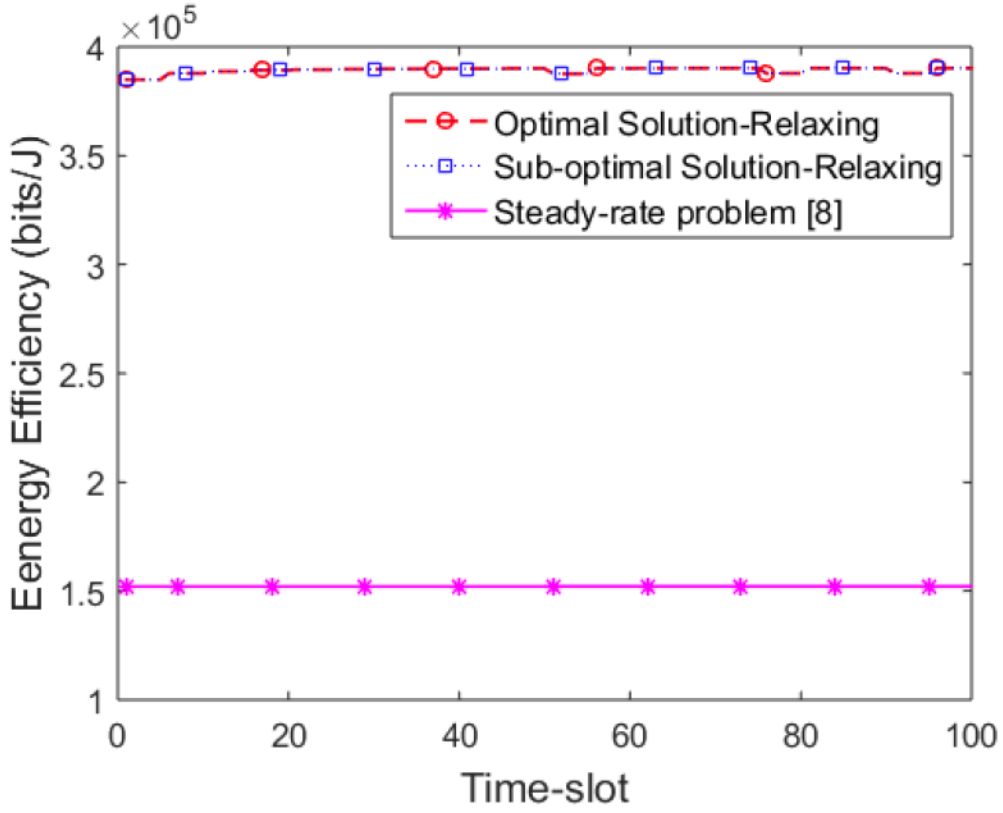

Fig. 3.4: Optimal and suboptimal energy efficiency of WBAN in relaxing state.

$P_{t,i} = 10^{\frac{X_\sigma}{10}}\beta_i r_i + \theta_i$, where X_σ is the Gaussian random variable denoted as $\mathcal{N}(0, \sigma_s^2)$. The standard deviation σ_s depicts the different postures of the body such as relaxing, walking or running [8, 58]. In this regard, X_σ is chosen as 1 in the relaxing state as the direction, and the distance from a SN to the aggregator remains unchanged in the relaxing state. However, the arbitrary movements of the human body change the direction and distance between the SN and the aggregator and cause variations in the path loss. Therefore, based on the experimental and measured results in [58], σ_s for the walking and the running activities are chosen as 2.15 dB and 3.49 dB, respectively.

Fig. 3.4 shows the performance of the optimal and suboptimal solution of the EE

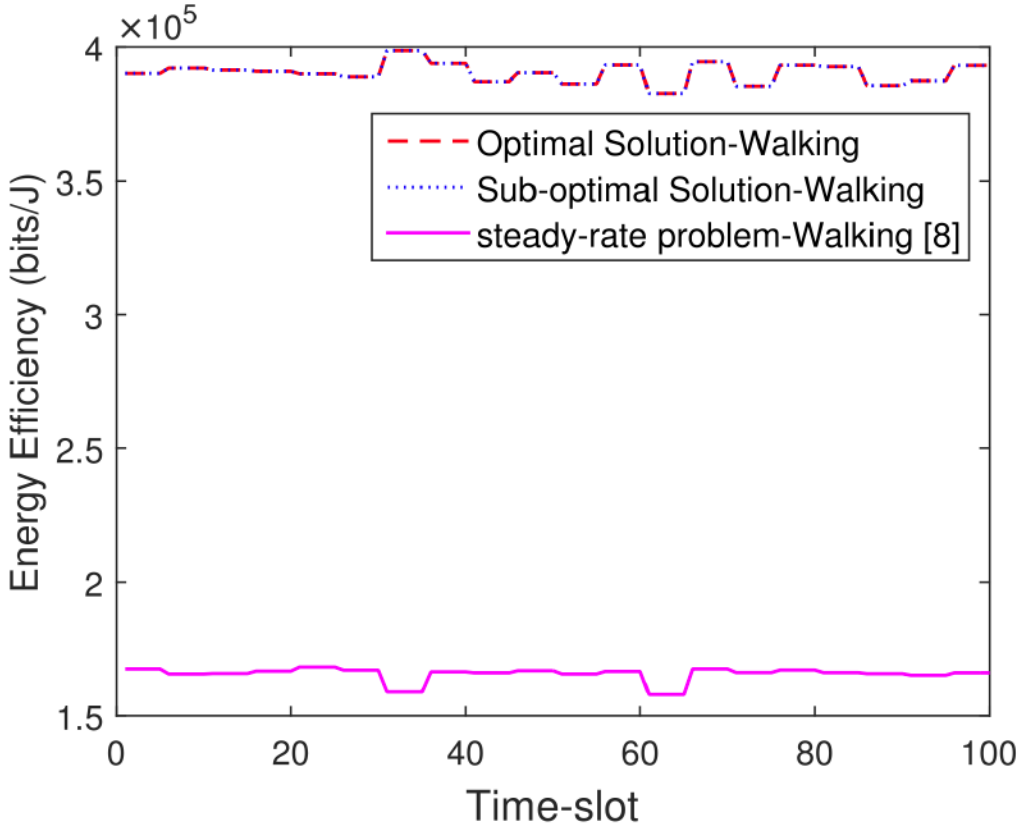

Fig. 3.5: Optimal and suboptimal energy efficiency of WBAN in walking state.

optimization problem in relaxing state in comparison with the steady-rate problem [8]. It can be noticed that the EE optimization problem provides higher EE in comparison with the steady rate problem. The EE remains almost static during the time slots because the distance and the direction from the SN to the aggregator remain unchanged in a relaxing state. Moreover, the performance of a suboptimal solution is very close to the optimal solution.

Fig. 3.5 illustrates the effect of EE when the patient is in the walking state. The EE varies due to the change of path loss and the distance from the SN to the aggregator.

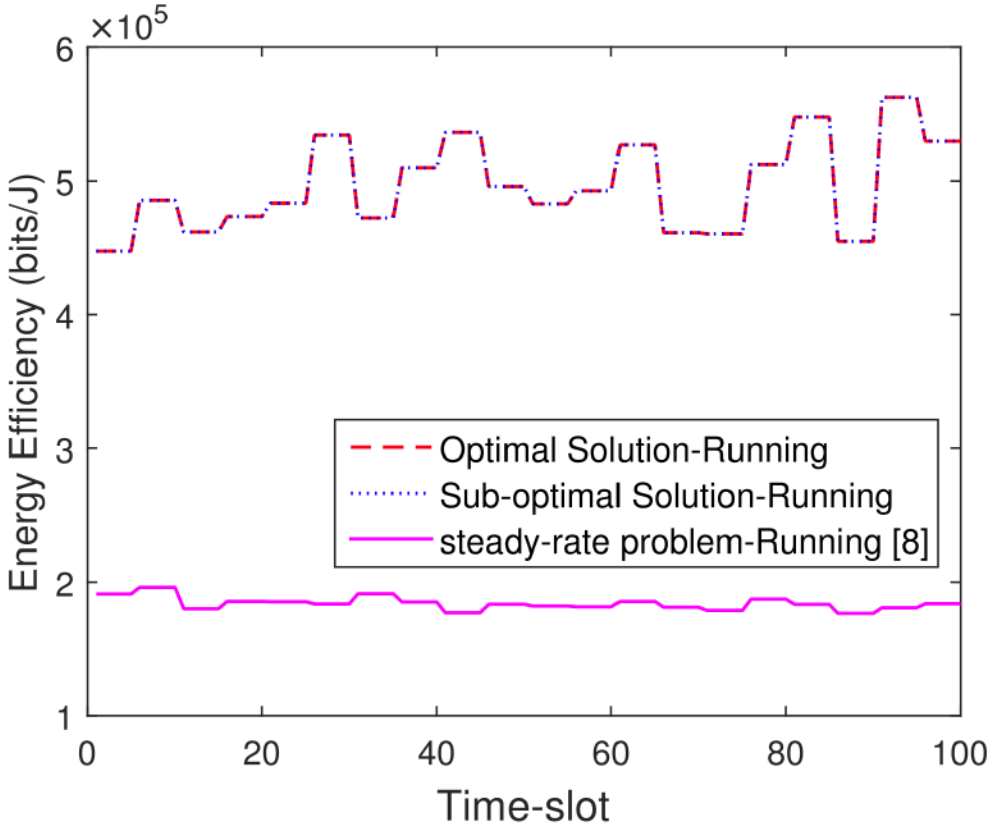

Fig. 3.6: Optimal and suboptimal energy efficiency of WBAN in running state.

Moreover, the energy harvesting rate also changes due to dynamic behavior. Therefore, for a particular time slot, if the harvested energy is more than the energy consumed, EE will increase, and if the harvested energy is less than the power consumed, EE will decrease. As depicted from Fig. 3.6, in the running state, the EE is higher as compared to the walking state as the harvested energy is higher due to the aggressive body movements.

3.5 Conclusion

In the design of an eHealth monitoring WBAN, due to the limited battery life of the SNs, saving energy is of paramount importance. Therefore, maximizing the EE enables efficient use of the energy critical nodes. This chapter formulates and solves a novel optimization problem to maximize the EE of the WBAN equipped with energy harvesting capabilities. The optimization problem is transformed from the linear fractional problem to a linear function, and the resultant problem is solved using numerical methods. For further in-depth analysis, we exploited the structure of the optimization problem and derived the upper and the lower bounds of the source rates, and a suboptimal solution is proposed that approaches the optimal solution with lower computational complexity. Simulation results validate the proficiency of the proposed schemes, and the performance merits in terms of EE of the eHealth monitoring network.

3.6 Publication Resulted From This Chapter

- O. Amjad, E. Bedeer, and S. Ikki, "Energy-Efficiency Maximization of Self-Sustained Wireless Body Area Sensor Networks," *IEEE Sensors Letters*, vol. 3, no. 12, pp. 14, Oct. 2019.

Chapter 4

Robust Energy Efficiency Optimization Algorithm for Health Monitoring System with Wireless Body Area Networks

4.1 Introduction

The aging population poses several challenges for healthcare providers as people aged over 65 years are expected to account for nearly 12% of the world population by 2030. Such challenges motivate the research community and healthcare providers to investigate new techniques to reduce costs and cut unnecessary hospitals/clinics visits while maintaining the expected high quality of care. eHealth is a new paradigm—bridging concepts from bio-sensing, signal processing, and communication theory—proposed mainly to support and

improve the existing health services. In eHealth, sensors are deployed on, in, or around the human body to perform real-time monitoring of physiological attributes, and hence, detect any vital sign abnormalities [61].

4.1.1 Related Work

One of the implementation challenges of eHealth solutions is that not all the sensors' batteries can be easily replaced, especially if they are implanted in the patient's body. That said, improving the sensors' lifetime or EE is crucial. Such a design objective has been overlooked in the literature [25], [61–66]. In [25], a multi-point WBAN is proposed that aims to maximize the throughput by considering the normal and abnormal scenarios to promote reliable information transmission and to improve the performance of the system. In this regard, time switching protocol and hybrid time switching and power splitting protocols are proposed. In time switching protocol, SNs transmit command signals to the access point in the uplink, and the access point then broadcasts the energy signals to distributed sensors in the downlink. As a result, SNs provide data information to the access point in the uplink. In the hybrid time switching and power splitting protocol, after the access point transmits wireless energy and commands to all SNs, the SNs take turns to simultaneously send the needed physiological data in the opposite direction. The transmission time of SNs, time spend by the access point in transmitting the energy signals, and power splitting ratios are optimized to obtain the solution of the proposed throughput maximization problems.

The authors in [61] proposed the design and development of an eHealth system that keeps track of patient parameters to support disease management during daily life activities. The presented system combines patient health monitoring, status logging for

recording various difficulties or symptoms encountered, and social sharing of the recorded data within the patient's community, all with the goal of making illness treatment easier. A prototype for unobtrusive vital sign monitoring via a wearable multi-sensing device is built on a mobile device, demonstrating the feasibility and application of the current work. In addition, a study involving 16 hypertensive patients was done to determine user acceptance, usability, and the merits of the proposed scheme.

The authors in [62] proposed two TDMA based scheduling algorithms to improve the reliability and EE of WBAN such as to guarantee better QoS in unexpected emergency situations while minimizing energy consumption. In this regard, an adaptive scheduling scheme is proposed that dynamically allocates the time slots to the SNs by observing their channel conditions. In addition, another dynamic scheduling scheme is proposed that allocates the time slots to the SNs based on the status of their buffer. Both normal and emergency situations are considered to evaluate the performance of the proposed algorithms to ensure WBAN reliability, EE, and better QoS.

In [63], EE optimization for WBAN is performed that considers the QoS required from each SN, intelligent time and power resource allocation for energy saving. In this regard, global energy minimization and network lifetime maximization problems are solved to improve the EE by considering the minimum power consumption of a SN in an active state, required throughput of a SN, and the global energy constraint of an eHealth network.

In [64], an investigation of the real-time health monitoring system is provided for the patients suffering from the threatening disease of diabetic ketoacidosis by using the C-band sensing techniques. In [65], a remote eHealth system is designed that optimizes clinician time with reduced medical costs and improved healthcare. A system-level design with a specific focus on early detection of patient deterioration provided in [66] utilizes the various wireless sensors to monitor patient activities.

4.1.2 Contributions

Compared to the existing literature, in this chapter, a robust optimization algorithm is designed to save the power of energy-constrained sensors, which does not require perfect CSI from the transmitting sensor to the gateway. The optimization algorithm is robust in a sense that it utilizes a generalized gamma distribution that supports various patient conditions and can efficiently model both everyday and dynamic activities. EE objective function is defined as the ratio of the transmission power consumption of the SN to a transmission rate of the SN while considering the retransmissions due to error. The formulated problem optimizes the EE (measured in J/bits) by optimizing the transmit power and encoding rate of a SN while considering outage probability and packet retransmission. It is shown that optimization problem is semi-strictly quasi-convex in each decision variable, and an alternative approach is utilized to determine its solution at reduced complexity.

The remainder of this chapter is organized as follows: Section 4.2 presents the system model and problem formulation. The problem is analyzed and solved in Section 4.3. Section 4.4 provides the numerical results, and the chapter is finally concluded in Section 4.5.

4.2 System Model and Problem Formulation

In order to design a robust communication system for WBAN that can support different patient conditions is a challenging task as each condition has its own propagation characteristics. For instance, the channel propagation of patients with everyday activities like walking, outdoor jogging, regular home, and office activities was found to be characterized by Weibull or gamma distributions [67,68]. Such activities can be referred to as "*everyday activities*". For patients with more "*dynamic activities*" such as running or exercising, the authors in [68] showed that the channel propagation characteristics follow a lognor-

mal distribution. The propagation characteristics of everyday and dynamic activities were confirmed later in [69] and it was also shown that Rayleigh distribution—which is usually assumed for WBAN transmission—is a poor fit for such scenarios.

We consider a WBAN with one aggregator carried by the patient that acts as a gateway. The sensors are deployed on, in, or around the human body to monitor the patient's vital signs. Each sensor inquires a dedicated guaranteed time slot from the aggregator, during which it periodically transmits its data directly (i.e., no need for a relay) to a gateway without having perfect CSI using the standard TDMA scheme [41]. The maximum transmission rate of sensor n for infinite packet length can be expressed as follows [70]

$$C_n = B \log_2(1 + \gamma_n s_n), \tag{4.1}$$

where B is the bandwidth and s_n is the transmit power of sensor n. $\gamma_n = |h_n|^2/\sigma_n^2$ is the instantaneous channel gain to noise ratio (CNR), h_n is the complex channel coefficient between sensor n and the gateway and σ_n^2 is the noise variance. From [70], C_n in (4.1) can be approximated to characterize the channel capacity of a finite packet length given as

$$C_{approx} \approx C_n - \sqrt{\frac{V(\gamma_n s_n)}{L}} Q^{-1}(\epsilon), \tag{4.2}$$

where L is a finite number of bits per packet, $Q^{-1}(.)$ is the inverse of the Gaussian cumulative distribution function, and $\epsilon \in (0, 1)$ is the average error probability. $V(\gamma_n, s_n)$ is the Gaussian dispersion function that measures the stochastic variability of the channel relative to a deterministic channel with the same capacity given as follows

$$V(\gamma_n, s_n) = \log^2 e. \frac{\gamma_n s_n(\gamma_n s_n + 2)}{2(\gamma_n s_n + 1)^2}. \tag{4.3}$$

From (4.2), the numerator in the second term mainly depends upon $V(\gamma_n, s_n)$, since $Q^{-1}(\epsilon)$ is not a large value. Therefore, by looking at the term $V(\gamma_n, s_n)$ in (4.3), it can be observed

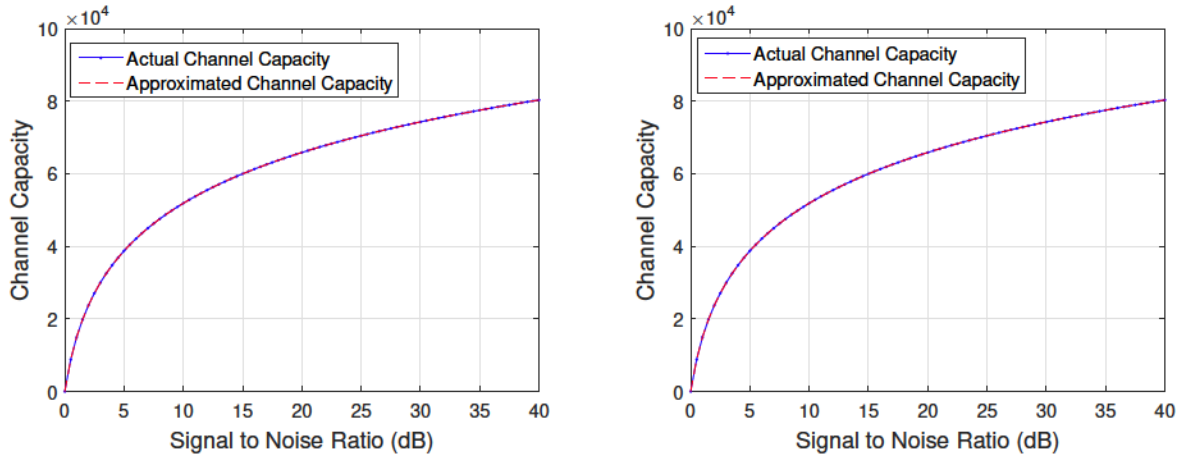

(a) Packet length of $L = 50$ bits (b) Packet length of $L = 200$ bits

Fig. 4.1: Actual and approximated channel capacity vs. SNR for different packet lengths.

that it is a function of γ_n and s_n. It can be noticed from (4.3), if the sensor transmits its data using a fixed s_n, the term $V(\gamma_n, s_n)$ is always small for any practical value of γ_n, because both numerator and denominator are of the same order. Moreover, in the worst case, if γ_n approaches infinity and for a fixed s_n, $V(\gamma_n, s_n)$ becomes as follows

$$\lim_{\gamma_n \to \infty} V(\gamma_n, s_n) = \log^2 e. \lim_{\gamma_n \to \infty} \left(\frac{\gamma_n s_n (\gamma_n s_n + 2)}{2(\gamma_n s_n + 1)^2} \right) = \frac{1}{2} \log^2 e. \tag{4.4}$$

Therefore, from (4.2), it can be noticed that for a fixed s_n, and any practical value of γ_n, the numerator in the second term is significantly small in comparison to a finite packet length of L bits, consequently the term $\sqrt{\frac{V(\gamma_n, s_n)}{L}} Q^{-1}(\epsilon)$ reaches a very small value. Therefore, based on the simulation results in Fig. 4.1, for $L \geq 50$ the approximation of achievable rate is found to be significantly good to the Shannon's capacity given in (4.1), and thus (4.1) is sufficiently acceptable to characterize the channel capacity for $L \geq 50$ bits.

We do not assume knowledge of the instantaneous value of h_n, and hence, knowledge of γ_n, at the transmitting sensor n due to the lack of a feedback channel from the gateway

to sensor n. Accordingly, sensor n transmits its information using a fixed encoding rate $\gamma_{n,0}$ and its transmission rate is given as

$$R_n = B \log_2(1 + \gamma_{n,0} s_n). \tag{4.5}$$

A packet sent from sensor n to the gateway is received correctly if $R_n \leq C_n$, and is received in error if $R_n > C_n$ and outage occurs. The outage probability is given by

$$P_{\text{out}} = p(\gamma_n < \gamma_{n,0}) = F(\gamma_{n,0}), \tag{4.6}$$

where $p(.)$ is the probability and $F(.)$ is the cumulative distribution function. In order to design a robust and reliable WBAN system that supports both everyday and dynamic activities of patients, a generalized gamma distribution for γ_n is adopted that can easily capture Weibull, gamma, and lognormal distributions [69].

Sensor n transmits its information to the gateway in packets each of length L bits. If any of the L bits are received in error, an outage occurs and the gateway requests retransmission of the whole packet. The retransmission is assumed to be repeated until the packet is received correctly. The average number of retransmissions of a given packet (N_{av}) until it is received correctly is derived as follows

$$\begin{aligned} N_{\text{av}} &= \sum_{i=1}^{\infty} i(PER)^{i-1}(1 - PER) \\ &= (1 - PER)^{-2}(1 - PER) \\ &= (1 - PER)^{-1}, \end{aligned} \tag{4.7}$$

where i is the number of retransmissions and the and the infinite geometric series in (4.7)

has a convergent sum given as $\sum_{i=1}^{\infty} i(PER)^{i-1} = (1-PER)^{-2}$. The packet error rate (PER) of a given packet can be expressed as [56]

$$PER = 1 - (1 - P_e)^L. \tag{4.8}$$

where P_e is the bit error probability. Consequently, substituting PER from (4.8) in (4.7) the average number of retransmissions of a given packet N_{av} until it is received correctly is given as follows

$$N_{\text{av}} = (1 - P_e)^{-L}, \tag{4.9}$$

In the considered system model, since the majority of errors are due to the outage, therefore, in the rest of this chapter, the outage probability is considered to be approximately equal to the probability of error, and hence, $P_e \approx F(\gamma_{n,0})$. The total transmit power of sensor n, S_n, is given as [41]

$$S_n = \kappa_n s_n + s_{n,\text{c}}, \tag{4.10}$$

where κ_n represents the amplifier efficiency of sensor n and $s_{n,\text{c}}$ is the fixed power consumed in transmission by sensor n. That said, the EE η_n (measured in J/bits) for sensor n considering the retransmissions due to errors is represented as

$$\eta_n = \frac{\kappa_n s_n + s_{n,\text{c}}}{B \log_2(1 + \gamma_{n,0} s_n)} (1 - F(\gamma_{n,0}))^{-L}. \tag{4.11}$$

The aim of this work is to optimize the sensor transmit power s_n and its encoding CNR value $\gamma_{n,0}$ to optimize the EE η_n.

4.3 Optimization Problem Analysis and Solution

In this section, the optimization problem is analyzed and solved to optimize the EE η_n of sensor n without knowledge of perfect CSI. The EE optimization problem can be formally expressed as

$$\begin{aligned} \min_{s_n,\, \gamma_{n,0}} \quad & \eta_n = \frac{\kappa_n s_n + s_{n,\mathrm{c}}}{B\, \log_2(1+\gamma_{n,0} s_n)} (1 - F(\gamma_{n,0}))^{-L} \\ \text{s. t.} \quad & s_n \leq s_{n,\max}, \end{aligned} \tag{4.12}$$

where $s_{n,\max}$ represents the maximum transmit power of sensor n. The EE objective function in (4.12) is analyzed in order to facilitate obtaining a solution in a low complexity manner. The power term in the numerator in (4.12) is affine in s_n and positive assuming that $s_{n,\mathrm{c}} > 0$, while the transmission rate term in the denominator is positive and bi-concave in s_n and $\gamma_{n,0}$. To analyze the term $(1 - F(\gamma_{n,0}))^{-L}$, its second derivative can be found as follows

$$\frac{\partial^2 (1 - F(\gamma_{n,0}))^{-L}}{\partial \gamma_{n,0}^2} = \quad L(L+1) f^2(\gamma_{n,0}) (1 - F(\gamma_{n,0}))^{-L-2} + L f^{'}(\gamma_{n,0}) (1 - F(\gamma_{n,0}))^{-L-1}, \tag{4.13}$$

where $f^{'}(\gamma_{n,0})$ is the first derivative of the probability density function (PDF) $f(\gamma_{n,0})$ of the random variable $\gamma_{n,0}$. One can see that the second derivative is positive if and only if

$$(L+1) f^2(\gamma_{n,0}) + f^{'}(\gamma_{n,0}) (1 - F(\gamma_{n,0})) > 0. \tag{4.14}$$

The question now is whether (4.14) holds for the generalized gamma distribution adopted for WBAN to model propagation characteristics of various patient conditions. The PDF

$f(\gamma_{n,0})$ of generalized gamma distribution is given as [69]

$$f(\gamma_{n,0}; a, b, c) = \frac{c}{b^{ac}\Gamma(a)} \gamma_{n,0}^{ac-1} \exp\left(-\left(\frac{\gamma_{n,0}}{b}\right)^{c}\right), \tag{4.15}$$

where $\Gamma(.)$ is the standard gamma function, a and c represents the shape parameters of the generalized gamma distribution, respectively, and b is its scale parameter. The Weibull and gamma distributions can be reached from the generalized gamma distribution PDF by setting $a = 1$ and $c = 1$, respectively; however, the lognormal distribution can be reached from the generalized gamma distribution in the limiting case when $c \longrightarrow 0$ and $a = 2/(c^2 b^c)$ [69].

Lemma 1. *The PDF of the generalized gamma distribution that characterizes various patient conditions of WBAN is log-concave if* $c \geq 1$ *and* $ac \geq 1$.

Proof: The second derivative of the log of the generalized gamma distribution, i.e., $\log(f(\gamma_{n,0}; a, b, c))$, is found as

$$\frac{\partial^2 \log(f(\gamma_{n,0}; a, b, c))}{\partial \gamma_{n,0}^2} = -\frac{1}{\gamma_{n,0}^2}\left(c(c-1)\left(\frac{\gamma_{n,0}}{b}\right)^{c} + ac - 1\right). \tag{4.16}$$

For the generalized gamma distribution PDF to be log-concave, its second derivative in (4.16) has to be non-negative. One can see that this can be achieved when both $c \geq 1$ and $ac \geq 1$. For Weibull distribution, i.e. $a = 1$, this condition reduces to $c \geq 1$. On the other hand, for gamma distribution, i.e. $c = 1$, the condition reduces to $a \geq 1$. ■

The fact that the generalized gamma distribution PDF is log-concave for a certain operating region implies that $(1 - F(\gamma_{n,0}))$ is log-concave as well. From the properties of a twice differentiable log-concave function, it is known that $(1 - F(\gamma_{n,0}))\, \nabla^2 (1 - F(\gamma_{n,0})) \leq (\nabla (1 - F(\gamma_{n,0})))^2$ [71]. This implies that $-f'(\gamma_{n,0})\,(1 - F(\gamma_{n,0})) \leq f^2(\gamma_{n,0})$, and hence,

the condition in (4.14) is always satisfied for $L \geq 1$. This concludes that the term $(1 - F(\gamma_{n,0}))^{-L}$ is strictly-convex.

Recalling that the transmission rate in the denominator of (4.12) is bi-concave, the power consumption in the numerator is affine, and the average number of retransmission is strictly-convex, hence, the EE optimization problem of WBAN without knowing the CSI at the transmitting sensor is semi-strictly quasi-convex with respect to s_n and $\gamma_{n,0}$ individually.

To obtain a low-complexity solution to the optimization problem in (4.12), an alternate optimization approach is followed where first the EE is optimized with respect to s_n while treating $\gamma_{n,0}$ as a constant. Later optimized is the EE with respect to $\gamma_{n,0}$ while treating s_n as a constant. This process repeats until convergence is reached such that the change in EE is no greater than $\epsilon = 0.001$. In particular, we start by finding the local minimum with respect to s_n by setting $\frac{\partial \eta_n}{\partial s_n} = 0$ which results in

$$(1 + \gamma_{n,0} s_n) \ln(1 + \gamma_{n,0} s_n) = \gamma_{n,0} s_n + \frac{s_{n,c}}{\kappa_n} \gamma_{n,0}, \tag{4.17}$$

Then, the transmit power s_n of sensor n can be given as

$$s_n = \frac{1}{\gamma_{n,0}} \left[-1 + \exp\left(1 + \mathcal{W}\left(e^{-1} \left(\frac{s_{n,c}}{\kappa_n} \gamma_{n,0} - 1 \right) \right) \right) \right], \tag{4.18}$$

where $\mathcal{W}(.)$ is the Lambert-W function. To consider the maximum transmit power constraint in (4.12), the transmit power s_n^* of sensor n can be expressed as

$$s_n^* = \min(s_n, s_{n,\max}). \tag{4.19}$$

Algorithm 2 Robust energy-efficient iterative algorithm for optimizing EE of eHealth monitoring WBAN

1: **INPUT:** κ_n, $s_{n,c}$, L, and B.

2: Assume initial values of s_n and $\gamma_{n,0}$.

3: Calculate the transmit power of sensor s_n^* using (4.19).

4: Calculate the encoding rate $\gamma_{n,0}^*$ numerically from (4.20).

5: Repeat steps 3 and 4 until convergence is reached such that change in EE is no greater than $\epsilon = 0.001$.

6: **OUTPUT:** s_n^* and $\gamma_{n,0}^*$.

Second, the local minimum is found with respect to $\gamma_{n,0}$ by setting $\frac{\partial \eta_n}{\partial \gamma_{n,0}} = 0$ as follows

$$\frac{f(\gamma_{n,0}^*)}{1 - F(\gamma_{n,0}^*)}(1 + \gamma_{n,0}^* s_n)\ln(1 + \gamma_{n,0}^* s_n) = \frac{s_n}{L}. \tag{4.20}$$

Unfortunately, a closed-form solution of $\gamma_{n,0}^*$ cannot be reached; however, (4.20) can be efficiently solved numerically. The proposed Algorithm 2 to optimize the EE of WBAN without knowing the perfect CSI at the transmitting sensor is formally summarized at the top of this page.

4.4 Simulation Results

We consider an eHealth system with WBAN to evaluate the performance of the proposed algorithm. In this regard, the amplifier efficiency κ_n of the sensor n is set to 35%. From [41], the fixed power consumed in transmission by sensor n, i.e., $s_{n,c}$ is set to 5×10^{-8} W. The

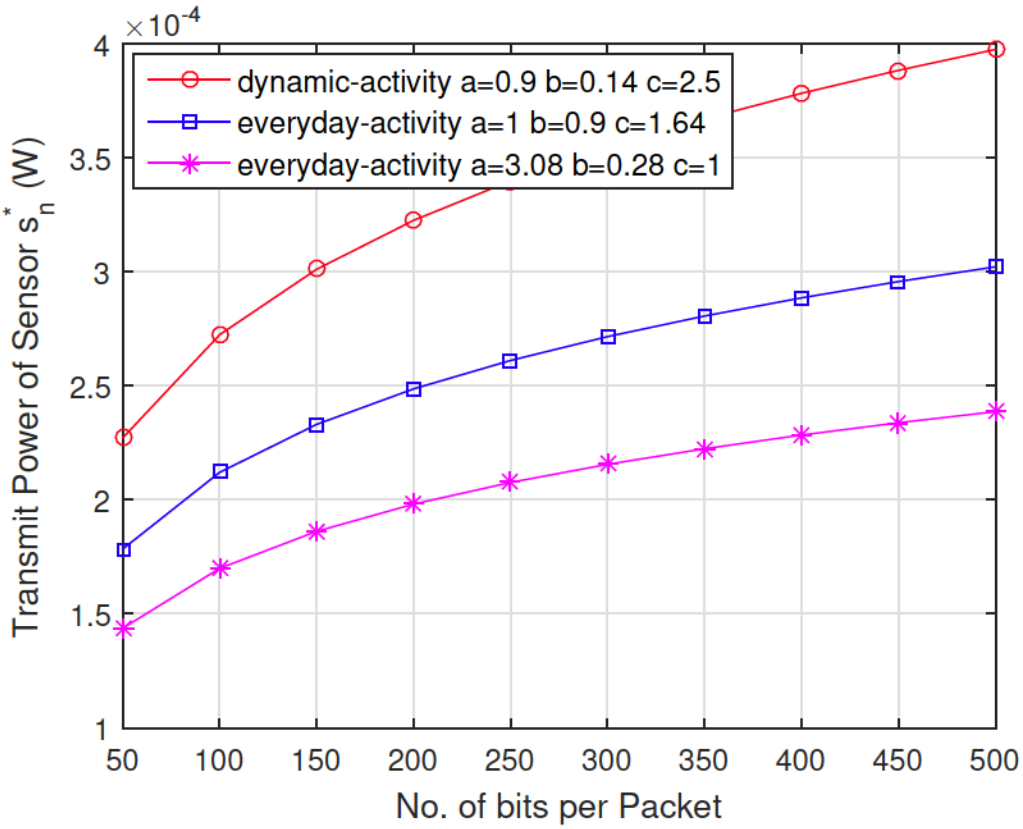

Fig. 4.2: Optimized transmit power of the sensor for different everyday and dynamic activities.

maximum transmit power $s_{n,\max}$ of the sensor n is set as 10 mW, and the bandwidth B is set to 1 MHz. The parameters of the generalized gamma distribution depend on the measured data under different activities and based on that best fitting distribution model is applied. From the experimental results in [68] the shape parameters are chosen as $a = 3.08$ and $c = 1$, and scale parameter is set as $b = 0.28$ to model the everyday activities. Similarly, the dynamic activities are modeled by setting the $a = 0.9$, $b = 0.14$, and $c = 2.5$.

Fig. 4.2 shows the transmit power of a sensor for different patient's conditions calculated from the analytical solution in (4.19). It can be noticed that for higher L, the sensor

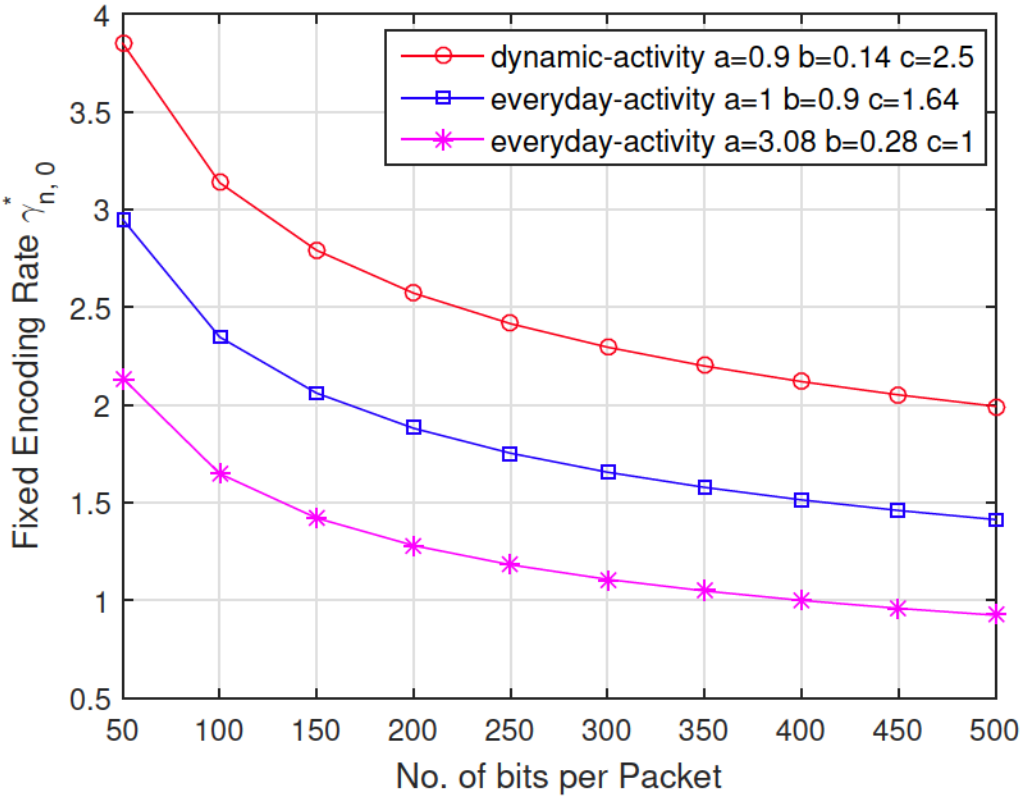

Fig. 4.3: Optimized fixed encoding rate of the sensor for different everyday and dynamic activities.

transmits its information with higher transmit power for both everyday and dynamic activities. Moreover, it can be observed that with an increased L, the transmit power of a sensor in dynamic activities is higher as compared to everyday activities.

Fig. 4.3 shows the optimized fixed encoding rate $\gamma^*_{n,0}$ of the sensor for different packet lengths obtained from solving (4.20) using bisection and inverse quadratic interpolation methods [71]. The simulation results and the mathematical solution shows that s^*_n and $\gamma^*_{n,0}$ are inversely proportional to each other. However, compared to everyday activities, dynamic activities have a higher encoding rate.

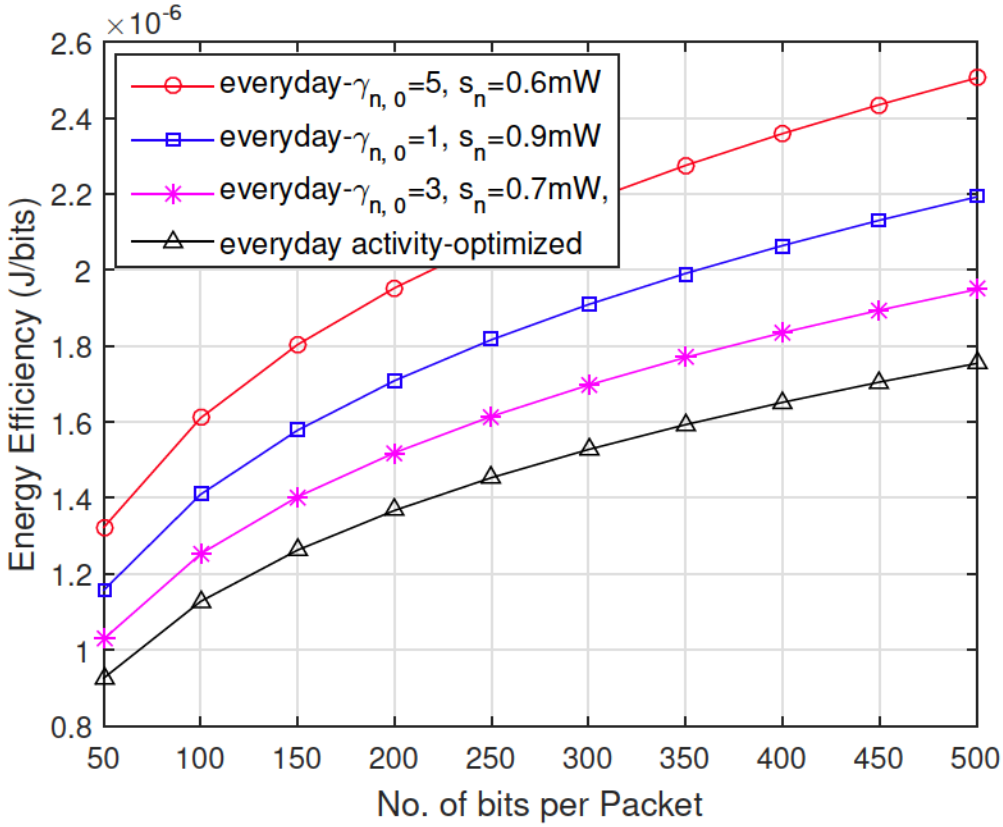

Fig. 4.4: Comparison of optimized and suboptimal energy efficiency of the sensor for everyday activities.

Fig. 4.4 depicts the solution of the optimization problem and achieved EE at s_n^* and $\gamma_{n,0}^*$ for everyday activities. Since the EE is a function of J/bits, to transmit a higher number of bits per packet higher transmit power is required by the sensor that ultimately results in the increase of EE. Moreover, from (4.9) if a packet contains a higher L, PER and N_{av} are also increased, due to which more energy will be consumed by the sensor to retransmit the same packet again. Therefore, it is better to transmit the shorter packets instead of sending the information in a single burst to avoid the number of retransmission request from the gateway of incorrectly received bits, and to ultimately save the energy of

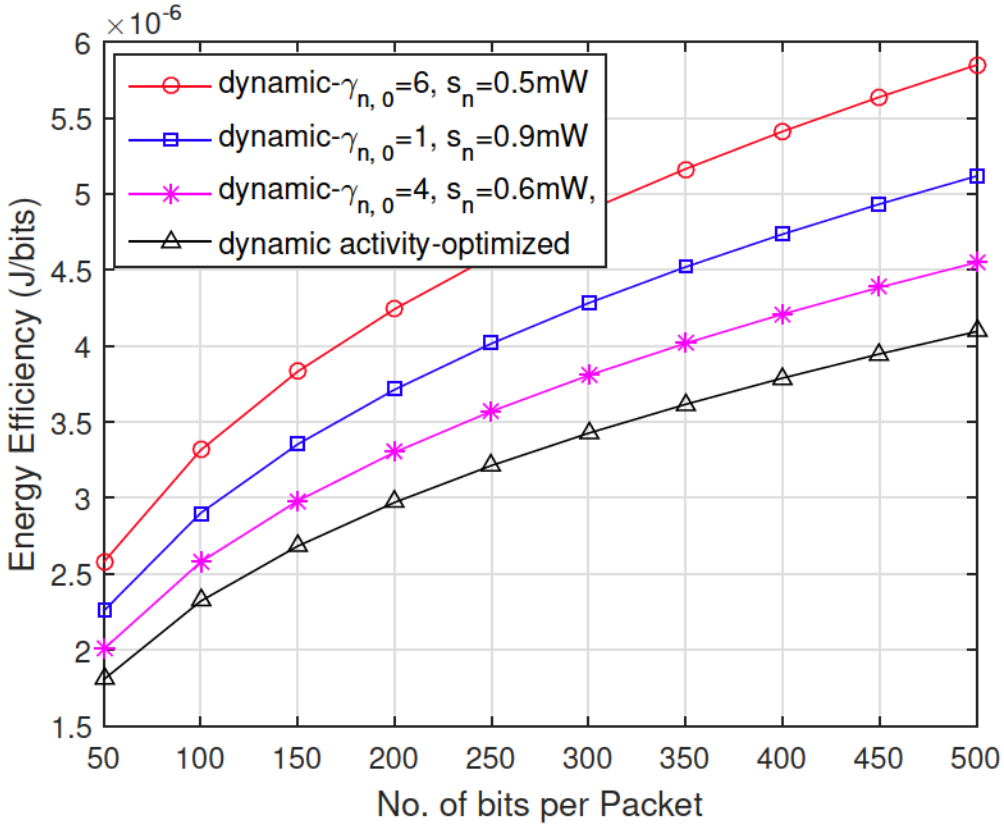

Fig. 4.5: Comparison of optimized and suboptimal energy efficiency of the sensor for dynamic activities.

the sensor. The comparison of the optimized solution with the suboptimal results obtained by using different values of s_n and $\gamma_{n,0}$ other than calculated from (4.19) and (4.20) shows that the optimized solution provides better EE.

Fig. 4.5 shows the optimized EE for dynamic activities. In comparison with everyday activities, the EE for dynamic activities is higher due to the higher transmit power required to transmit the fixed number of bits per packet. For various suboptimal values of $\gamma_{n,0}$, and s_n other than calculated from (4.19) and (4.20), the EE curve shifts upwards which shows that the sensor requires more energy/bit as compared to the optimized solution.

4.5 Conclusion

In the design of WBAN, due to the limited battery life of the sensors, saving energy is of paramount importance. Consequently, optimizing the EE enables efficient use of the energy-constrained sensors. This chapter formulates a novel optimization problem that aims to minimize the EE (measured in J/bits) of WBAN by optimizing transmit power and encoding rate of the sensor while considering outage and packet retransmission. The simulation results demonstrate that for a packet length of $L = 50$ bits the proposed algorithm is 47% more energy-efficient in comparison with $L = 500$ bits. Therefore, transmitting the information in smaller packets is preferable to avoid the retransmission request for any incorrectly received bits, and thus to save the energy of overall WBAN system. Additionally, the proposed algorithm is 30% more energy efficient when compared to sub-optimal solution with a constant encoding rate and transmit power of 5 dB, and 0.6 mW, respectively.

4.6 Publication Resulted from This Chapter

- O. Amjad, E. Bedeer, N. A. Ali, and S. Ikki, "Robust Energy Efficiency Optimization Algorithm for Health Monitoring System with Wireless Body Area Networks," *IEEE Communications Letters*, vol. 24, no. 5, pp. 11421145, Feb. 2020.

Chapter 5

Energy Efficient Resource Allocation for eHealth Monitoring Wireless Body Area Networks with Backscatter Communication

5.1 Introduction

With the evolution of low-power wearable sensors and advancement in wireless communications, WBANs have experienced remarkable growth in providing the aging population with more proactive and affordable healthcare solutions [2]. eHealth monitoring, among prominent applications of WBAN, allows continuous monitoring of patients' health and helps early detection and prevention of any abnormal physiological activities. eHealth system with WBAN consists of several SNs deployed on, or implanted inside the human body

and a central coordinator node known as an aggregator (e.g., a smart cell phone) [72]. The SNs collect the patient's vitals (e.g., heart rate, blood pressure, body temperature, and pulse rate) and send it wirelessly to the aggregator [2, 73]. By deploying an eHealth system, patients can perform their daily life activities without constantly requiring specialized medical services, thus reducing the unnecessary hospital visits and creating significant enhancement in the standard of living.

To facilitate the efficient and seamless implementation of WBANs, there are certain challenges that need to be addressed. For what concerns the major issues to be addressed, increasing battery life or EE of the SNs is of significant importance. Body SNs require a sustainable energy supply to perform a perpetual operation. Conventionally, these SNs are powered by batteries, which have a limited lifespan and are needed to be replaced/recharged manually once the energy is depleted. Moreover, battery maintenance and replacement are not preferable sometimes, especially when SNs are implanted within the human body. Therefore, wireless energy harvesting emerged as an alternative and a promising approach that allows the energy-constrained SNs to harvest energy from a variety of energy sources and ultimately helps enable self-sustained body SNs operations [41, 74].

BackCom technology is considered as a promising solution in overcoming the limited life span challenge in next-generation wireless networks such as WBANs. It has a remarkable potential to decrease or even eliminate the reliance on batteries and allows self-sustainable operations to energy-constrained SNs to transmit information by reflecting and modulating the incident signal of the aggregator. Unlike a conventional radio architecture that requires a chain of power-hungry modules, a backscatter node does not need any active RF components, therefore, can be deployed to have miniature hardware with exceptionally low power consumption [21].

5.1.1 Related Work

Most studies regarding WBANs in the literature focus on devices that harvest energy through a rectenna-based energy harvesting device that converts the signals captured either from ambient, or biomechanical and biochemical energy sources available inside the human body. Despite the fact that this technique of harvesting energy is feasible, the amount of harvested energy is typically very limited. On the other hand, BackCom has gained significant attention due to the fact that it can extend the battery life of the wireless network by consuming less power. However, BackCom has not been thoroughly investigated for eHealth systems. There is only a limited number of works in the literature that considered BackCom technology for eHealth systems. In [75], Kwan *et al.* studied a two-way data transmission optimization problem for wireless powered communication network (WPCN) consisting of multiple on/in body SNs and multiple hybrid access points (H-APs). More specifically, a blind adaptive beamforming with combination sensors (MS2-BABF/combo) protocol with time switching and power splitting structure is studied on a time block divided into three phases that includes energy harvesting/backscatter uplink phase, downlink data decoding phase, and uplink data transmission phase. The MS2-BABF/combo protocol optimizes the beamforming vector at each H-AP, duration of time used by H-AP in transmitting energy signals, power splitting ratio between energy harvesting and data decoding, and system timings such as to maximize the total throughput of WPCN, including the throughput fairness between sensors by adopting the Jain's fairness index. MS2-BABF/combo algorithm attempts to maximize the throughput of WPCN by using the optimal beamforming vector for each H-AP and the duration of time used by the RF source in transmitting energy signals for each H-AP by initially considering no SN in the BackCom mode. Later on, the algorithm considers one SN at a time starting with the SN with the lowest signal-to-noise ratio (SNR) to be operated in a BackCom mode.

Based on the previous SNs operation mode configuration, the algorithm keeps a check to observe if adding more SNs to the BackCom mode will result in any improvement in the WPCN throughput. If there is no improvement, it shows that adding more SNs to the BackCom mode will not enhance the throughput any further indicating that the global optimal solution has already been reached.

Ling *et al.* in [76] proposed an optimal resource allocation for point-to-point WBAN by employing BackCom and harvest-then-transmit (HTT) modes. The authors treated each mode independently and solved the throughput maximization problem by optimizing the time slots, reflection coefficient, and the SN's transmit power by considering only one SN. Zang *et al.* in [77] investigated an experimental study of a throughput maximization of BackCom-based WBAN studied on a time block that only considers the BackCom mode in which SNs take turns to transmit data to the gateway using passive BackCom technology. The proposed optimization scheme utilizes the CVX toolbox to jointly optimize the emitting power of the source as well as the backscatter time by collecting real-time WBAN data of a patient in a walking scenario.

BackCom technology has also been studied in the literature to prolong the lifetime of wireless powered backscatter communication networks (WPCNs). In this regard, Ye *et al.* in [78] considered a WPCN consisting of one transmitter-receiver pair and one BackCom node to maximize the EE by optimizing the transmit power, time allocation, and reflection coefficient by only considering the passive BackCom mode. In [79], Lyu *et al.* studied a WPCN that considers a power beacon (PB), an access point, one hybrid device (HD) operating in HTT mode, and one BackCom device operating in BackCom mode. The proposed scheme maximizes the EE by optimizing the beamforming vector adopted at PB, time, and power allocation by using fractional programming and a semidefinite relaxation approach. Shi *et al.* in [80] studied a WPCN consisting of a PB, a reader node, and

multiple HDs that can either operate in the BackCom or HTT modes. The proposed scheme maximizes the EE by optimizing the PB's and HDs transmit power and the time allocation between the BackCom and HTT modes to obtain the optimal solution using the iterative algorithm. In [81], Xu *et al.* studied a multi-subcarrier WPCN consisting of a dedicated power source and one information transmitter-receiver pair to solve the rate maximization problem by optimizing the power allocation, time allocation, energy allocation, and reflection coefficient. Yang *et al.* in [82], proposed an unmanned aerial vehicle (UAV) enabled hybrid BackCom-HTT IoT network in which UAV serves as a mobile PB to provide energy signals to the IoT nodes. The proposed scheme maximizes the EE by optimizing the UAV's transmit power and trajectory, BackCom reflection coefficients of the nodes, and time allocation by using fractional programming to obtain the solution.

5.1.2 Contributions

Based on the above discussion on BackCom based resource allocation, in comparison with the throughput maximization problem [75,76], and [81], the problem formulation, analysis, and the solution of a proposed problem in our work are different as it focuses on maximizing the EE of WBAN defined as ratio of the overall achievable throughput to the sum of total transmission and circuit power consumption of WBAN [83]. Considering the fractional EE objective function makes the optimization problem more complex to solve due to the coupling of the decision variables. Moreover, unlike MS2-BABF/combo algorithm [75] that initially considers no SN in the BackCom mode and then, later on, considers one SN at a time starting with the SN with the lowest SNR to be operated in a BackCom mode such that not all the SNs are always selected to be operated in BackCom mode, in our work all SNs take turns to operate in the BackCom mode during the passive BackCom phase.

Similarly, in comparison with the related works that only considered one SN [76, 78, 79], in [81], and the studies that treated both BackCom and HTT modes independently [76], or only considered the BackCom mode as in [78], our work considers the WBAN with multiple SNs that are supported to operate under both BackCom and HTT modes. eHealth system with multiple SNs and considering the time frame in which BackCom and HTT modes are not independent makes the optimization problem more challenging and complex to solve due to the more optimization variables being involved. In [75,76,78,79], and [81], there are no constraints that restrict the transmit power of the SNs, which is unsuitable for WBANs as excessive transmission power of SNs can be hazardous to human health [84]. Moreover, in order to fully exploit the information transmission time, the aggregator in our work is assumed to operate both in the downlink frequency for sending energy signals to the SNs, and the corresponding uplink frequency on which the SNs can either backscatter or perform active data transmission to the aggregator. Based on such an assumption, we have considered an energy harvesting model such that, when a specific SN is transmitting data to the aggregator during the active data transmission phase the remaining SNs can still harvest energy from the aggregator's signal and store it for operations in next time frame. Therefore, in comparison to the existing literature with an assumption that the aggregator stays silent during the active data transmission phase, our optimization problem involves coupling of the BackCom and data transmission time variables.

In this work, we investigate the energy-efficient resource allocation problem for BackCom-based WBAN. The objective of any resource allocation framework in WBAN is to better exploit the network resources given a particular transmission scenario while ensuring a satisfactory performance level for each SN. In this regard, the proposed model is studied on a time frame divided into two phases, i.e., the passive BackCom phase and the active data transmission phase. The main contributions of this work are summarized as follows

- A resource allocation optimization framework is proposed to maximize the EE of eHealth monitoring WBAN subject to energy harvesting and power budget constraints, whereas the communication between SNs and aggregator is assisted by adopting BackCom. In order to design an energy-efficient system, and to make the best use of available resources, the SNs are supported to operate in two different communication modes, i.e., the BackCom and HTT modes. In this regard, an EE maximization problem is formulated that optimizes the aggregator's transmit power, BackCom time, and data transmission time of each SN, with the principal aim of using the power of energy-constrained WBAN with a stricter economy.

- One of our aims in this work is to design an eHealth system that can incorporate different movements/activities of the patients during daily life. This is a challenging task as each arbitrary movement of the patient has its own specific propagation characteristics, and accurate modeling of the WBAN radio propagation channel is required that is appropriate for a variety of body movements. Numerous statistical characterizations based on real-time measurements are studied in literature to approximate the human body radio propagation channel [69]. In this regard, the channel model of patients with activities like walking, outdoor jogging, driving a car, general home, and office activities was found to be characterized by Weibull or gamma distributions [67, 68]. For more aggressive activities such as running, the authors in [68] showed that the propagation characteristics of the communication channel can be best modeled by a lognormal distribution. Later, in [69] it is shown that the well-known Rayleigh distribution, commonly assumed for WBAN communication channel—is a poor fit for such scenarios. Therefore, in this work, instead of utilizing a different distribution to model various patient conditions, a generalized gamma distribution is adopted for the BackCom based eHealth monitoring WBAN.

A generalized gamma distribution can support propagation scenarios under different body movements and helps model the radio-propagation channel that can easily characterize the Weibull, gamma, and lognormal distributions [85]. In this regard, the EE optimization problem formulation in our work utilizes the generalized gamma distribution for channel gain to noise ratio whose parameters are used to model the different body movements of the patient.

- To facilitate obtaining the solution, we first prove that the nonlinear fractional EE objective function is quasi-concave and then it is converted to an equivalent parametric form by using the Dinkelbach algorithm, and the corresponding KKT conditions are solved. Based on the expected value of the overall throughput, we obtain the throughput performance lower and upper bounds to show that the results of the EE maximization problem using both the bounds are tight. To reduce the computational complexity, the structure of the EE optimization problem is analyzed and an iterative suboptimal solution is provided whose performance is fairly close to the optimized solution. Extensive simulations are provided to evaluate the performance of the proposed schemes in comparison with related work from the literature that show the superiority of the proposed algorithm in terms of EE. Simulation results reveal that optimal allocation of aggregator's transmit power, BackCom and data transmission times helps improve EE of the WBAN.

The remaining chapter is organized as follows: In Section 5.2, the system model is described. Section 5.3 formulates the BackCom-based EE optimization problem. Section 5.4 details the optimization problem analysis including optimized and suboptimal solutions. Finally, simulation results are presented in Section 5.5, whereas conclusions are drawn in Section 5.6.

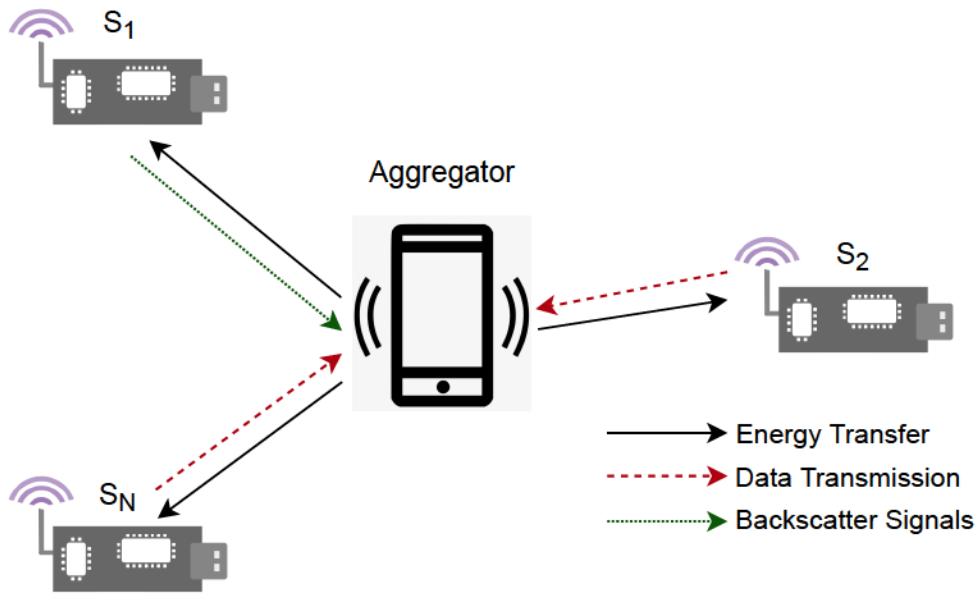

Fig. 5.1: WBAN system model with backscatter communication [83].

5.2 System Model

5.2.1 WBAN Topology

We consider an eHealth monitoring WBAN with one central coordinator node (i.e, an aggregator) that is carried by the patient which serves as both the gateway and energy source for the SNs, as shown in Fig. 5.1. There are N SNs in the network denoted by S_i, where, $i = 1, \ldots, N$. These SNs could be either deployed on the patient's body surface, or they can be embedded inside the body to monitor the vital signs. The SNs are connected in a star topology such that each SN communicates directly with the aggregator. The aggregator is assumed to be connected with a reliable and steady energy supply within easy reach, e.g., a power outlet or a high capacity portable power bank. Note that, for energy harvesting rather than transmitting a random burst signal the aggregator node has to

broadcast the CW signal. In contrast, the SNs are energy-constrained with limited battery capacity and are supposed to have a rechargeable battery with an accompanying energy harvesting device to harvest energy. The downlink frequency upon which the aggregator broadcasts the energy signals to the SNs is represented by f_1. The corresponding uplink frequency upon which the SNs either backscatter the data passively or perform active data transmissions to the aggregator is represented by f_2. The SNs can harvest energy from the CW signals transmitted by the aggregator, which upon storage in their batteries, can be used to support internal operations as well as data transmission to the aggregator. Alternatively, the SNs may exploit the incident broadcast signals to transmit data to the aggregator by performing BackCom.

5.2.2 Time frame Structure

As illustrated in Fig. 5.2, the transmission frame structure is considered to have two operating phases, i.e., the passive BackCom phase, and the active data transmission phase. During the BackCom phase, the SNs can either backscatter signals to transmit data to the aggregator by modulating and reflecting the incident signals of the aggregator, or alternatively, the SNs can harvest and store the energy signals for transmitting their data later in the active data transmission phase. It is important to emphasize that, when a SN S_i is backscattering the data, the remaining $N - i$ SNs in the WBAN can still harvest energy from incident signals of the aggregator. This feature ensures the maximum utilization of the energy signals broadcasted by the aggregator. However, if at a particular time slot more than one SN backscatter their data at the same time, they can create interference for each other. Thus, to avoid such a situation, each SN in the considered WBAN model is equipped with a single antenna, meaning that at a specific time slot, it can only either

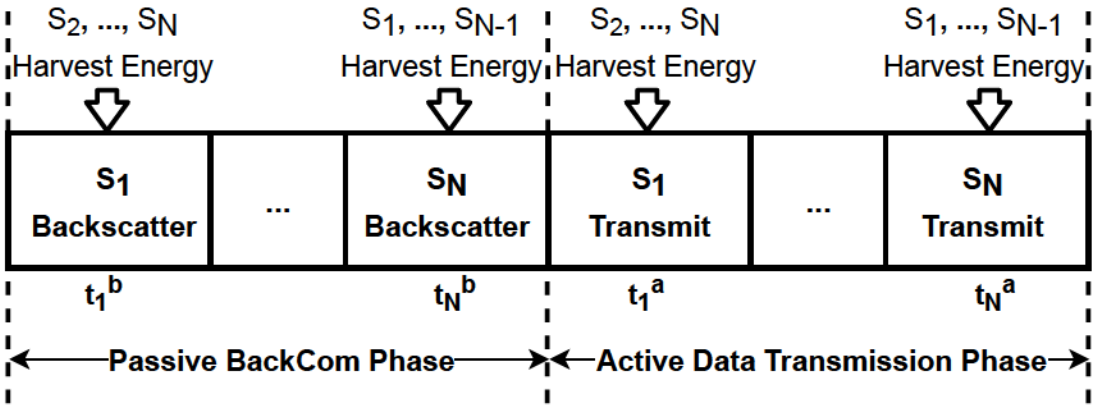

Fig. 5.2: Normalized time frame structure of WBAN.

harvest energy from the signals transmitted by the aggregator or backscatter signals. That said, no two SNs are allowed to backscatter at the same time, assuring the elimination of any possibility for interference.

The backscatter time is allocated to the SN based on multiple factors that include its energy harvesting efficiency, data backscattering rate, and the aggregator's transmit power to maximize the overall EE of the WBAN. The passive BackCom phase and the active data transmission phase of the WBAN under consideration are not independent. As a result, if the SNs spend more time backscattering data in the passive BackCom phase, less duration of time will be allocated to the SNs for transmitting data in the second phase. Moreover, since the SNs are energy-constrained we focus on maximizing the overall EE of the WBAN subject to the energy harvesting and transmission power of the SNs.

In each transmission frame, let t_i^b denotes the normalized amount of time during which sensor S_i backscatter data information to the aggregator and t_i^a represents the normalized time duration allocated to the sensor S_i for transmitting data to the aggregator. Since during a particular transmission frame, t_i^b and t_i^a are the portions of the time allocated to sensor S_i either for data backscattering or performing active data transmission, respectively,

therefore in a particular transmission frame the total normalized time is given by the following constraints

$$\begin{cases} \sum_{i=1}^{N} t_i^b + \sum_{i=1}^{N} t_i^a \leq 1, \\ \\ t_i^b, t_i^a \geq 0, \quad \forall i \in \{1, \ldots, N\}. \end{cases} \tag{5.1}$$

5.3 Energy Efficiency Optimization Problem Formulation

In this section, we discuss and formulate the optimization problem that aims to maximize the EE of a BackCom-assisted WBAN. In particular, the optimization problem optimally allocates the transmit power of the aggregator, backscatter and transmission times of energy-constrained SNs subject to energy harvesting and transmission power constraints. Additionally, the WBAN under consideration is supposed to operate under two communication modes: 1) BackCom mode and 2) HTT mode, whose details are provided in the subsections. Furthermore, the structure of the optimization problem is analyzed to propose a suboptimal solution at a significantly lower computational complexity.

5.3.1 Passive BackCom Phase

Data backscattering depends only on the first operating phase of the transmission frame. During the passive BackCom phase, the SNs exploit the incident broadcast signals of the aggregator to backscatter their data to the aggregator by employing TDMA as described in Fig. 5.2. In order to obtain a closed-form of the backscatter throughput, the

receiver/aggregator must be able to sample the received backscatter signal for demodulating and decoding the data information. Obtaining the digital samples, on the other hand, necessitates the use of an ADC, which is often avoided in ultra-low-power designs. In this regard, the decoding mechanism proposed in [86] allows the receiver to decode the data information with high efficiency by utilizing an envelope detector and averaging circuit and a threshold computation circuit. In order to evaluate the feasibility of the proposed mechanism the hardware prototype is implemented and real time experiments were performed in a metropolitan area at different indoor and outdoor locations to account for the multipath and attenuation effect by considering the channel between the backscatter transmitter and receiver that is not ideal. Firstly, the envelope detection and averaging circuit smoothes by averaging out the variations of the received signals, then, based on the two signal levels produced at the output of the averaging circuit the threshold value is calculated. Finally, the comparison circuit consisting of an RC circuit and a comparator compares the average envelope signal and the threshold to distinguish between the output "0" and the "1" bits.

Under the proposed decoding mechanism in [86], the closed-form of the backscatter throughput for the BackCom mode can not be derived as it explicitly depends on the decoding circuit, and the BackCom rate can be regulated by adjusting the RC circuit elements of the aggregator node. As a result, for a given BackCom system, the BackCom achievable rate can only be determined through real experiments [87] as performed in [86] by considering practical channel conditions in which the channel between the backscatter transmitter and receiver is not ideal.

In [88], a hybrid BackCom for WPCNs is proposed. The authors have considered two zones such as long-range WiFi-zone and short-range Macro-zone in which the achievable BackCom rates for each zone are specified with different rate equations. For instance, short-range Macro-zone transmission up to 15 meters the achievable rates are prototype

dependent and the BackCom rate is limited by the transceiver design. Since the achievable rate of the short-range BackCom transmission is unknown [88], therefore based on the designed prototype in [86] the authors have used the fixed BackCom rate that depends on the real experiments.

Since the communication in WBAN is in the range of few meters only, and the focus of our work is to design an energy-efficient WBAN, therefore by following the decoding mechanism [86], we have assumed that the achievable BackCom rate can be determined in advance by means of testing through real-time experiments as considered in [87–92], which is more relevant and related to the short-range WBAN communications. Therefore, the BackCom throughput of SN S_i during data BackCom phase denoted as $\mathcal{R}_i^b$, can be expressed as follows

$$\mathcal{R}_i^b = t_i^b B_i^b, \tag{5.2}$$

where B_i^b represents the achievable backscatter rate of sensor S_i, i.e., the number of data bits successfully decoded at the aggregator by using BackCom [87–92]. It is worth noting that when a sensor S_i is backscattering its data signals to the aggregator, in the mean-time other SNs in the WBAN simultaneously harvest energy from the signals broadcasted by the aggregator, and this guarantees that the SNs have sufficient time for both data backscattering and energy harvesting.

5.3.2 Active Data Transmission Phase

The data transmission of SNs depends on both the passive BackCom phase and the active data transmission phase of the time frame. The SNs adopt the HTT protocol to harvest the energy first in the passive BackCom phase from the signals broadcast by the aggregator.

Then, the SNs utilize the harvested energy for transmitting data in the active data transmission phase using TDMA. Since the aggregator is transmitting and receiving on different frequency channels, therefore in order to efficiently utilize the available resources, it should be noted that when the SN S_i is transmitting the data to the aggregator during the active data transmission phase the remaining SNs in the network can still harvest energy from the aggregator's signal and store it for the operations in next transmission block. In the following, we formulate the energy harvesting model, power consumption model, and the total throughput of the SNs in the active data transmission phase.

1) Energy Harvesting Model:

As stated in [93], the energy received by the sensor S_i from the signals transmitted by the aggregator can be computed by using Friis free space propagation model, which can be mathematically given as follows

$$P_i^{\mathrm{R}} = \delta_i P_t \frac{G^{\mathrm{T}} G_i^{\mathrm{R}} \lambda^2}{(4\pi d_i)^2}, \tag{5.3}$$

where P_i^{R} is the harvested power of sensor S_i and δ_i is its energy harvesting efficiency. The transmit power and the antenna gain of the aggregator are denoted by P_t, G^{T}, respectively. G_i^{R} is the antenna gain of SN S_i. λ represents the wavelength, and d_i is the distance of S_i from the aggregator.

In a particular transmission frame, the SN S_i uses t_i^b amount of time for data backscattering and t_i^a amount of time is utilized for active data transmission, whereas all the remaining slots are used for harvesting energy. Therefore, based on the received energy signals from the aggregator, the total energy harvesting time of sensor S_i in each transmission frame is given as $\left(\left(\sum_{n=1}^{N} t_n^b\right) - t_i^b + \left(\sum_{n=1}^{N} t_n^a\right) - t_i^a\right)$. Thus, the total energy harvested

by S_i in one transmission frame, denoted as E_i^h, which is equal to the total energy harvesting time of SN S_i multiplied by the harvested power P_i^{R}. This can be mathematically expressed as follows

$$E_i^h = \left(\left(\sum_{n=1}^{N} t_n^b \right) - t_i^b + \left(\sum_{n=1}^{N} t_n^a \right) - t_i^a \right) P_i^{\mathrm{R}}, \tag{5.4}$$

***2) Power Consumption Model*:**

The energy consumption of a SN mainly depends on sensing, data processing and data communication for transmitting data to the aggregator. The sensing power consumption is mainly responsible for sensing operations including the signal amplification and ADC. The ADC converts the analog signals of the sensors into digital signals, which are subsequently supplied into the processing unit. The key functions of the data processing module are sensor controlling and data processing using the microcontroller unit (MCU). The power consumption of the amplification and ADC block is usually very low (in μW), and the TI MS430P microcontrollers family generally used in health monitoring also have low power consumption [94].

The SN S_i utilizes the harvested energy to transmit its data to the aggregator during the time slot t_i^a in the data transmission phase. Let P_i^{a} represents the transmit power of the SN S_i during the transmission time slot t_i^a, which can be obtained as E_i^h/t_i^a. Note that, the major power consumption is due to the communication module in which the SNs transmit their data during the active data transmission phase [95]. In order to better understand this concept [95] showed through an example by comparing the energy consumption costs of the data processing by radio and data transmission. It is showed that for ground-to-ground transmission, 3 J of energy is consumed to send 1 kb of data across a distance of

100 m. In contrast, a general purpose processor with a modest processing capability of 100 million instructions per second can execute 300 million instructions for the same amount of energy. Therefore, the total transmission power consumption of N SNs in eHealth monitoring WBAN can be written as follows [52, 96, 97]

$$\begin{aligned} P_{\text{sum}} &= P_c + \sum_{i=1}^{N} P_i^{\text{a}} \\ &= P_c + \sum_{i=1}^{N} \left[\frac{\left(\left(\sum_{n=1}^{N} t_n^b \right) - t_i^b + \left(\sum_{n=1}^{N} t_n^a \right) - t_i^a \right) P_i^{\text{R}}}{t_i^a} \right], \end{aligned} \tag{5.5}$$

where power consumption P_c is written as $P_c = p_a + p_b + p_c$, where p_a represents the fixed circuit power consumption of the aggregator [79], p_b is the total circuit power consumption in the BackCom phase [76, 98], and p_c is the total power consumption required to transmit the information from SNs to the aggregator including the sensing and processing power consumption [52, 81].

Let r_i^a be the maximum achievable transmission rate of SN S_i during active data transmission phase, which can be written as follows [99]

$$r_i^a = W \log_2(1 + \gamma_i P_i^{\text{a}}), \tag{5.6}$$

where W is the bandwidth of the channel from SN to the aggregator. $\gamma_i = |g_i|^2/N_0$ is the instantaneous channel gain to noise ratio of SN S_i, where g_i is the complex channel coefficient between SN S_i and the aggregator, and N_0 is the noise power. Then, the total number of data bits transmitted by SN S_i during the active data transmission time t_i^a

denoted as $\mathcal{R}_i^a$ can be given as follows

$$\mathcal{R}_i^a = \psi_i t_i^a \log_2 \left(1 + \gamma_i \frac{\left(\left(\sum_{n=1}^{N} t_n^b \right) - t_i^b + \left(\sum_{n=1}^{N} t_n^a \right) - t_i^a \right) P_i^{\mathrm{R}}}{t_i^a} \right), \tag{5.7}$$

where $\psi_i = \epsilon_i W$, and $\epsilon_i \in (0, 1)$ represents the transmission efficiency coefficient. The total throughput of the sensor S_i is the sum of the number of bits transmitted during the passive BackCom and active data transmission phases, i.e., $\mathcal{R}_i = \mathcal{R}_i^b + \mathcal{R}_i^a$, written as follows

$$\mathcal{R}_{\mathrm{i}} = t_i^b B_i^b + \psi_i t_i^a \log_2 \left(1 + \gamma_i \frac{\left(\left(\sum_{n=1}^{N} t_n^b \right) - t_i^b + \left(\sum_{n=1}^{N} t_n^a \right) - t_i^a \right) P_i^{\mathrm{R}}}{t_i^a} \right), \tag{5.8}$$

Thus, the overall achievable throughput of N sensors in a WBAN, denoted as $\mathcal{R}_{\mathrm{sum}}$, can be written as follows

$$\mathcal{R}_{\mathrm{sum}} = \sum_{i=1}^{N} \left[t_i^b B_i^b + \psi_i t_i^a \log_2 \left(1 + \gamma_i \frac{\left(\left(\sum_{n=1}^{N} t_n^b \right) - t_i^b + \left(\sum_{n=1}^{N} t_n^a \right) - t_i^a \right) P_i^{\mathrm{R}}}{t_i^a} \right) \right]. \tag{5.9}$$

Note that, in this work, we consider the average value of the total throughput over a large number of channel realizations. The average value of the throughput does not require an estimation of the channel coefficients every coherence time, which significantly reduces the complexity of the system. The overall average throughput of the WBAN represented as $\mathcal{R}_{\mathrm{avg}} = \mathbb{E}[\mathcal{R}_{\mathrm{sum}}]$, which can be calculated as follows

$$\mathbb{E}[\mathcal{R}_{\mathrm{sum}}] = \sum_{i=1}^{N} \left[\mathbb{E}\left[t_i^b B_i^b \right] + \mathbb{E}\left[\psi_i t_i^a \log_2 \left(1 + \gamma_i \frac{E_i^h}{t_i^a} \right) \right] \right], \tag{5.10}$$

where $\mathbb{E}[\cdot]$ represents the expected value. Let $f(\cdot)$ be a real-valued concave function with respect to x, where x be the random variable with finite expectation, then the Jensen's inequality [100] can be stated as $\mathbb{E}[f(x)] \leq f(\mathbb{E}[x])$. Since γ_i is the only random variable in (5.10), therefore it can be easily verified that (5.10) is a concave function of γ_i by showing that the second derivative $\mathcal{R}''_{\text{sum}}(\gamma_i) \leq 0$. Accordingly, by applying the Jensen's inequality on (5.10) as $\mathbb{E}\left[\log\left(1+x\right)\right] \leq \log(1+\mathbb{E}\left[x\right])$, expected value of the overall throughput performance upper bound can be written as

$$\mathcal{R}_{\text{avg}} \leq \sum_{i=1}^{N} \left[t_i^b B_i^b + \psi_i t_i^a \log_2 \mathbb{E}\left[1 + \gamma_i \frac{E_i^h}{t_i^a}\right]\right]. \tag{5.11}$$

Consequently, after simple mathematical manipulations and by using the expectation properties, the expected value of the overall throughput performance upper bound can be written as follows

$$\mathcal{R}_{\text{avg}} \leq \sum_{i=1}^{N} \left[t_i^b B_i^b + \psi_i t_i^a \log_2 \left(1 + \frac{E_i^h}{t_i^a} \mathbb{E}\left\{\gamma_i\right\}\right)\right]. \tag{5.12}$$

Similarly, by convexity of $\log_2\left(1+1/z\right)$, where $z = 1/x$ for $z > 0$, and by applying the Jensen's inequality, the overall throughput performance lower bound can be written as follows [101]

$$\mathcal{R}_{\text{avg}} \geq \sum_{i=1}^{N} \left[t_i^b B_i^b + \psi_i t_i^a \log_2 \left(1 + \frac{E_i^h}{t_i^a} \mathbb{E}\left\{\frac{1}{\gamma_i}\right\}^{-1}\right)\right]. \tag{5.13}$$

Note that, the exact value of the overall throughput expression given in (5.10) is bounded between the throughput performance upper and lower bounds given in (5.12)

and (5.13), which can be written as follows

$$\underbrace{\sum_{i=1}^{N}\left[\eta_i t_i^b B_i^b + \psi_i t_i^a \log_2\left(1+\frac{E_i^h}{t_i^a}\mathbb{E}\left\{\frac{1}{\gamma_i}\right\}^{-1}\right)\right]}_{\text{Lower bound of throughput}} \leq \sum_{i=1}^{N}\left[\eta_i t_i^b B_i^b + \mathbb{E}\left\{\psi_i t_i^a \log_2\left(1+\gamma_i\frac{E_i^h}{t_i^a}\right)\right\}\right] \leq$$

$$\underbrace{\sum_{i=1}^{N}\left[\eta_i t_i^b B_i^b + \psi_i t_i^a \log_2\left(1+\frac{E_i^h}{t_i^a}\mathbb{E}\left\{\gamma_i\right\}\right)\right]}_{\text{Upper bound of throughput}}. \tag{5.14}$$

As discussed earlier, one of our aims in this work is to design a WBAN that can incorporate different movements/activities of the patients during daily life and their corresponding transmission requirements. Therefore, in order to design a reliable WBAN communication system, a generalized gamma distribution for γ_i is adopted to model the radio-propagation channel that can support propagation scenarios under different body movements [85]. The PDF of γ_i is given as follows

$$f(\gamma_i; a_i, b_i, c_i) = \frac{c_i}{b_i^{a_i c_i}\Gamma(a_i)}\gamma_i^{a_i c_i - 1}\exp\left(-\left(\frac{\gamma_i}{b_i}\right)^{c_i}\right), \tag{5.15}$$

where $\Gamma(.)$ is the standard gamma function, a_i and c_i are the shape parameters of the generalized gamma distribution, respectively, and b_i is the scale parameter. From overall throughput performance upper bound in (5.14), the expected value of well-known generalized gamma distribution $\mathbb{E}\{\gamma_i\}$ can be written as [102]

$$\mathbb{E}\{\gamma_i\} = \frac{b_i\Gamma(a_i + 1/c_i)}{\Gamma(a_i)} = \chi_{UB}. \tag{5.16}$$

Similarly, from overall throughput performance lower bound in (5.14), the expected value of the inverse of the generalized gamma distribution $\mathbb{E}\left\{\frac{1}{\gamma_i}\right\}$ can be calculated by

doing the integration as follows

$$\begin{aligned}
\mathbb{E}\left\{\frac{1}{\gamma_i}\right\} &= \int_0^{\infty} \frac{1}{\gamma_i} \frac{c_i}{b_i^{a_i c_i}\Gamma(a_i)} \gamma_i^{a_i c_i - 1} \exp\left(-\left(\frac{\gamma_i}{b_i}\right)^{c_i}\right), \\
&= \int_0^{\infty} \frac{c_i \Gamma(a_i - 1/c_i)}{b_i b_i^{a_i c_i - 1}\Gamma(a_i - 1/c_i)\Gamma(a_i)} \gamma_i^{a_i c_i - 2} \exp\left(-\left(\frac{\gamma_i}{b_i}\right)^{c_i}\right), \\
&= \frac{\Gamma(a_i - 1/c_i)}{b_i \Gamma(a_i)} \int_0^{\infty} \frac{c_i}{b_i^{a_i c_i - 1}\Gamma(a_i - 1/c_i)} \gamma_i^{a_i c_i - 2} \exp\left(-\left(\frac{\gamma_i}{b_i}\right)^{c_i}\right), \\
&= \frac{\Gamma(a_i - 1/c_i)}{b_i \Gamma(a_i)}, \qquad (5.17)
\end{aligned}$$

From (5.17), $\mathbb{E}\left\{\frac{1}{\gamma_i}\right\}^{-1}$ can be written as

$$\mathbb{E}\left\{\frac{1}{\gamma_i}\right\}^{-1} = \frac{b_i \Gamma(a_i)}{\Gamma(a_i - 1/c_i)} = \chi_{LB}. \qquad (5.18)$$

Therefore, the exact value of the overall throughput bounded between the lower and the upper bounds of the throughput can be written as

$$\underbrace{\sum_{i=1}^{N}\left[\eta_i t_i^b B_i^b + \psi_i t_i^a \log_2\left(1 + \frac{E_i^h \chi_{LB}}{t_i^a}\right)\right]}_{\text{Lower bound of throughput}} \leq \sum_{i=1}^{N}\left[\eta_i t_i^b B_i^b + \mathbb{E}\left\{\psi_i t_i^a \log_2\left(1 + \gamma_i \frac{E_i^h}{t_i^a}\right)\right\}\right] \leq$$

$$\underbrace{\sum_{i=1}^{N}\left[\eta_i t_i^b B_i^b + \psi_i t_i^a \log_2\left(1 + \frac{E_i^h \chi_{UB}}{t_i^a}\right)\right]}_{\text{Upper bound of throughput}}. \qquad (5.19)$$

Thus, the EE objective function η_{EE} (measured in bits/Joule) is defined as the ratio of the overall achievable throughput of WBAN to the sum of the total transmission power

and circuit power consumption of all the SNs in the network, can be written as follows

$$\eta_{EE} = \frac{\sum_{i=1}^{N}\left[t_i^b B_i^b + \psi_i t_i^a \log_2\left(1+\frac{E_i^h \kappa_i}{t_i^a}\right)\right]}{P_c + \sum_{i=1}^{N}\left[\frac{\left(\left(\sum_{n=1}^{N} t_n^b\right) - t_i^b + \left(\sum_{n=1}^{N} t_n^a\right) - t_i^a\right) P_i^{\mathrm{R}}}{t_i^a}\right]}. \tag{5.20}$$

Consequently, the optimization problem to maximize the EE of eHealth monitoring WBAN can be formally expressed as follows

$$\begin{aligned}
\max_{t^a,\, t^b,\, P_t} \quad & \frac{\sum_{i=1}^{N}\left[t_i^b B_i^b + \psi_i t_i^a \log_2\left(1+\frac{E_i^h \kappa_i}{t_i^a}\right)\right]}{P_c + \sum_{i=1}^{N}\left[\frac{\left(\left(\sum_{n=1}^{N} t_n^b\right) - t_i^b + \left(\sum_{n=1}^{N} t_n^a\right) - t_i^a\right) P_i^{\mathrm{R}}}{t_i^a}\right]} \\
\text{s. t.} \quad & \mathcal{C}_1 : \frac{\left(\left(\sum_{n=1}^{N} t_n^b\right) - t_i^b + \left(\sum_{n=1}^{N} t_n^a\right) - t_i^a\right) P_i^{\mathrm{R}}}{t_i^a} \leq P_i^{\max}, \\
& \mathcal{C}_2 : \left(\left(\sum_{n=1}^{N} t_n^b\right) - t_i^b + \left(\sum_{n=1}^{N} t_n^a\right) - t_i^a\right) P_i^{\mathrm{R}} \geq E_i^{\min}, \\
& \mathcal{C}_3 : \left(\left(\sum_{n=1}^{N} t_n^b\right) - t_i^b + \left(\sum_{n=1}^{N} t_n^a\right) - t_i^a\right) P_i^{\mathrm{R}} \leq E_i^{\max}, \\
& \mathcal{C}_4 : \sum_{i=1}^{N} t_i^b + \sum_{i=1}^{N} t_i^a \leq 1, \\
& \mathcal{C}_5 : P_t \leq P_t^{\max}, \\
& \mathcal{C}_6 : t_i^b, t_i^a \geq 0.
\end{aligned} \tag{5.21}$$

Note that, the term κ_i in (5.21) can either take the value $\chi_{_{UB}}$ or $\chi_{_{LB}}$ as given in (5.16) and (5.18) to obtain the EE optimization problem using the throughput performance upper or lower bound, respectively. In optimization problem (5.21), the variables $\boldsymbol{t^b} = [t_1^b, \ldots, t_N^b]$, and $\boldsymbol{t^a} = [t_1^a, \ldots, t_N^a]$, are vectors of the data BackCom and data transmission times of all the SNs in the WBAN, respectively. The variable P_t represents the transmit power of the aggregator. Note that, the term E_i^h in the total throughput of the EE objective is a function of t_i^b, t_i^a, and P_t. Similarly, in the total power consumption, the term P_i^{R} is a function of P_t, such that all the decision variables are coupled in the numerator and the denominator of the EE objective function. In order to avoid the harmful effects of the transmit power of the SNs on the human body, the constraint $\mathcal{C}_1$ bounds the transmit power of each SN such that it should be less than or equal to the maximum transmit power threshold of the SN denoted as $P_i^{\max}$. The constraint $\mathcal{C}_2$ ensures the total harvested energy of each SN must not be less than the minimum energy $E_i^{\min}$ needed to be maintained at the SN. Due to the finite battery capacity of the SN, $\mathcal{C}_3$ guarantees that the total harvested energy of each SN must not exceed its maximum battery capacity $E_i^{\max}$. The constraint $\mathcal{C}_4$ reflects that the total normalized time during both the operating phases must be less than or equal to one. The constraint $\mathcal{C}_5$ requires that P_t should be no greater than the predefined maximum power threshold of the aggregator denoted as $P_t^{\max}$.

5.4 Optimization Problem Analysis and Solution

In this section, the EE optimization problem is analyzed and solved by using the concepts of fractional programming. To facilitate obtaining the solution, the Dinkelbach algorithm is utilized to convert the nonlinear fractional problem to an equivalent parametric problem. To balance between the computational complexity and achievable performance, the

inherent structure of the EE optimization problem is analyzed to provide an iterative based suboptimal heuristic solution.

5.4.1 Optimization Problem Solution

In order to find the solution of the formulated EE optimization problem, we first prove (as shown in the Appendix A) that the overall throughput function in the numerator of (5.21) is concave with respect to (t_i^a, t_i^b, P_t), and the total power consumption in the denominator is convex with respect to (t_i^a, t_i^b), and affine with respect to P_t. That said, the concave-convex fractional EE optimization problem in (5.21) is a quasi-concave with respect to time variables $\forall\ (t_i^a, t_i^b)$, where $i \in \{1, \ldots, N\}$, and the aggregator's transmit power P_t, individually. Such characteristics allow us to utilize the primal Dinkelbach algorithm [103] to solve the parametric concave-convex optimization problem. Accordingly, the nonlinear fractional EE problem in (5.21) can be converted to an equivalent parametric problem, written as follows

$$\begin{aligned}
&\max_{t^a,\, t^b,\, P_t} \sum_{i=1}^{N} \left[t_i^b B_i^b + \psi_i t_i^a \log_2 \left(1 + \frac{E_i^h \kappa_i}{t_i^a} \right) \right] \\
&\quad -q \left(P_c + \sum_{i=1}^{N} \left[\frac{\left(\left(\sum_{n=1}^{N} t_n^b \right) - t_i^b + \left(\sum_{n=1}^{N} t_n^a \right) - t_i^a \right) P_i^{\mathrm{R}}}{t_i^a} \right] \right) \\
&\text{s. t.} \quad \mathcal{C}_1, \mathcal{C}_2, \mathcal{C}_3, \mathcal{C}_4, \mathcal{C}_5, \mathcal{C}_6.
\end{aligned} \tag{5.22}$$

where q is a constant non-negative parameter whose optimized value, denoted as q^*, is the maximum EE, i.e., $q^* = \max \eta_{_{EE}}$. The parametric EE maximization problem in (5.22) can

be solved by using the KKT conditions to obtain the solution. The corresponding partial Lagrangian function $\mathcal{L}$ can be written as follows

$$\begin{aligned}
\mathcal{L}(\boldsymbol{t}^a, \boldsymbol{t}^b, P_t, \boldsymbol{\lambda}, \boldsymbol{\beta}, \boldsymbol{\gamma}, \zeta, \sigma) = & \sum_{i=1}^{N} \left[t_i^b B_i^b + \psi_i t_i^a \log_2 \left(1 + \frac{E_i^h \kappa_i}{t_i^a} \right) \right] \\
& - q \left(P_c + \sum_{i=1}^{N} \left[\frac{\left(\left(\sum_{n=1}^{N} t_n^b \right) - t_i^b + \left(\sum_{n=1}^{N} t_n^a \right) - t_i^a \right) P_i^{\mathrm{R}}}{t_i^a} \right] \right) \\
& - \sum_{i=1}^{N} \lambda_i \left(\left(\left(\sum_{n=1}^{N} t_n^b \right) - t_i^b + \left(\sum_{n=1}^{N} t_n^a \right) - t_i^a \right) P_i^{\mathrm{R}} - t_i^a P_i^{\max} \right) \\
& - \sum_{i=1}^{N} \beta_i \left(E_i^{\min} - \left(\left(\sum_{n=1}^{N} t_n^b \right) - t_i^b + \left(\sum_{n=1}^{N} t_n^a \right) - t_i^a \right) P_i^{\mathrm{R}} \right) \\
& - \sum_{i=1}^{N} \gamma_i \left(\left(\left(\sum_{n=1}^{N} t_n^b \right) - t_i^b + \left(\sum_{n=1}^{N} t_n^a \right) - t_i^a \right) P_i^{\mathrm{R}} - E_i^{\max} \right) \\
& - \zeta \left(\sum_{i=1}^{N} t_i^b + \sum_{i=1}^{N} t_i^a - 1 \right) \\
& - \sigma \left(P_t - P_t^{\max} \right), \qquad (5.23)
\end{aligned}$$

where $\boldsymbol{\lambda} = [\lambda_1, \ldots, \lambda_N]$, $\boldsymbol{\beta} = [\beta_1, \ldots, \beta_N]$, $\boldsymbol{\gamma} = [\gamma_1, \ldots, \gamma_N]$, ζ, and σ are the non-negative Lagrange multipliers associated with the constraints $\mathcal{C}_1, \mathcal{C}_2, \mathcal{C}_3$, $\mathcal{C}_4$, and $\mathcal{C}_5$ respectively, given in (5.21). Since the optimization problem is quasi-concave, the necessary and sufficient KKT conditions can be solved to obtain the solution [71]. The corresponding KKT

conditions of the EE maximization problem can be written as follows

$$\frac{\partial \mathcal{L}(t_i^a, t_i^b, P_t, \lambda_i, \beta_i, \gamma_i, \zeta, \sigma)}{\partial t_i^a} = 0, \tag{5.24}$$

$$\frac{\partial \mathcal{L}(t_i^a, t_i^b, P_t, \lambda_i, \beta_i, \gamma_i, \zeta, \sigma)}{\partial t_i^b} = 0, \tag{5.25}$$

$$\frac{\partial \mathcal{L}(t_i^a, t_i^b, P_t, \lambda_i, \beta_i, \gamma_i, \zeta, \sigma)}{\partial P_t} = 0, \tag{5.26}$$

$$\lambda_i \left(\left(\left(\sum_{n=1}^{N} t_n^b \right) - t_i^b + \left(\sum_{n=1}^{N} t_n^a \right) - t_i^a \right) P_i^{\mathrm{R}} - t_i^a P_i^{\max} \right) = 0, \tag{5.27}$$

$$\beta_i \left(E_i^{\min} - \left(\left(\sum_{n=1}^{N} t_n^b \right) - t_i^b + \left(\sum_{n=1}^{N} t_n^a \right) - t_i^a \right) P_i^{\mathrm{R}} \right) = 0, \tag{5.28}$$

$$\gamma_i \left(\left(\left(\sum_{n=1}^{N} t_n^b \right) - t_i^b + \left(\sum_{n=1}^{N} t_n^a \right) - t_i^a \right) P_i^{\mathrm{R}} - E_i^{\max} \right) = 0, \tag{5.29}$$

$$\zeta \left(\sum_{i=1}^{N} t_i^b + \sum_{i=1}^{N} t_i^a - 1 \right) = 0, \tag{5.30}$$

$$\sigma \left(P_t - P_t^{\max} \right) = 0 \tag{5.31}$$

$$\left(\left(\sum_{n=1}^{N} t_n^b \right) - t_i^b + \left(\sum_{n=1}^{N} t_n^a \right) - t_i^a \right) P_i^{\mathrm{R}} - t_i^a P_i^{\max} \leq 0, \tag{5.32}$$

$$E_i^{\min} - \left(\left(\sum_{n=1}^{N} t_n^b \right) - t_i^b + \left(\sum_{n=1}^{N} t_n^a \right) - t_i^a \right) P_i^{\mathrm{R}} \leq 0, \tag{5.33}$$

$$\left(\left(\sum_{n=1}^{N} t_n^b \right) - t_i^b + \left(\sum_{n=1}^{N} t_n^a \right) - t_i^a \right) P_i^{\mathrm{R}} - E_i^{\max} \leq 0, \tag{5.34}$$

$$\sum_{i=1}^{N} t_i^b + \sum_{i=1}^{N} t_i^a - 1 \leq 0, \tag{5.35}$$

$$P_t - P_t^{\max} \leq 0, \tag{5.36}$$

$$t_i^a, t_i^b, \lambda_i, \beta_i, \gamma_i, \zeta, \sigma \geq 0. \tag{5.37}$$

From (5.24), (5.25), and (5.26) we can obtain (5.38), (5.39), and (5.40) shown below and the top of the next page. For simplification and to save space, the term p_i in (5.40) has its definition in (5.3), such that $P_i^{\mathrm{R}} = \rho_i P_t$. It is important to note that, the term κ_i in (5.38)-(5.40) can either take the value $\chi_{_{UB}}$ or $\chi_{_{LB}}$ as given in (5.16) and (5.18) to obtain the EE optimization problem solution and to evaluate the tightness of the results using the throughput performance upper and lower bound, respectively. It can be seen from (5.24)-(5.31) that there are $5N+3$ equations with $5N+3$ unknown variables that include $\boldsymbol{t}^a, \boldsymbol{t}^b, P_t, \boldsymbol{\lambda}, \boldsymbol{\beta}, \boldsymbol{\gamma}$, ζ, and σ.

$$\sum_{\substack{j=1\\ j\neq i}}^{N} \frac{\psi_j t_j^a P_j^{\mathrm{R}} \kappa_j}{\ln 2 \left[t_j^a + \left(\left(\sum_{n=1}^{N} t_n^b \right) - t_j^b + \left(\sum_{n=1}^{N} t_n^a \right) - t_j^a \right) P_j^{\mathrm{R}} \kappa_j \right]} - \frac{\psi_i E_i^h \kappa_i}{\ln 2 \left[t_i^a + E_i^h \kappa_i \right]}$$
$$+ \psi_i \log_2 \left(1 + \frac{E_i^h \kappa_i}{t_i^a} \right) - q \left(\sum_{\substack{j=1\\ j\neq i}}^{N} \frac{P_j^{\mathrm{R}}}{t_j^a} - \frac{\left(\left(\sum_{n=1}^{N} t_n^b \right) - t_i^b + \left(\sum_{n=1}^{N} t_n^a \right) - t_i^a \right) P_i^{\mathrm{R}}}{t_i^{a2}} \right)$$
$$+ \lambda_i P_i^{\max} - \sum_{\substack{j=1\\ j\neq i}}^{N} \lambda_j P_j^{\mathrm{R}} + \sum_{\substack{j=1\\ j\neq i}}^{N} \beta_j P_j^{\mathrm{R}} - \sum_{\substack{j=1\\ j\neq i}}^{N} \gamma_j P_j^{\mathrm{R}} - \zeta = 0, \quad \forall i = 1, \ldots, N, \quad (5.38)$$

$$B_i^b + \sum_{\substack{j=1\\ j\neq i}}^{N} \frac{\psi_j t_j^a P_j^{\mathrm{R}} \kappa_j}{\ln 2 \left[t_j^a + \left(\left(\sum_{n=1}^{N} t_n^b \right) - t_j^b + \left(\sum_{n=1}^{N} t_n^a \right) - t_j^a \right) P_j^{\mathrm{R}} \kappa_j \right]} - q \left(\sum_{\substack{j=1\\ j\neq i}}^{N} \frac{P_j^{\mathrm{R}}}{t_j^a} \right)$$
$$- \sum_{\substack{j=1\\ j\neq i}}^{N} \lambda_j P_j^{\mathrm{R}} + \sum_{\substack{j=1\\ j\neq i}}^{N} \beta_j P_j^{\mathrm{R}} - \sum_{\substack{j=1\\ j\neq i}}^{N} \gamma_j P_j^{\mathrm{R}} - \zeta = 0, \quad \forall i = 1, \ldots, N, \quad (5.39)$$

$$\sum_{i=1}^{N} \frac{\psi_i t_i^a \left(\left(\sum_{n=1}^{N} t_n^b \right) - t_i^b + \left(\sum_{n=1}^{N} t_n^a \right) - t_i^a \right) \rho_i \kappa_i}{\ln 2 \left[t_i^a + \left(\left(\sum_{n=1}^{N} t_n^b \right) - t_i^b + \left(\sum_{n=1}^{N} t_n^a \right) - t_i^a \right) P_i^{\mathrm{R}} \kappa_i \right]} - q \left(\sum_{i=1}^{N} \frac{\left(\left(\sum_{n=1}^{N} t_n^b \right) - t_i^b + \left(\sum_{n=1}^{N} t_n^a \right) - t_i^a \right) \rho_i}{t_i^a} \right)$$

$$- \sum_{i=1}^{N} \lambda_i \left(\left(\sum_{n=1}^{N} t_n^b \right) - t_i^b + \left(\sum_{n=1}^{N} t_n^a \right) - t_i^a \right) \rho_i + \sum_{i=1}^{N} \beta_i \left(\left(\sum_{n=1}^{N} t_n^b \right) - t_i^b + \left(\sum_{n=1}^{N} t_n^a \right) - t_i^a \right) \rho_i$$

$$- \sum_{i=1}^{N} \gamma_i \left(\left(\sum_{n=1}^{N} t_n^b \right) - t_i^b + \left(\sum_{n=1}^{N} t_n^a \right) - t_i^a \right) \rho_i - \sigma = 0, \qquad (5.40)$$

The parametric optimization problem in (5.22), can be solved by numerically solving the KKT conditions separately over the time variables (t_i^a, t_i^b), and P_t. In order to find the time variables t_i^a and t_i^b a system of $5N+1$ equations with $5N+1$ unknowns as given in (5.38), (5.39), and equations (5.27)-(5.30) are solved simultaneously using the nonlinear equation solver at a specific initial value of q using the primal Dinkelbach iterative algorithm. The MATLAB nonlinear equation solver utilizes the interior-point method to solve the system of equations as described in [71]. After each iteration the value of q is updated with the results obtained from the previous iteration and the parametric problem in (5.22) is solved again until t_i^a and t_i^b are optimized with no further change in values. Later on, by using the optimized values of t_i^a and t_i^b, the transmit power of the aggregator P_t is optimized separately by numerically solving (5.31) and (5.40). The iterative procedure is repeated over time variables and the transmit power of the aggregator until the values of the decision variables are optimized with no further change in the values. The optimized values of time variables t_i^{*a}, t_i^{*b}, and transmit power P_t^* can be used to find the converged q^*. This

converged q^* is the maximum EE value, given as follows

$$q^* = \frac{\sum_{i=1}^{N}\left[t_i^{*b}B_i^b + \psi_i t_i^{*a}\log_2\left(1+\frac{E_i^{*h}\kappa_i}{t_i^{*a}}\right)\right]}{P_c + \sum_{i=1}^{N}\left[\frac{\left(\left(\sum_{n=1}^{N} t_n^{*b}\right)-t_i^{*b}+\left(\sum_{n=1}^{N} t_n^{*a}\right)-t_i^{*a}\right)P_i^{*R}}{t_i^{*a}}\right]}, \tag{5.41}$$

where P_t^* is the optimized transmit power of the aggregator, t_i^{*a}, and t_i^{*b} are the optimized values of the data transmission and data backscattering times of sensor S_i, respectively.

5.4.2 Suboptimal Solution

In this subsection, the structure of the EE optimization problem is analyzed to obtain a low-complexity suboptimal solution. It can be seen that (5.38) and (5.39) are $2N$ equations in $2N$ unknowns for known values of the Lagrange multipliers. Similarly, (5.40) is one equation in one unknown P_t for known values of Lagrange multipliers and time variables t_i^a, t_i^b. Unfortunately, the closed-form expression of time allocation from (5.38) and (5.39), and aggregator's transmit power P_t from (5.40) can not be reached; however, they can be solved efficiently using numerical techniques. In this regard, to reduce the computational complexity of EE optimization problem, an iterative method is used to find the values of decision variables t_i^a, t_i^b, and P_t. Whereas the subgradient method [104] is used to tune the values of the Lagrange multipliers after each iteration such as to converge to the optimal values that satisfies the constraints. The subgradient Lagrange multiplier update rule is given as

$$\lambda_i^{l+1} = \lambda_i^l - \upsilon_i^l(t_i^a P_i^{\max} - E_i^h), \qquad \forall i = 1,\ldots,N, \tag{5.42}$$

$$\beta_i^{l+1} = \beta_i^l - \upsilon_i^l(E_i^h - E_i^{\min}), \qquad \forall i = 1,\ldots,N, \tag{5.43}$$

$$\gamma_i^{l+1} = \gamma_i^l - \upsilon_i^l(E_i^{\max} - E_i^h), \qquad \forall i = 1, \ldots, N, \tag{5.44}$$

$$\zeta^{l+1} = \zeta^l - \upsilon^l\left(1 - \sum_{i=1}^{N} t_i^b + \sum_{i=1}^{N} t_i^a\right), \qquad \forall i = 1, \ldots, N, \tag{5.45}$$

$$\sigma^{l+1} = \sigma^l - \upsilon^l\left(P_t^{\max} - P_t\right), \qquad \forall i = 1, \ldots, N. \tag{5.46}$$

where υ_i represents the sufficiently small step sizes associated with the corresponding Lagrange multipliers, chosen as $\sqrt{0.1}/l$, and l represents the index number. Note that, the MATLAB is used for testing the performance of the proposed algorithm, however it can be implemented in any programming language as an application that can be run on a smart phone. As the goal of the proposed study is to maximize the battery life or EE of energy-constrained SNs that rely on the energy signals harvested from the aggregator, therefore the algorithm needs to be run on the aggregator instead of running it on each SN as a distributed algorithm. As mentioned that we focus on saving energy of the energy-constrained SNs, therefore running the algorithm on an aggregator will incur the operational overhead cost such as computation and processing on the aggregator node rather than the SNs. Therefore, in this regard, the aggregator node in our work is supposed to have sufficient energy and has stable charging access within reach. The suboptimal algorithm to maximize the EE of BackCom assisted eHealth monitoring WBAN is summarized in Algorithm 3 shown at the top of next page.

5.4.3 Complexity Analysis

The computational complexity of the proposed suboptimal algorithm is analyzed as follows: Given the number of iterations needed to update the Lagrange multipliers denoted as $K_{\max}$, to solve the Lagrangian dual method in (5.23) by using the subgradient method

Algorithm 3 Proposed iterative based suboptimal algorithm for energy efficiency maximization problem

1: **INPUT:** $G^T, G_i^R, \lambda, d_i, \delta_i, W, \epsilon_i, a_i, b_i, c_i, B_i^b$.
2: Start with the initial values of $q, t_i^a, t_i^b, P_t, \lambda_i, \beta_i, \gamma_i, \zeta, \sigma$.
3: Calculate the data transmission time t_i^a numerically from (5.38) using the interior-point method in MATLAB.
4: Calculate the data backscattering time t_i^b numerically from (5.39) using the interior-point method in MATLAB.
5: Calculate the transmit power of the aggregator P_t numerically from (5.40) using the interior-point method in MATLAB.
6: Repeat steps 3-5 until the convergence is reached.
7: Update the Lagrange multipliers $\lambda_i^l, \beta_i^l, \gamma_i^l, \zeta^l$, and σ according to (5.42), (5.43), (5.44), (5.45), and (5.46), respectively.
8: Repeat steps 3-7 until the constraints are satisfied or certain stopping criterion is fulfilled.
9: Calculate the value of energy efficiency η_{EE} from (5.20).
10: Update the value of q as with η_{EE} obtained from step 9.
11: Repeat steps 3-10 until the convergence is reached such that the change in η_{EE} is no greater than $\varphi = 0.001$.
12: **OUTPUT:** The suboptimal solution of EE maximization problem.

after each iteration calculated from (5.42), (5.43), (5.44), (5.45), and (5.46), respectively, is of computational complexity $\mathcal{O}(K_{\max}N)$. For each iteration, to solve the optimization problem in (5.22) numerically using the interior point method has a computational complexity of $\mathcal{O}(\sqrt{m_1}\log(m_1))$, where m_1 represents the number of inequality constraints in (5.22) [71, 105]. Given the number of iterations needed to reach the convergence of the Dinkelbach denoted as $L_{\max}$, and $I_{\max}$ are the number of iterations required to alternately solve the time variables t_i^a, t_i^b, and transmit power of the aggregator P_t are calculated according to (5.38), (5.39), and (5.40), respectively. Therefore, the total computational complexity of Algorithm 3 becomes $\mathcal{O}\big[(K_{\max}N + \sqrt{m_1}\log(m_1))L_{\max}I_{\max}\big]$.

5.5 Simulation Results

In this section, simulation results are presented to demonstrate the performance of the proposed EE optimization scheme for eHealth monitoring system. As illustrated in Fig. 5.1, we consider a BackCom-based WBAN with $N = 3$ SNs and one aggregator that not only serves as a gateway but also acts as a power source to stimulate the SNs transmission in WBAN. In the energy harvesting model, the distance d_i from the SN to aggregator is set between 0.3 to 0.7 m [8]. The transmission antenna gain of the aggregator G^T and the SNs G_i^R are chosen as 6 dBi, respectively [106]. In the power consumption model, the power consumption p_c including sensing and processing consumption is considered as 5 mW [79], and the circuit power consumption in the BackCom phase is 10 μW [98]. The transmission efficiency ϵ_i and energy harvesting efficiency δ_i are given as 60% [84,89]. The length of each normalized time frame is set as 1 s. From [8], the minimum energy $E_i^{\min}$ and maximum battery capacity $E_i^{\max}$ of the SN is set to 0.01 J and 0.11 J, respectively. The maximum transmit power $P_i^{\max}$ of the SN is set to 1.5 mW [84]. The parameters of the generalized gamma distribution depend on the measured data under different arbitrary movements of the patient's body during routine activities of daily life, and based on that, the best fitting distribution model is applied. From the experimental results in [68], three most common body postures are modeled using the generalized gamma distribution, i.e., relaxing, walking, and running state.

5.5.1 Energy Efficiency of the WBAN Under Different Body Movements

Fig. 5.3 shows the optimized and suboptimal EE (in bits/Joule) of the WBAN in a relaxing state with generalized gamma distribution parameters set as $a_i = 3.84, b_i = 0.0026$, and

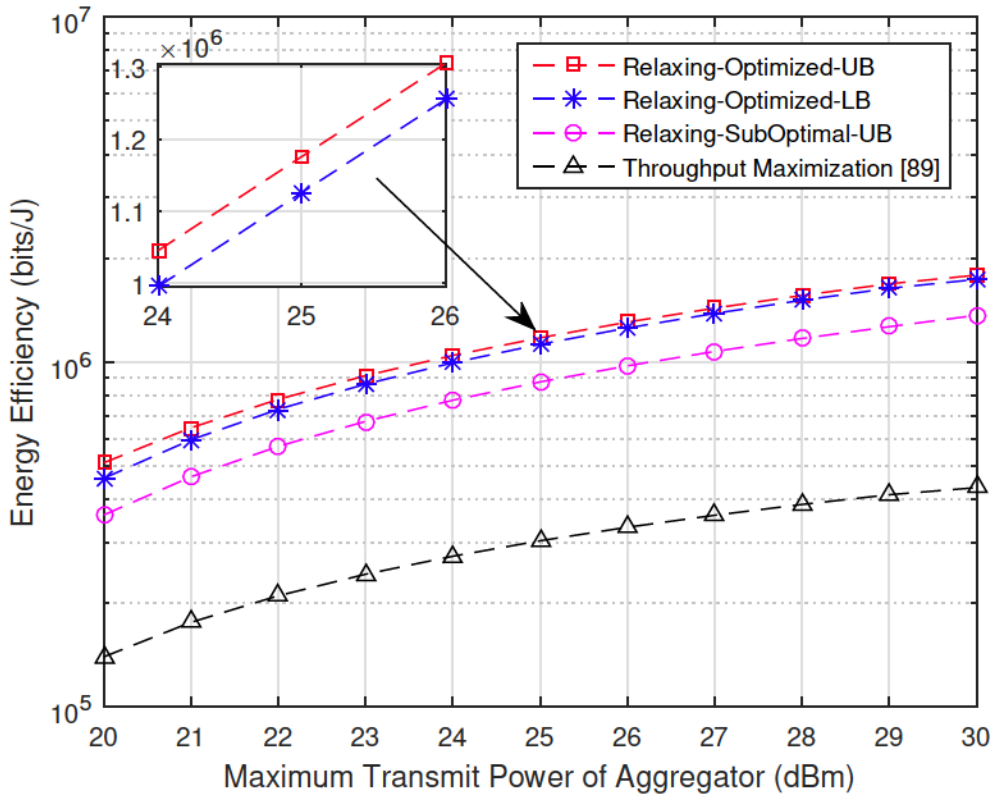

Fig. 5.3: Optimized and suboptimal EE of WBAN for relaxing state with $a_i = 3.84, b_i = 0.0026$, and $c_i = 1$.

$c_i = 1$ [68]. By following the Federal Communications Commission (FCC) rules in [106] that allows the maximum transmit power of a device in an ISM band up to 36 dBm, the simulation results are plotted against the predefined maximum transmit power threshold of the aggregator $P_t^{\max}$ varying from 20 dBm to 30 dBm. It can be readily observed that the performance of the suboptimal solution is reasonably close to that of the optimized case. In order to provide a fair comparison and to evaluate the performance of the proposed optimization framework, the results are compared with the throughput maximization problem in [89]. It can be clearly noticed that the proposed EE maximization problem provides

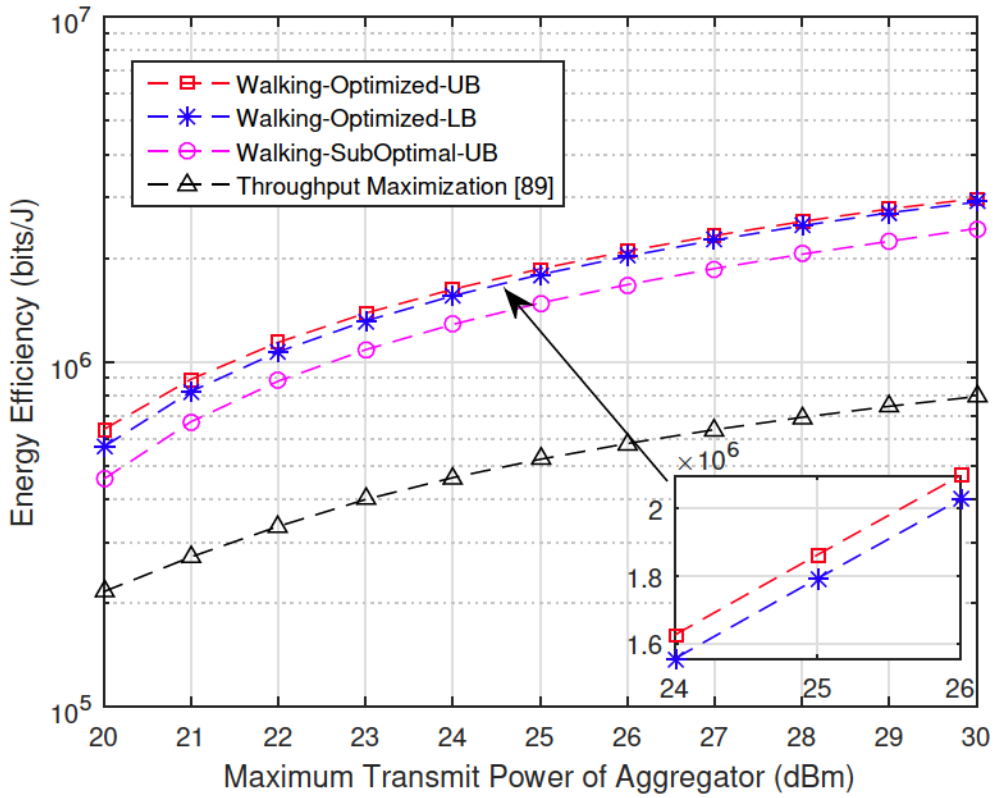

Fig. 5.4: Optimized and suboptimal EE of WBAN for walking state with $a_i = 3.52, b_i = 0.251$, and $c_i = 1$.

higher EE in comparison with the throughput maximization problem, in which the SNs transmit data to the aggregator with maximum transmit power. Moreover, the obtained EE of system by using both the throughput performance lower and upper bounds is fairly close to each other that validates that the obtained bounds are tight.

Fig. 5.4 depicts the EE of eHealth monitoring WBAN by considering the patient in the walking state. Based on the experimental results from [68] to model the walking posture, generalized gamma distribution with shape parameters chosen as $a_i = 3.52$ and $c_i = 1$, and scale parameter set as $b_i = 0.251$. It can be noticed that EE (in bits/Joule) follows the

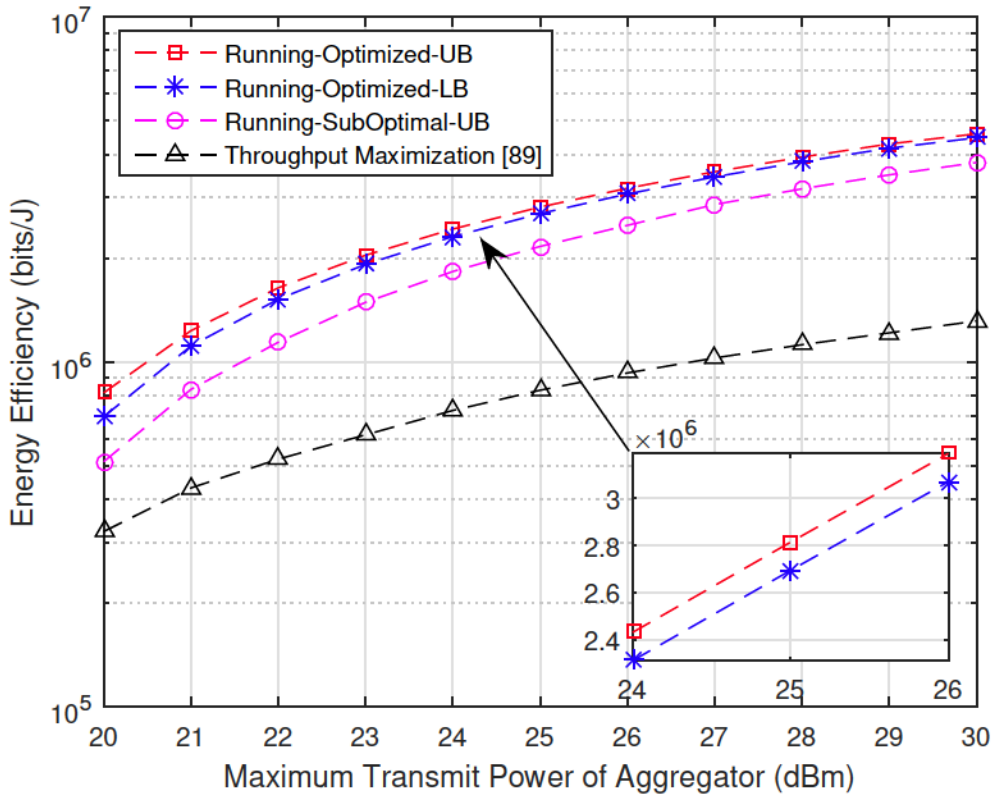

Fig. 5.5: Optimized and suboptimal EE of WBAN for running state with $a_i = 1, b_i = 0.948$, and $c_i = 1.64$.

increasing trend with the increase in maximum transmit power of the aggregator. It is due to the fact that, since the aggregator acts as the energy source for the SNs by broadcasting energy signals at a certain transmit power, therefore when the maximum transmit power threshold of the aggregator is increased the SNs can harvest more energy that ultimately results in higher EE. Moreover, it can be observed that the EE of the optimized and suboptimal solutions are close to each other.

Fig. 5.5 illustrates the EE of BackCom based WBAN in running state. From [68], the running state of the patient is modeled using the generalized gamma distribution with shape

parameters chosen as $a_i = 1$ and $c_i = 1.64$, and scale parameter is set as $b_i = 0.948$. Similar to the relaxing and walking state, the EE in running state also follows the same increasing behavior with the increased maximum transmit power threshold of the aggregator.

5.5.2 Effect of Backscatter Rate on Energy Efficiency of the System in BackCom and HTT Modes

In order to observe the performance of the proposed algorithm in both the passive BackCom phase and the active data transmission phase, we calculated the EE of the individual phases, which are referred to as BackCom and HTT modes. The EE of the BackCom mode and HTT mode is calculated as the ratio of the throughput in the passive BackCom phase or the active data transmission phase, to the total power consumption of the WBAN such that the sum of the EE of both the modes is equal to the EE of the overall WBAN.

Fig. 5.6 shows the EE of the WBAN in a relaxing state against the backscatter rate varying from 2 kbps to 30 kbps, by considering a throughput performance lower bound. For a fixed maximum transmit power threshold of the aggregator set as 20 dBm and δ_i as 40%, it can be seen that by increasing the backscatter rate, the EE of the WBAN also increases. Moreover, another interesting result that can be deduced is the effect of the backscatter rate on the BackCom and HTT modes of operation. In a specific time frame, as the backscatter rate increases, the SNs will spend most of their time in backscattering data to the aggregator in the passive BackCom phase and ultimately less duration of time will be spent by SNs for transmitting data in the active data transmission phase. As a result, when the backscatter rate increases the solution of the EE maximization problem switches to the BackCom mode. Since the SNs spend less time for data transmission due to the increasing backscatter rate, the EE in the HTT mode is less than that in the BackCom

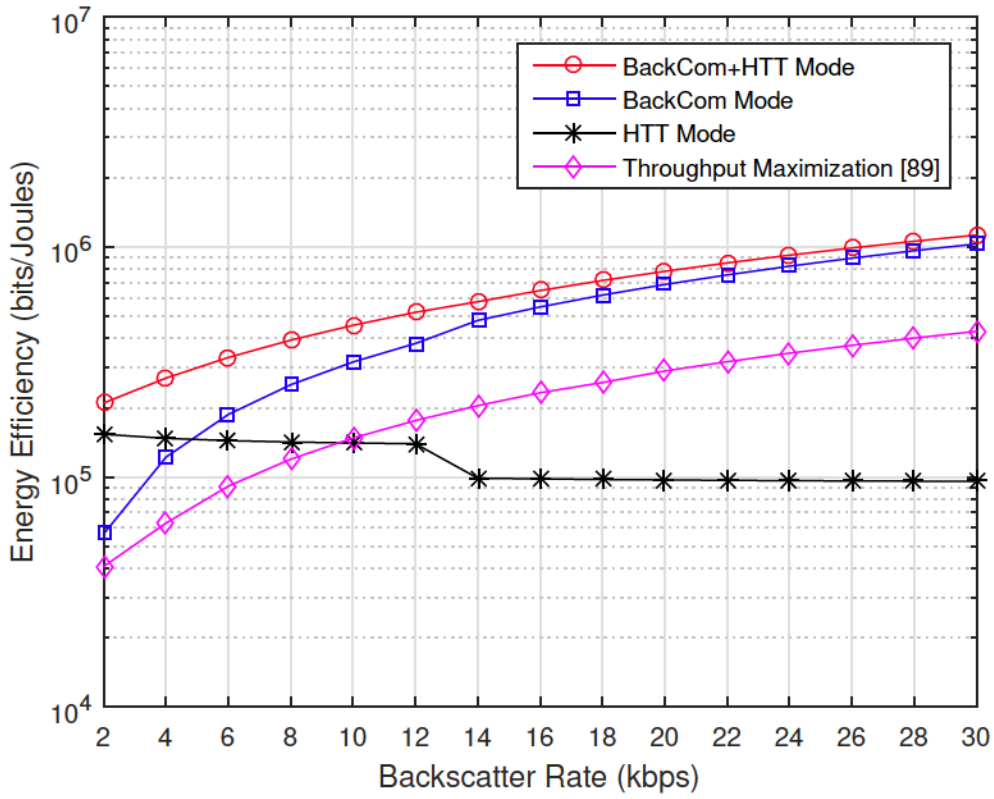

Fig. 5.6: Effect of backscatter rate on EE of the system in BackCom and HTT modes.

mode and far from the EE maximization solution.

5.5.3 Effect of Maximum Transmit Power of Aggregator on Energy Efficiency in BackCom and HTT Modes

Fig. 5.7 illustrates the effect of the maximum transmit power threshold of the aggregator on different communications modes as well as the EE of the WBAN system in the running state by considering throughput performance lower bound, and a fixed backscatter rate of 4 kbps. The maximum transmit power threshold of the aggregator is an important

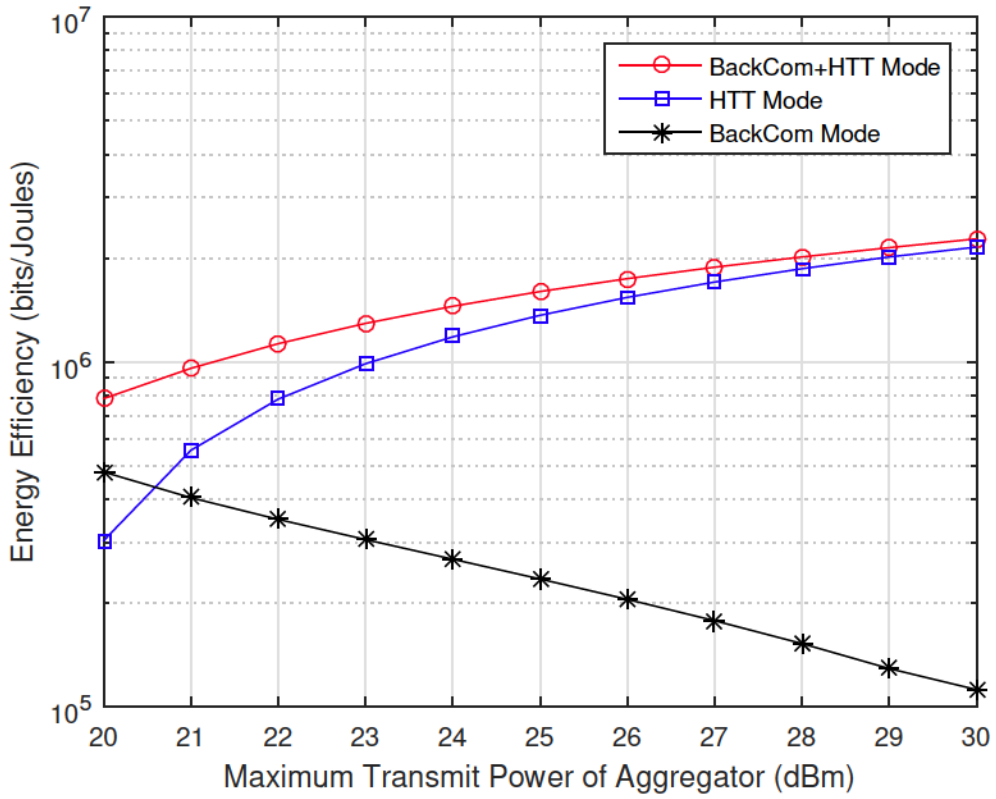

Fig. 5.7: Effect of aggregator's maximum transmit power on EE of the system in BackCom and HTT modes.

factor that affects the time allocated to the SNs during the passive BackCom and active data transmission phases. As mentioned earlier that the aggregator node also acts as the energy source for the SNs by broadcasting the energy signals, therefore by increasing the aggregator's maximum transmit power, the SNs will spend more time for harvesting energy during the first phase. Consequently, when the maximum transmit power of the aggregator increases, the SNs utilize the harvested energy in the first phase to transmit data during the active data transmission phase. As a result, the solution of the EE maximization problem switches to the HTT mode. By increasing the maximum transmit power threshold, the

EE of the HTT mode is reasonably close to the EE maximization solution. In comparison with the BackCom mode, it can be noticed that the EE in BackCom mode decreases with the increase of maximum transmit power of the aggregator.

5.6 Conclusion

In this chapter, we proposed an energy-efficient resource allocation framework for a BackCom-based eHealth system to provide sustainable and high-quality medical services by maximizing the EE of WBAN. BackCom technology is envisioned to be highly desirable for the EE system catering to severe and life-threatening illness by keeping the energy-constrained SNs alive and thus assuring the self-sustainable and perpetual WBAN operations. The significance of the proposed optimization scheme and the EE maximization algorithm is important for widespread adoption in the eHealth monitoring WBAN, as the optimal allocation of aggregator's transmit power, data BackCom and data transmission times demonstrate the effectiveness of the proposed scheme in maximizing the EE of the WBAN. Furthermore, for a practical dynamic environment, the adopted generalized gamma distribution is appropriate for a variety of body movements and can efficiently model different activities/movements of the patient during daily life.

Since improving the SNs lifetime or EE is a crucial design objective in the eHealth systems, in this regard simulation results demonstrate that the proposed EE maximization framework outperforms in comparison with the throughput maximization scheme from the literature. In addition, in a specific time frame if the BackCom rate is increased the SNs will spend more time backscattering their data to the aggregator, and to maximize the EE of the WBAN, the solution of the optimization problem switches to BackCom mode. Alternatively, the solution of the EE problem switches to the HTT mode by increasing

the maximum transmit power of the aggregator as more time will be spent by the SNs for harvesting energy in the first phase. Simulation results show the effect of varying aggregator's maximum transmit power and BackCom rate on the EE in different communication modes, along with the performance of the proposed scheme in maximizing the EE of the WBAN under different arbitrary movements.

5.7 Publication Resulted from This Chapter

- O. Amjad, E. Bedeer, N. A. Ali, and S. Ikki, "Energy Efficient Resource Allocation for eHealth Monitoring Wireless Body Area Networks with Backscatter Communication," doi:10.1109/JSEN.2022.3175754, *IEEE Sensors Journal*.

Chapter 6

Conclusions and Future Work

This chapter summarizes the contributions made in this dissertation and discusses potential extensions and future directions to our work.

6.1 Conclusions

One of the key challenges that limit the widespread usage of eHealth solutions in practical healthcare facilities is the limited battery life of the SNs that are needed to be replaced/recharged manually once the energy is depleted. In most scenarios, battery replacement is not preferable, and it becomes highly unsuitable and impractical, especially when the SNs are implanted inside the human body. This limited battery capacity of the SNs not only causes a performance bottleneck but is also likely to disrupt the future operations of the SNs, which may cause a life hazard. In order to have seamless and efficient implementation of an eHealth monitoring WBAN, improving the SNs' lifetime or EE is of paramount importance.

In this regard, we have formulated and solved the EE optimization problems under different system models and communication systems. Firstly, an optimization problem is proposed and solved to maximize the EE of an eHealth monitoring WBAN consisting of SNs equipped with energy harvesting capabilities in which the energy harvesting process of the SN is modeled using the discrete-time Markov chain. The EE objective function is defined as the ratio of the sum of the source rate of all the SNs to the power consumption of all the SNs in the network. The optimization problem aims to maximize the overall EE of the self-sustained eHealth monitoring system with WBAN. It can be concluded from this research that the source rate of the SNs is an important parameter that affects the EE of the system, and by optimally allocating each SN's source rate the overall EE of the WBAN can be improved.

Secondly, a robust eHealth monitoring communication system is proposed that can characterize the propagation characteristics of various patient conditions by only utilizing the generalized gamma distribution and can efficiently model both everyday and dynamic activities. More specifically, an optimization problem is formulated to optimize the EE of WBAN without requiring the CSI from the transmitting SNs to the aggregator and by considering outage probability and packet retransmission. The transmit power and encoding rate of the SNs are important parameters that can be optimized to improve the EE of the system.

Finally, considering a BackCom-assisted WBAN in the proposed research has its basis on exceptionally low-power consumption and enabling the energy-constrained SNs with self-sustaining capabilities by utilizing an energy harvesting mechanism can help improve the efficiency of the healthcare system globally. In this regard, the significance of the proposed optimization framework and EE maximization algorithm is that it shows potential in tackling the implementation difficulty faced by an eHealth system that requires a sus-

tainable energy supply. In this way, it can facilitate the realization of eHealth solutions in real-life healthcare settings by efficiently utilizing the network resources while guaranteeing a satisfactory performance of the WBAN. Furthermore, the healthcare sector is projected to be overwhelmed by the growing population. In this regard, the proposed scheme also has the potential to provide adaptable health services under various body postures without limiting the patients' mobility, thereby limiting unnecessary hospital visits. This can ultimately reduce healthcare expenses by eliminating the need for expensive in-hospital patient monitoring and alleviating overburdening of healthcare facilities. Simulation results demonstrate the performance of the proposed algorithm in comparison with the existing literature, along with the effectiveness of the proposed scheme in maximizing EE of the WBAN under different arbitrary movements.

6.2 Future Work

There are various future directions that can serve a source of inspiration in future development and advancement of eHealth monitoring WBANs, which can be briefly outlined as follows:

- It would be worthwhile researching to extend BackCom assisted eHealth monitoring WBAN to the scenario of multi-input-multi-output (MIMO) system. More specifically, the BackCom assisted EE optimization problem can be extended to a case in which the aggregator instead of having only a single antenna has multiple antennas. Extending the work to the MIMO system is expected to enhance the system performance in terms of EE of the system.
- Interference is a critical issue in WBANs and has a significant impact on system

performance, including lifetime, EE, and reliability. In real applications, multiple WBANs patients may coexist in the same local region, such as a hospital ward. Multiple types of interference sources, such as Bluetooth and WiFi, may coexist in such an environment. When numerous SNs use the same channel and time slot at the same time, interference occurs, resulting in transmission problems for those SNs. In this regard, interference mitigation schemes are another interesting research direction that can be focused on to help improve the performance of eHealth monitoring WBANs in the real-life practical healthcare environment.

- WBANs have usually used the 2.4 GHz microwave Industrial, Scientific, and Medical (ISM) band. It is anticipated that the 2.4 GHz microwave band, on the other hand, will be insufficient for the PHY channel of future WBANs, as evidenced by the expanding requirements for real-time high-speed communication of WBANs. Furthermore, many existing services use the 2.4 GHz spectrum, which would interfere with the reliability of WBAN connections. In this regard, a 60 GHz mmWave band can serve as a potential alternative that can offer high data rates with low-power consumption in short-range networks. However, the exact potential and limitations of this band have yet to be completely investigated. Large-scale testing and research of 60 GHz communication environments are required for the development of WBAN solutions in 5G networks. [11].

Appendix A

Proof of the Quasi-Concavity of the Objective Function of EE Maximization Problem

A.1 Proof of Quasi-Concavity of BackCom-Assisted EE Objective Function

The EE objective function defined in (5.20) is a quasi-concave function $\forall$ (t_i^a, t_i^b), where $i \in \{1, \ldots, N\}$, and the aggregator's transmit power P_t, individually, satisfying the given constraints. Recalling the EE objective function in (5.20) is a ratio of the overall throughput of WBAN in the passive BackCom phase and the active data transmission phase to the total power consumption of all the SNs in the network. In order to find the solution of the EE optimization problem, we need to verify the concavity of the total throughput in the numerator and the total power consumption term in the denominator. For simplicity,

we will show that the total throughput of sensor S_i is a concave function in each decision variable, i.e., (t_i^a, t_i^b, P_t). In this regard, we study the concavity of total throughput function $\mathcal{R}_i(t_i^a, t_i^b, P_t)$ by computing the Hessian matrix as follows $\mathbf{H}_1 = \bigtriangledown^2 \mathcal{R}_i(t_i^a, t_i^b, P_t)$, which is found to be written as

$$\mathbf{H}_1\left(\mathcal{R}_i(t_i^a, t_i^b, P_t)\right) = \frac{2\psi_i \rho_i {E_i^h}^2 \kappa_i^2}{P_i^R \ln 2 \left[t_i^a + E_i^h \kappa_i\right]^2} \begin{bmatrix} \frac{-{P_i^R}^2}{t_i^a} & 0 & \rho_i P_i^R \\ 0 & 0 & 0 \\ \rho_i P_i^R & 0 & -t_i^a \rho_i^2 \end{bmatrix}, \tag{A.1}$$

Then for any arbitrary real vector $\mathbf{z} = [z_1 \quad z_2 \quad z_3]$

$$\mathbf{z}^\top \mathbf{H}_1 \mathbf{z} = \frac{2\psi_i \rho_i {E_i^h}^2 \kappa_i^2}{P_i^R \ln 2 \left[t_i^a + E_i^h \kappa_i\right]^2} \left[\frac{-z_1^2 P_i^R}{2t_i^a \rho_i} + z_1 z_3 + \frac{-z_3^2 t_i^a \rho_i}{2P_i^R}\right], \tag{A.2}$$

From (A.2), we can write the following

$$\left(\sqrt{\frac{z_1^2 P_i^R}{2t_i^a \rho_i}} - \sqrt{\frac{z_3^2 t_i^a \rho_i}{2P_i^R}}\right)^2 = \frac{z_1^2 P_i^R}{2t_i^a \rho_i} - z_1 z_3 + \frac{z_3^2 t_i^a \rho_i}{2P_i^R} \geq 0, \tag{A.3}$$

Accordingly, by multiplying (A.3) with -1, the sign of the inequality is reversed as follows

$$\frac{-z_1^2 P_i^R}{2t_i^a \rho_i} + z_1 z_3 - \frac{z_3^2 t_i^a \rho_i}{2P_i^R} \leq 0, \tag{A.4}$$

Since for $t_i^a, t_i^b, P_t \geq 0$, $\psi_i, \rho_i, \kappa_i, E_i^h > 0$, $\forall i \in \{1, \ldots, N\}$, and by utilizing (A.4), it can be seen from (A.2) that $\mathbf{z}^\top \mathbf{H}_1 \mathbf{z} \leq 0$, $\forall i \in \{1, \ldots, N\}$. Hence, from (A.1), the Hessian matrix $\mathbf{H}_1\big(\mathcal{R}_i(t_i^a, t_i^b, P_t)\big)$ is negative semi-definite ($\forall i \in N$), therefore the total throughput function of sensor S_i, i.e., $\mathcal{R}_i(t_i^a, t_i^b, P_t)$ is concave with respect to t_i^a, t_i^b, and P_t.

In order to analyze the the total power consumption term in the denominator of EE

objective function in (5.20), i.e., $P_{\text{sum}}(t_i^a, t_i^b)$, the Hessian matrix $\mathbf{H}_2 = \bigtriangledown^2 P_{\text{sum}}(t_i^a, t_i^b)$ can be computed as follows

$$\mathbf{H}_2\big(P_{\text{sum}}(t_i^a, t_i^b)\big) = \frac{2\left(\left(\sum_{n=1}^{N} t_n^b\right) - t_i^b + \left(\sum_{n=1}^{N} t_n^a\right) - t_i^a\right) P_i^{\text{R}}}{t_i^{a3}} \begin{bmatrix} 1 & 0 \\ 0 & 0 \end{bmatrix}, \tag{A.5}$$

For any arbitrary real vector $\mathbf{z} = [z_1 \quad z_2]$

$$\mathbf{z}^\top \mathbf{H}_2 \mathbf{z} = \frac{2z_1^2}{t_i^{a3}} \left(\left(\sum_{n=1}^{N} t_n^b\right) - t_i^b + \left(\sum_{n=1}^{N} t_n^a\right) - t_i^a\right) P_i^{\text{R}} \geq 0. \tag{A.6}$$

As, $\mathbf{z}^\top \mathbf{H}_2 \mathbf{z} \geq 0$, the Hessian matrix $\mathbf{H}_2\big(P_{\text{sum}}(t_i^a, t_i^b)\big)$ in (A.5) is positive semi-definite ($\forall i \in N$), which proves that the total power consumption term, i.e., $P_{\text{sum}}(t_i^a, t_i^b)$ is convex with respect to t_i^a and t_i^b. Similarly, for a specific t_i^a and t_i^b, the total power consumption is positive and affine with respect to P_t. Therefore, the objective function to maximize the EE of WBAN is concave-convex fractional program which in turn is a quasi-concave function in t_i^a and t_i^b, and separately with respect to P_t [107]. In the similar manner the above mentioned analysis can be adopted to show that the overall EE of N SNs in the WBAN is a quasi-concave function. ■

References

[1] Department of Economic and Social Affairs, Population Division, "World Population Ageing 2020 Highlights: Living arrangements of older persons," United Nations, Tech. Rep., 2020, last Accessed: Jun. 01, 2022. [Online]. Available: https://www.un.org/development/desa/pd/sites/www.un.org.development.desa.pd/files/undesa_pd-2020_world_population_ageing_highlights.pdf

[2] S. Movassaghi, M. Abolhasan, J. Lipman, D. Smith, and A. Jamalipour, "Wireless body area networks: A survey," *IEEE Commun. Surveys Tuts.*, vol. 16, no. 3, pp. 1658–1686, 3rd Quart., 2014.

[3] R. Cavallari, F. Martelli, R. Rosini, C. Buratti, and R. Verdone, "A survey on wireless body area networks: Technologies and design challenges," *IEEE Commun. Surveys Tuts.*, vol. 16, no. 3, pp. 1635–1657, 3rd Quart., 2014.

[4] M. S. Hajar, M. O. Al-Kadri, and H. K. Kalutarage, "A survey on wireless body area networks: architecture, security challenges and research opportunities," *Computers & Security*, vol. 104, p. 102211, May 2021.

[5] R. Jaana, L. Katherine, and S. Shubham. Prioritizing health: A prescription for prosperity. Last Accessed: Jun. 01, 2022. [Online].

Available: https://www.mckinsey.com/industries/healthcare-systems-and-services/our-insights/prioritizing-health-a-prescription-for-prosperity

[6] A. Bouazizi, G. Zaibi, M. Samet, and A. Kachouri, "Wireless body area network for e-health applications: Overview," in *Proc. IEEE Int. Conf. on Smart, Monitored and Controlled Cities (SM2C)*, 2017, pp. 64–68.

[7] P. K. D. Pramanik, A. Nayyar, and G. Pareek, "WBAN: Driving e-healthcare beyond telemedicine to remote health monitoring: Architecture and protocols," in *Telemedicine technologies.* Elsevier, May 2019, pp. 89–119.

[8] Y. He, W. Zhu, and L. Guan, "Optimal resource allocation for pervasive health monitoring systems with body sensor networks," *IEEE Trans. Mob. Comput.*, vol. 10, no. 11, pp. 1558–1575, May 2011.

[9] A. K. Sagar, S. Singh, and A. Kumar, "Energy-aware WBAN for health monitoring using critical data routing (CDR)," *Wirel. Pers. Commun.*, vol. 112, no. 1, pp. 273–302, Jan. 2020.

[10] I. Al Barazanchi, W. Hashim, A. A. Alkahtani, H. H. Abbas, and H. R. Abdulshaheed, "Overview of WBAN from literature survey to application implementation," in *Proc. 8th IEEE Int. Conf. Electr. Eng. Inform. (EECSI)*, Oct. 2021, pp. 16–21.

[11] B. Cornet, H. Fang, H. Ngo, E. W. Boyer, and H. Wang, "An overview of wireless body area networks for mobile health applications," *IEEE Netw.*, vol. 36, no. 1, pp. 76–82, Mar. 2022.

[12] E. Jafer, S. Hussain, and X. Fernando, "A wireless body area network for remote observation of physiological signals," *IEEE Consum. Electron. Mag*, vol. 9, no. 2, pp. 103–106, Feb. 2020.

[13] X. Yang, L. Wang, and Z. Zhang, "Wireless body area networks MAC protocol for energy efficiency and extending lifetime," *IEEE Sens. Lett.*, vol. 2, no. 1, pp. 1–4, Mar. 2018.

[14] B. Liu, Z. Yan, and C. W. Chen, "Medium access control for wireless body area networks with QoS provisioning and energy efficient design," *IEEE Trans. Mobile Comput.*, vol. 16, no. 2, pp. 422–434, Feb. 2016.

[15] F. Akhtar and M. H. Rehmani, "Energy harvesting for self-sustainable wireless body area networks," *IT Prof.*, vol. 19, no. 2, pp. 32–40, Apr. 2017.

[16] S. M. Demir, F. Al-Turjman, and A. Muhtaroğlu, "Energy scavenging methods for WBAN applications: A review," *IEEE Sens. J.*, vol. 18, no. 16, pp. 6477–6488, Jun. 2018.

[17] F. Hu, X. Liu, M. Shao, D. Sui, and L. Wang, "Wireless energy and information transfer in WBAN: An overview," *IEEE Netw.*, vol. 31, no. 3, pp. 90–96, May 2017.

[18] J. Ramis-Bibiloni and L. Carrasco-Martorell, "Energy harvesting effect on the sensors battery lifespan of an energy efficient smartBAN network," in *Proc. IEEE Int. Wireless Commun. and Mobile Computing (IWCMC)*, Aug. 2021, pp. 1593–1598.

[19] N. Van Huynh, D. T. Hoang, X. Lu, D. Niyato, P. Wang, and D. I. Kim, "Ambient backscatter communications: A contemporary survey," *IEEE Commun. Surveys Tuts.*, vol. 20, no. 4, pp. 2889–2922, 4th Quart., 2018.

[20] G. Yang, Q. Zhang, and Y.-C. Liang, "Cooperative ambient backscatter communications for green Internet-of-Things," *IEEE Internet Things J.*, vol. 5, no. 2, pp. 1116–1130, Jan. 2018.

[21] F. Jameel, R. Duan, Z. Chang, A. Liljemark, T. Ristaniemi, and R. Jantti, "Applications of backscatter communications for healthcare networks," *IEEE Netw.*, vol. 33, no. 6, pp. 50–57, Dec. 2019.

[22] D. D. Olatinwo, A. M. Abu-Mahfouz, and G. P. Hancke, "Energy-aware hybrid MAC protocol for IoT enabled WBAN systems," *IEEE Sens. J.*, Dec. 2021.

[23] V. Esteves, A. Antonopoulos, E. Kartsakli, M. Puig-Vidal, P. Miribel-Català, and C. Verikoukis, "Cooperative energy harvesting-adaptive MAC protocol for WBANs," *Sens.*, vol. 15, no. 6, pp. 12 635–12 650, May 2015.

[24] C. Liu, H. Liu, Y. Cong, P. Li, Z. Mao, and H. H. Zhang, "Throughput maximization by time switching in multipoint WBAN with fairness consideration," *IEEE Access*, vol. 8, pp. 107 661–107 668, Jun. 2020.

[25] H. Liu, F. Hu, S. Qu, Z. Li, and D. Li, "Multipoint wireless information and power transfer to maximize sum-throughput in WBAN with energy harvesting," *IEEE Internet of Things J.*, vol. 6, no. 4, pp. 7069–7078, Apr. 2019.

[26] S. Li, F. Hu, Z. Mao, Z. Ling, and Y. Zou, "Sum-throughput maximization by power allocation in WBAN with relay cooperation," *IEEE Access*, vol. 7, pp. 124 727–124 736, Aug. 2019.

[27] A. Astrin, "IEEE standard for local and metropolitan area networks part 15.6: Wireless body area networks," *IEEE Std 802.15. 6*, Feb. 2012.

[28] M. Ghamari, B. Janko, R. S. Sherratt, W. Harwin, R. Piechockic, and C. Soltanpur, "A survey on wireless body area networks for ehealthcare systems in residential environments," *Sens.*, vol. 16, no. 6, p. 831, Jun. 2016.

[29] W. Dargie and C. Poellabauer, *Fundamentals of wireless sensor networks: theory and practice*. John Wiley & Sons, 2010.

[30] P. Kaushik and P. Sethi, "A comprehensive study on blood pressure measurement techniques," in *Proc. IEEE 4th Int. Conf. on Computing Communication and Automation (ICCCA)*, Dec. 2018, pp. 1–3.

[31] N. Watanabe, Y. K. Bando, T. Kawachi, H. Yamakita, K. Futatsuyama, Y. Honda, H. Yasui, K. Nishimura, T. Kamihara, T. Okumura *et al.*, "Development and validation of a novel cuff-less blood pressure monitoring device," *Basic to Translational Science*, vol. 2, no. 6, pp. 631–642, Dec. 2017.

[32] D. M. Bard, J. I. Joseph, and N. van Helmond, "Cuff-less methods for blood pressure telemonitoring," *Front. cardiovasc. med.*, vol. 6, p. 40, Apr. 2019.

[33] Q. Zhang, N. Zhang, L. Kang, G. Hu, X. Yan, X. Ding, Q. Fu, Y.-t. Zhang, N. Zhao, J. Gao *et al.*, "Technology development for simultaneous wearable monitoring of cerebral hemodynamics and blood pressure," *IEEE J. Biomed. Health Inform.*, vol. 23, no. 5, pp. 1952–1963, Oct. 2018.

[34] V. G. Ganti, A. Carek, B. N. Nevius, J. Heller, M. Etemadi, and O. Inan, "Wearable cuff-less blood pressure estimation at home via pulse transit time," *IEEE J. Biomed. Health Inform.*, Sep. 2020.

[35] "IEEE standard for wearable, cuffless blood pressure measuring devices - amendment 1," *IEEE Std 1708a-2019 (Amendment to IEEE Std 1708-2014)*, pp. 1–35, 2019.

[36] A. Darwish and A. E. Hassanien, "Wearable and implantable wireless sensor network solutions for healthcare monitoring," *Sens.*, vol. 11, no. 6, pp. 5561–5595, May 2011.

[37] H. Taleb, A. Nasser, G. Andrieux, N. Charara, and E. Motta Cruz, "Wireless technologies, medical applications and future challenges in WBAN: a survey," *Wirel. Netw.*, vol. 27, no. 8, pp. 5271–5295, Sep. 2021.

[38] M. Salayma, A. Al-Dubai, I. Romdhani, and Y. Nasser, "Wireless body area network (WBAN) a survey on reliability, fault tolerance, and technologies coexistence," *ACM Comput. Surv.*, vol. 50, no. 1, pp. 1–38, Mar. 2017.

[39] R. Negra, I. Jemili, and A. Belghith, "Wireless body area networks: Applications and technologies," *Procedia Comput. Sci.*, vol. 83, pp. 1274–1281, May 2016.

[40] D. P. Tobón, T. H. Falk, and M. Maier, "Context awareness in WBANs: a survey on medical and non-medical applications," *IEEE Wirel. Commun.*, vol. 20, no. 4, pp. 30–37, Aug. 2013.

[41] O. Amjad, E. Bedeer, and S. Ikki, "Energy-efficiency maximization of self-sustained wireless body area sensor networks," *IEEE Sens. Lett.*, vol. 3, no. 12, pp. 1–4, Oct. 2019.

[42] M. Boumaiz, M. El Ghazi, S. Mazer, M. Fattah, A. Bouayad, M. El Bekkali, and Y. Balboul, "Energy harvesting based WBANs: EH optimization methods," *Procedia Comput. Sci.*, vol. 151, pp. 1040–1045, May 2019.

[43] S. Cosnier, A. Le Goff, and M. Holzinger, "Towards glucose biofuel cells implanted in human body for powering artificial organs," *Electrochem. commun.*, vol. 38, pp. 19–23, Jan. 2014.

[44] A. J. Bandodkar and J. Wang, "Wearable biofuel cells: a review," *Electroanalysis*, vol. 28, no. 6, pp. 1188–1200, Feb. 2016.

[45] B. Shi, Z. Li, and Y. Fan, "Implantable energy-harvesting devices," *Adv. Mater.*, vol. 30, no. 44, p. 1801511, Jul. 2018.

[46] F. Invernizzi, S. Dulio, M. Patrini, G. Guizzetti, and P. Mustarelli, "Energy harvesting from human motion: materials and techniques," *Chem. Soc. Rev.*, vol. 45, no. 20, pp. 5455–5473, Jul. 2016.

[47] A. Ghosh, S. Khalid, V. Harigovindan *et al.*, "Performance analysis of wireless body area network with thermal energy harvesting," in *Proc. Global Conf. on Communication Technologies (GCCT)*, Apr. 2015, pp. 916–920.

[48] H. M. Saraiva, L. M. Borges, P. Pinho, R. Goncalves, R. Chavez-Santiago, N. Barroca, J. Tavares, P. T. Gouveia, N. B. Carvalho, I. Balasingham *et al.*, "Experimental characterization of wearable antennas and circuits for RF energy harvesting in WBANs," in *Proc. IEEE 79th Vehicular Technology Conference (VTC Spring)*, May 2014, pp. 1–5.

[49] Powercast. Tx91501b powercaster transmitter. Last Accessed: Jun. 05, 2022. [Online]. Available: https://www.powercastco.com/products/powercaster-transmitter/

[50] W. Liu, K. Huang, X. Zhou, and S. Durrani, "Backscatter communications for Internet-of-Things: Theory and applications," *arXiv preprint arXiv:1701.07588*, Aug. 2017.

[51] E. Ibarra, A. Antonopoulos, E. Kartsakli, J. J. Rodrigues, and C. Verikoukis, "QoS-aware energy management in body sensor nodes powered by human energy harvesting," *IEEE Sensors J.*, vol. 16, no. 2, pp. 542–549, Jan. 2016.

[52] P.-V. Mekikis, A. Antonopoulos, E. Kartsakli, N. Passas, L. Alonso, and C. Verikoukis, "Stochastic modeling of wireless charged wearables for reliable health mon-

itoring in hospital environments," in *Proc. Int. Conf. on Communications (ICC)*. IEEE, Jul. 2017, pp. 1–6.

[53] B. Liu, Z. Yan, and C. W. Chen, "Medium access control for wireless body area networks with QoS provisioning and energy efficient design," *IEEE Trans. Mobile. Comput.*, vol. 16, no. 2, pp. 422–434, Feb. 2017.

[54] Z. Ling, F. Hu, L. Wang, J. Yu, and X. Liu, "Point-to-point wireless information and power transfer in WBAN with energy harvesting," *IEEE Access*, vol. 5, pp. 8620–8628, Apr. 2017.

[55] M. Wahbah, M. Alhawari, B. Mohammad, H. Saleh, and M. Ismail, "Characterization of human body-based thermal and vibration energy harvesting for wearable devices," *IEEE Trans. Emerg. Sel. Topics Circuits Syst.*, vol. 4, no. 3, pp. 354–363, Sep. 2014.

[56] Z. Liu, B. Liu, and C. W. Chen, "Joint power-rate-slot resource allocation in energy harvesting-powered wireless body area networks," *IEEE Trans. Veh. Technol.*, vol. 67, no. 12, pp. 12 152–12 164, Dec. 2018.

[57] W. R. Heinzelman, A. Chandrakasan, and H. Balakrishnan, "Energy-efficient communication protocol for wireless microsensor networks," in *Proc. IEEE 33rd annual Hawaii international conference on system sciences*, Jan. 2000, pp. 1–10.

[58] R. DErrico and L. Ouvry, "A statistical model for on-body dynamic channels," *Int. J. Wirel. Inf. Netw.*, vol. 17, no. 3-4, pp. 92–104, Dec. 2010.

[59] M. B. Hasan and S. Acharjee, "Solving LFP by converting it into a single LP," *Int. J. Ops. Research*, vol. 8, no. 3, pp. 1–14, Jun. 2011.

[60] P. R. Thie and G. E. Keough, *An Introduction to Linear Programming and Game Theory*. John Wiley & Sons, Sep. 2011.

[61] A. K. Triantafyllidis, V. G. Koutkias, I. Chouvarda, and N. Maglaveras, "A pervasive health system integrating patient monitoring, status logging, and social sharing," *IEEE J. Biomed. Health inform.*, vol. 17, no. 1, pp. 30–37, Jan. 2012.

[62] M. Salayma, A. Al-Dubai, I. Romdhani, and Y. Nasser, "Reliability and energy efficiency enhancement for emergency-aware wireless body area networks (WBANs)," *IEEE Trans. Green Commun. Netw.*, vol. 2, no. 3, pp. 804–816, Mar. 2018.

[63] X. Zhou, T. Zhang, L. Song, and Q. Zhang, "Energy efficiency optimization by resource allocation in wireless body area networks," in *Proc. IEEE 79th Vehicular Technology Conference (VTC Spring)*, May 2014, pp. 1–6.

[64] X. Yang, D. Fan, A. Ren, N. Zhao, and M. Alam, "5G-based user-centric sensing at C-band," *IEEE Trans. Ind. Informat.*, vol. 15, no. 5, pp. 3040–3047, May 2019.

[65] N. Alshurafa, C. Sideris, M. Pourhomayoun, H. Kalantarian, M. Sarrafzadeh, and J.-A. Eastwood, "Remote health monitoring outcome success prediction using baseline and first month intervention data," *IEEE J. Biomed. Health inform.*, vol. 21, no. 2, pp. 507–514, Mar. 2016.

[66] S. P. McGrath, I. M. Perreard, M. D. Garland, K. A. Converse, and T. A. Mackenzie, "Improving patient safety and clinician workflow in the general care setting with enhanced surveillance monitoring," *IEEE J. Biomed. Health inform.*, vol. 23, no. 2, pp. 857–866, Mar. 2018.

[67] L. Hanlen, V. Chaganti, B. Gilbert, D. Rodda, T. Lamahewa, and D. Smith, "Open-source testbed for body area networks: 200 sample/sec, 12 hrs continuous mea-

surement," in *Proc. IEEE Int. Symp. Pers., Indoor and Mobile Radio Commun. (PIMRC) Workshops*, Sep. 2010, pp. 66–71.

[68] D. B. Smith, L. W. Hanlen, J. A. Zhang, D. Miniutti, D. Rodda, and B. Gilbert, "First-and second-order statistical characterizations of the dynamic body area propagation channel of various bandwidths," *annals of telecommunications-annales des télécommunications*, vol. 66, no. 3-4, pp. 187–203, Dec. 2010.

[69] D. B. Smith, D. Miniutti, T. A. Lamahewa, and L. W. Hanlen, "Propagation models for body-area networks: A survey and new outlook," *IEEE Antennas Propag. Mag.*, vol. 55, no. 5, pp. 97–117, Oct. 2013.

[70] Y. Polyanskiy, H. V. Poor, and S. Verdú, "Channel coding rate in the finite block-length regime," *IEEE Trans. Inf. Theory*, vol. 56, no. 5, p. 2307, May 2010.

[71] S. Boyd and L. Vandenberghe, *Convex Optimization*. Cambridge University Press, 2004.

[72] J. C. Kwan and A. O. Fapojuwo, "Sum-throughput maximization in wireless sensor networks with radio frequency energy harvesting and backscatter communication," *IEEE Sens. J.*, vol. 18, no. 17, pp. 7325–7339, Jul. 2018.

[73] M. He, F. Hu, Z. Ling, Z. Mao, and Z. Huang, "A dynamic weights algorithm on information and energy transmission protocol based on WBAN," *IEEE Trans. Veh. Technol.*, vol. 70, no. 2, pp. 1528–1537, Jan. 2021.

[74] X. Lu, P. Wang, D. Niyato, D. I. Kim, and Z. Han, "Wireless networks with RF energy harvesting: A contemporary survey," *IEEE Commun. Surveys Tuts.*, vol. 17, no. 2, pp. 757–789, 2nd Quart., 2014.

[75] J. C. Kwan and A. O. Fapojuwo, "Performance optimization of a multi-source, multi-sensor beamforming wireless powered communication network with backscatter," *IEEE Sens. J.*, vol. 19, no. 22, pp. 10 898–10 909, Jul. 2019.

[76] Z. Ling, F. Hu, and D. Li, "Optimal resource allocation in point-to-point wireless body area network with backscatter communication," in *Proc. Int. Conf. on Computing, Networking and Communications (ICNC)*, Feb. 2020, pp. 780–784.

[77] W. Zang, F. Sun, and Y. Li, "Throughput improvement in backscatter-based wireless body area network," in *Proc. IEEE Int. Conf. on Human-Machine Systems (ICHMS)*, Sep. 2020, pp. 1–6.

[78] Y. Ye, L. Shi, R. Q. Hu, and G. Lu, "Energy-efficient resource allocation for wirelessly powered backscatter communications," *IEEE Commun. Lett.*, vol. 23, no. 8, pp. 1418–1422, Jun. 2019.

[79] B. Lyu, Z. Yang, F. Tian, and G. Gui, "Energy-efficient resource allocation for wireless-powered backscatter communication networks," in *Proc. Int. Conf. on Communication Systems (ICCS)*, Dec. 2018, pp. 72–77.

[80] L. Shi, R. Q. Hu, J. Gunther, Y. Ye, and H. Zhang, "Energy efficiency for RF-powered backscatter networks using HTT protocol," *IEEE Trans. Veh. Technol.*, vol. 69, no. 11, pp. 13 932–13 936, Aug. 2020.

[81] Y. Xu and G. Gui, "Optimal resource allocation for wireless powered multi-carrier backscatter communication networks," *IEEE Wireless Commun. Lett.*, vol. 9, no. 8, pp. 1191–1195, Apr. 2020.

[82] H. Yang, Y. Ye, X. Chu, and S. Sun, "Energy efficiency maximization for UAV-enabled hybrid backscatter-harvest-then-transmit communications," *IEEE Trans. Wirel. Commun.*, Oct. 2021.

[83] O. Amjad, E. Bedeer, N. A. Ali, and S. Ikki, "Energy efficient resource allocation for eHealth monitoring wireless body area networks with backscatter communication," *IEEE Sens. J.*, May 2022.

[84] Z. Ling, F. Hu, and M. Shao, "The optimal control policy for point-to-point wireless body area network based on simultaneous time-ratio and transmission power allocation," *IEEE Access*, vol. 7, pp. 46 454–46 460, Feb. 2019.

[85] O. Amjad, E. Bedeer, N. A. Ali, and S. Ikki, "Robust energy efficiency optimization algorithm for health monitoring system with wireless body area networks," *IEEE Commun. Lett.*, vol. 24, no. 5, pp. 1142–1145, Feb. 2020.

[86] V. Liu, A. Parks, V. Talla, S. Gollakota, D. Wetherall, and J. R. Smith, "Ambient backscatter: Wireless communication out of thin air," in *Proc. ACM Special Interest Group on Data Communication (SIGCOMM)*, Aug. 2013, pp. 39–50.

[87] D. T. Hoang, D. Niyato, P. Wang, D. I. Kim, and Z. Han, "Ambient backscatter: A new approach to improve network performance for RF-powered cognitive radio networks," *IEEE Trans. Commun.*, vol. 65, no. 9, pp. 3659–3674, Jun. 2017.

[88] S. H. Kim and D. I. Kim, "Hybrid backscatter communication for wireless-powered heterogeneous networks," *IEEE Trans. Wirel. Commun.*, vol. 16, no. 10, pp. 6557–6570, Jul. 2017.

[89] N. Van Huynh, D. T. Hoang, D. Niyato, P. Wang, and D. I. Kim, "Optimal time scheduling for wireless-powered backscatter communication networks," *IEEE Wireless Commun. Lett.*, vol. 7, no. 5, pp. 820–823, Apr. 2018.

[90] B. Lyu, Z. Yang, G. Gui, and Y. Feng, "Wireless powered communication networks assisted by backscatter communication," *IEEE Access*, vol. 5, pp. 7254–7262, Mar. 2017.

[91] N.-T. Nguyen, D. N. Nguyen, D. T. Hoang, N. Van Huynh, H.-N. Nguyen, Q. T. Nguyen, and E. Dutkiewicz, "Energy trading and time scheduling for energy-efficient heterogeneous low-power IoT networks," in *Proc. IEEE Global Communications Conference (GLOBECOM)*, Dec. 2020, pp. 1–6.

[92] X. Gao, D. Niyato, P. Wang, K. Yang, and J. An, "Contract design for time resource assignment and pricing in backscatter-assisted RF-powered networks," *IEEE Wireless Commun. Lett.*, vol. 9, no. 1, pp. 42–46, Sep. 2019.

[93] C. A. Balanis, *Antenna theory: analysis and design.* John wiley & sons, 2016.

[94] Texas Instruments, *MSP430 microcontrollers units (MCUs).* [Online]. Available: https://www.ti.com/microcontrollers-mcus-processors/microcontrollers/msp430-microcontrollers/overview.html

[95] K. Sohrabi, J. Gao, V. Ailawadhi, and G. J. Pottie, "Protocols for self-organization of a wireless sensor network," *IEEE Pers. Commun.*, vol. 7, no. 5, pp. 16–27, Oct. 2000.

[96] H. Azarhava and J. M. Niya, "Energy efficient resource allocation in wireless energy harvesting sensor networks," *IEEE Wirel. Commun. Lett.*, vol. 9, no. 7, pp. 1000–1003, Mar. 2020.

[97] H. Lim and T. Hwang, "User-centric energy efficiency optimization for MISO wireless powered communications," *IEEE Trans. Wirel. Commun.*, vol. 18, no. 2, pp. 864–878, Dec. 2018.

[98] B. Lyu, C. You, Z. Yang, and G. Gui, "The optimal control policy for RF-powered backscatter communication networks," *IEEE Trans. Veh. Technol.*, vol. 67, no. 3, pp. 2804–2808, Nov. 2017.

[99] D. Tse and P. Viswanath, *Fundamentals of Wireless Communication.* Cambridge university press, 2005.

[100] D. J. MacKay and D. J. Mac Kay, *Information Theory, Inference and Learning Algorithms.* Cambridge university press, 2003.

[101] T. L. Marzetta, *Fundamentals of massive MIMO.* Cambridge University Press, 2016.

[102] O. Gomès, C. Combes, and A. Dussauchoy, "Parameter estimation of the generalized gamma distribution," *Mathematics Comput. Simul*, vol. 79, no. 4, pp. 955–963, Dec. 2008.

[103] W. Dinkelbach, "On nonlinear fractional programming," *Management science*, vol. 13, no. 7, pp. 492–498, Mar. 1967.

[104] S. Boyd, L. Xiao, and A. Mutapcic, "Subgradient methods," Dept. Elect. Eng., Stanford University, Stanford, CA, USA, Lecture Notes of EE392o, 2003.

[105] L. Shi, Y. Ye, R. Q. Hu, and H. Zhang, "Energy efficiency maximization for SWIPT enabled two-way DF relaying," *IEEE Signal Process. Lett.*, vol. 26, no. 5, pp. 755–759, Mar. 2019.

[106] Federal Communications Commission, "Part 15: Radio frequency devices," Code of Federal Regulations, 2008.

[107] A. Cambini and L. Martein, *Generalized Convexity and Optimization: Theory and Applications*. Berlin, Germany: Springer-Verlag, 2008, vol. 616.